

Department of Organic and Macromolecular Chemistry
Research group: Supramolecular Chemistry Group

Responsive polymer hydrogel sensors and actuators

Thesis submitted to obtain

the degree of Master of Science in Chemistry by

Annelore PODEVYN

Academic year 2015-2016

Promoter: Prof. dr. Richard Hoogenboom

Supervisor: Zhanyao Hou

Acknowledgements

I would like to take this opportunity to thank the people who helped and supported me during this final thesis year. Without them this year would have been a lot more difficult.

First of all I would like to thank my promotor, Prof. dr. Richard Hoogenboom for giving me the opportunity to be part of this research group and his guidance during this project. A special thanks goes to my supervisor Zhanyao Hou for his support in the lab and his assistance in writing my thesis. I have learned a lot from him and he was always ready to answer my questions.
I would also like to thank my colleagues who were always willing to lend a hand and for creating a nice work environment.
Additionally, I would also like to mention Ir. Jan Goeman for his aid regarding LCMS measurements, Jos Van den Begin for all technical aid and Tim Courtin for the many NMR measurements, thank you.

Finally, I would like to thank my family for their endless support and patience in these stressful times. My cousin Silke, for being an amazing roommate and support these last years. And lastly, my friends for giving me an amazing and unforgettable five years in Ghent.

Abbreviations

Đ	dispersity
AIBN	azobisisobutyronitrile
AMA	aluminium oxide methanesulfonic acid
ATRP	atom transfer radical polymerization
$CBPQT^{4+}$	cyclobis(paraquat-*p*-phenylene)
CCl_4	carbon tetrachloride
CRP	controlled radical polymerization
CTA	chain transfer agent
DCC	*N,N'*-dicyclohexylcarbodiimide
DCM	dichloromethane
DMA	dimethylacetamide
DMAP	4-dimethylaminopyridine
DMF	dimethylformamide
DP	degree of polymerization
ESI-MS	electrospray ionization mass spectrometry
Et_2O	diethyl ether
EtOAc	ethyl acetate
EtOH	ethanol
GC	gas chromatography
I	initiator
LCST	lower critical solution temperature
M	monomer
MBTTC	methyl 2-(butylthiocarbonothioylthio)propanoate
MeCN	acetonitrile

M_n	number average molecular weight
M_w	weight average molecular weight
NBS	N-bromosuccinimide
NMP	nitroxide mediated polymerization
NMR	nuclear magnetic resonance spectroscopy
PNIPAM	poly(*N*-isopropylacrylamide)
RAFT	reversible addition-fragmentation chain transfer
SEC	size exclusion chromatography
T_{CP}	cloud point temperature
TLC	thin layer chromatography
UCST	upper critical solution temperature

Contents

1 Introduction

1.1 Supramolecular chemistry

Supramolecular chemistry is a very vibrant research topic and thanks its popularity to the fact that it is inspired by nature, making this a highly interdisciplinary field. After all, the initial motivation behind supramolecular chemistry was to design chemical systems which could mimic biological processes. Due to their dynamic nature, supramolecular interactions are quite common in biological systems and are among others responsible for the high adaptivity of living species. Some of the most well-known examples in nature include the self-assembly of double helical DNA,[1–3] enzyme-substrate recognition,[4,5] metal-ligand complexes,[6,7] the folding and assembly of proteins[8,9] and changes in protein assemblies such as focussing of the eye, healing processes and temperature regulation. Today, supramolecular chemistry is used in various applications such as drug delivery,[10–13] "smart" materials,[14–16] catalysis,[17–19] data storage and processing[20–23] and nanotechnology.[24,25]

Supramolecular chemistry differs from molecular chemistry, which focusses on the highly stable covalent bonds, in a way that it studies intermolecular interactions that are of a reversible nature. These non-covalent interactions are generally weaker than the covalent interactions but can be used in a multiple and cooperative manner to give the strength needed to form stable complexes and provide the adaptability and specificity required in most important biological processes.[26] So, while molecular chemistry rules the covalent bond, supramolecular chemistry tries to gain control over reversible non-covalent interactions between aggregates of molecules or ions. The non-covalent interactions comprise electrostatic interactions (ion-ion interactions, ion-dipole interactions, dipole-dipole interactions and induced dipole interactions), hydrogen bondings, aromatic and π-interactions

(π-π interactions, cation-π interactions and anion-π interactions) and Van der Waals forces (Figure 1.1). In addition, solvophobic effects are also important.

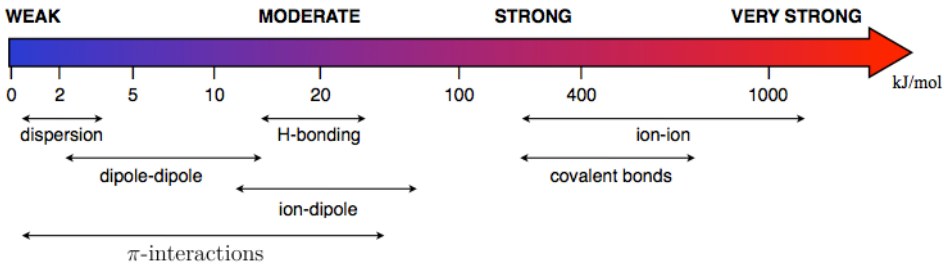

Figure 1.1: *Overview of the strength of different non-covalent interactions compared to covalent bonds. Dispersion forces are also known as induced dipole interactions, London (dispersion) forces or Van der Waals forces. Reprinted from reference*[27].

Generally, supramolecular chemistry can be divided into two broad categories: host-guest chemistry[28] and self-assembly,[29] in which the difference between these two areas is a question of size and shape. Host-guest chemistry occurs when one molecule is significantly larger than another molecule and the larger "host" molecule is capable of enclosing a smaller "guest" molecule *via* non-covalent forces, while self-assembly is the spontaneous process of different molecular components joining together to form a larger and more complex aggregate (Figure 1.2). In both cases, a maximum specificity and stability between both molecules is acquired with complementary surfaces (lock-key principle) and complementary distribution of the active groups.[26] So, host-guest chemistry can be seen as a specific case of self-assembly where the different molecular components joining together have a distinct difference in size.

1.1.1 Self-assembly

Molecular self-assembly is the autonomous and reversible organization of molecular components into ordered structures *via* non-covalent interactions without external guidance or intervention.[31] The self-assembled structure is the result of a thermodynamic equilibrium between this ordered structure (less Gibbs-free energy) and the more random, individual components. To obtain a stable, well-defined final assembly, three aspects need to be considered. First, the non-covalent interactions between the individual components should be

strong enough, either by one strong interaction or multiple weaker interactions. Secondly, these interactions should be energetically more favorable than the competing interactions with the solvent. Thirdly, they must be able to overcome the entropic disadvantage of the assembled state over the dissociated state.[32] Due to the reversible nature of this process, it is possible to form ordered structures that are relatively free of defects, representing the thermodynamically most stable state.

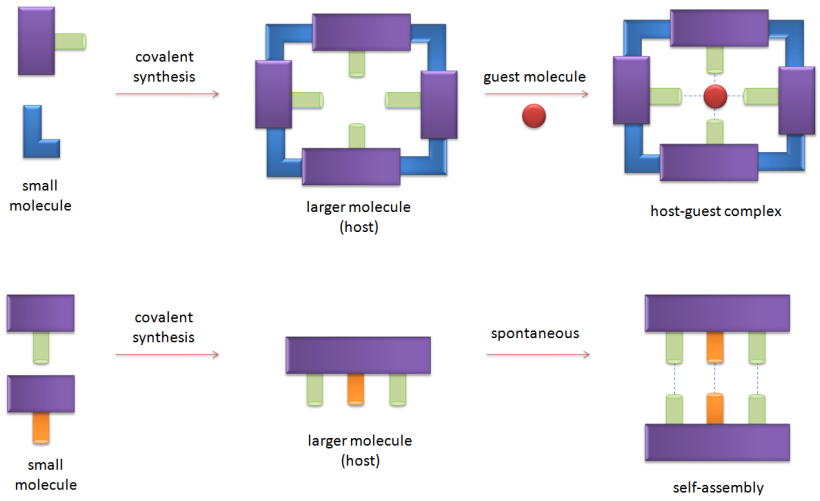

Figure 1.2: *The two broad categories of supramolecular chemistry: host-guest chemistry and self-assembly. Reprinted from Tiwari et al.*[30].

Molecular self-assembly is omnipresent in biological systems (where the most famous example is the lipid bilayer membrane in cells) and has become very important in nanotechnology where it is one of the most important strategies to make nanostructures from a bottom-up approach.[33–36]

1.1.2 Host-guest chemistry

In host-guest chemistry there is a very high binding selectivity of the guest(s) towards the host. The host and guest(s) need a compatible geometry and selective non-covalent interactions to get recognition. Successful molecular recognition depends on molecular complementarity regarding size, shape, chemical properties and functionalities of the host and the guest molecules. When a host can bind multiple guests, cooperativity can occur where the binding behavior of one binding site is influenced by another spatially separated binding site. Cooperativity can be positive or negative, depending whether the

occupation of the first binding site enhances or reduces the binding of the second guest. This means that the total binding strength will be higher than the sum of the individual interactions.

The strength of complexation in host-guest chemistry generally depends on different factors. A first determining factor is the size of both molecules. The size of the guest and the dimensions of the hosts cavity both need to be compatible to get sufficient interaction between the two compounds. A slight deviation from the optimal size will result in a weaker binding. Secondly, the type and number of interactions also influence the binding strength between the host and the guest. And finally, the same requirements as for self-assembly need to be considered to control the direction of the equilibrium (association over dissociation of the complex): a large number of non-covalent interactions, that are energetically more favorable than the competing interactions with the solvent; and can overcome the entropic disadvantage of the associated state over the dissociated state.
The most well-known examples in nature that exhibits host-guest interaction are enzymes and their substrates. Enzymes are the ideal host molecules and are constructed in such a way that they can undergo highly selective interaction with *one specific* substrate *via* various non-covalent interactions. These highly selective interactions allow enzymes to act as catalysts for various biochemical reactions with a high degree of efficiency and specificity.

For this project, the focus will be on host-guest chemistry, where the host is a macrocyclic cyclobis(paraquat-*p*-phenylene) structure and the guest is a 1,5-dialkoxynaphthalene derivative (Figure 1.3). Cyclobis(paraquat-*p*-phenylene) ($CBPQT^{4+}$) or "bluebox" thanks its name to its inventor J.F. Stoddart, who uses different colors to indicate specific molecular properties in his publications.[38] Since blue is the color he uses for electron-poor recognition units, the electron-accepting $CBPQT^{4+}$ looks essentially like a blue box.
The tetracationic electron accepting macrocycle $CBPQT^{4+}$ has been known in literature as a possible ring component for the construction of switchable donor-acceptor bistable catenanes and rotaxanes.[37] These molecular machines make it possible to process information at a molecular level *via* mechanical movements, in response to chemical or electrical energy, or light. $CBPQT^{4+}$ possesses a box-like structure with a well-defined electron poor cavity, which is lined with two electron-acceptor paraquat groups that are

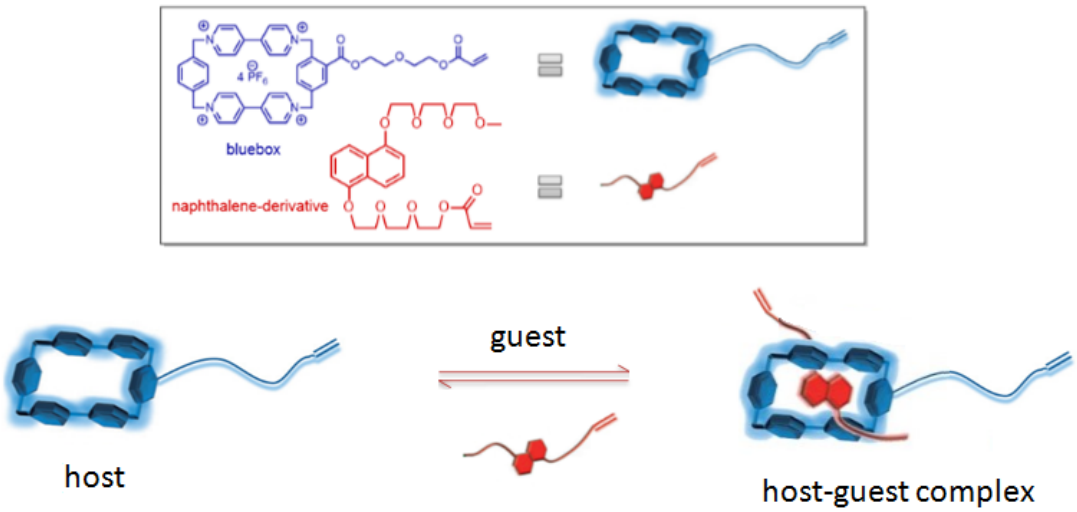

Figure 1.3: *Overview of the supramolecular host and guest molecules used in this project and the association equilibrium.*

separated by about 6.8 Å.[38] The distance, which perfectly matches the Van der Waals thickness of an aromatic ring, and the electron-accepting character make the cavity ideal for the inclusion of electron-rich aromatic subunits such as tetrathiafulvalene (TTF) and 1,5-dioxynaphthalene (DNP) derivatives.[39] The binding strength of the guest towards the bluebox not only depends on the characteristics of the donor, but also on the choice of counteranion for the bluebox. The π-electron density and the size of the π-system of the donor determine how well the guest fits into the cavity. For the choice of counteranion, both the nature and the concentration are examined in their influence on the association strength of the resulting host-guest complex. Andersen *et al.*[40] concluded that larger counteranions allow for the formation of stronger host-guest donor-acceptor complexes, because the larger size of the counteranions increases the distance between the $CBPQT^{4+}$ macrocycle and the negative charges of the counteranions. This causes the bluebox to become more naked and effectively a stronger π-electron acceptor.[40] Furthermore, the nature of the counteranion will determine if the bluebox is soluble in aqueous media (Br^-, Cl^-) or organic solvents (PF_6^-).

1.2 Stimuli-responsive polymers

A basic feature of biological systems is their responsiveness to changes in the local environment, which is responsible for the high adaptivity of living species. This adaptivity stems from the possibility to alter the non-covalent intermolecular bonds *via* a change in amount or nature of the interactions or a variation in conditions, such as temperature or concentration. Synthetic or modified biological materials that mimic this responsive behavior in a controlled and predictable fashion are of great interest for a wide range of applications[41] and are often called "smart" materials. By definition, supramolecular chemistry will always lead to the formation of "smart" materials.

So, "smart" polymers or stimuli-responsive polymer materials are polymers, that are able to reversibly respond to small changes in their physical and/or chemical environment (stimuli) through a large property change (response). Usually, they are classified according to the external stimuli to which they respond, such as temperature,[10,42–44] pH,[10,42,45,46] magnetic field,[47,48] ionic strength,[49,50] light[51,52] and ultrasound.[53,54] Smart polymers respond to these stimuli *via* a primary microscopic response mechanism on molecular level, which can be translated into a number of secondary macroscopic response types, allowing a visible readout. For instance, a change in temperature can lead to a coil-to-globule transition (the collapse of an initially solvated polymer chain ; primary response), which in turn leads to a phase separation (secondary response) of the solution. As in nature, the bulk response of the polymer is usually due to multiple cooperative interactions, such as progressive ionization or loss of hydrogen bonding, that, although individually small, ultimately evoke a large structural change in the material when summed over the whole polymer.[55]

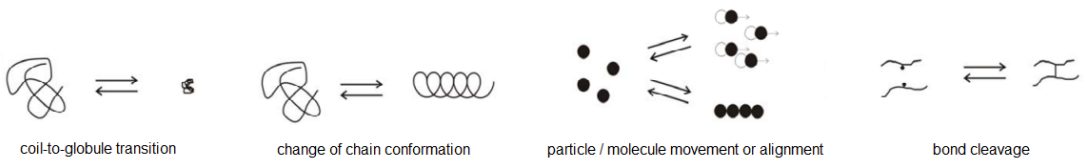

(a) *Primary response mechanisms in which the coil-to-globule transition is the most important. Incorporating acid-labile moieties in a copolymer chain or between drug molecules and copolymer nanostructures, can lead to release of the drug molecule via a pH-triggered bond cleavage.*[56]

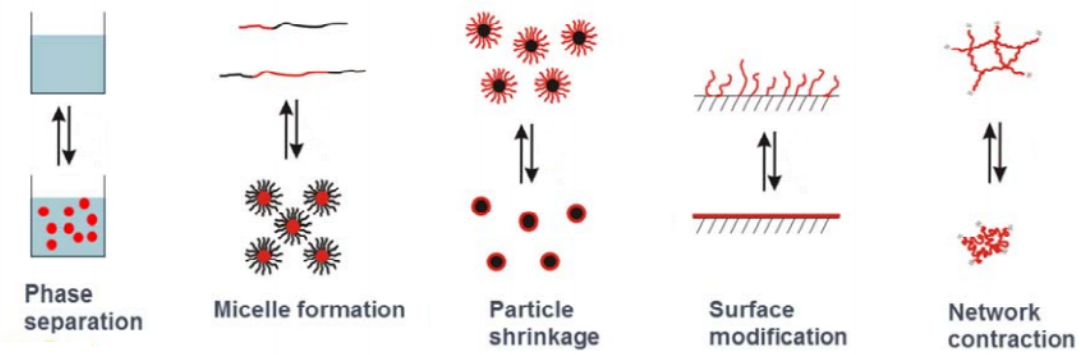

(b) *Possible secondary response mechanisms that follow a coil-to-globule transition.*

Figure 1.4: *Primary and secondary response mechanisms.*

When a "smart" material is exposed to a change in environment, it can initially counter this change *via* a primary response mechanism, which include coil-to-globule transitions,[57–60] change in chain conformation,[61–63] particle or molecule movement or alignment[64,65] and bond cleavage.[12,56,66] Since coil-to-globule transitions are the most important for this project, possible secondary response mechanisms that follow this primary response type are shown in Figure 1.4b and include phase separation, gelation,[67] micelle formation,[68] particle shrinkage, color change[69] and network contraction. The type of response mechanism that will occur is dependent on the polymer structure.

Hence, stimuli-responsive materials can adapt to the surrounding environment, regulate transport of ions and molecules or convert (bio)chemical signals into optical, electrical, thermal and mechanical signals, and *vice versa*.[41] This makes them extremely effective in (biomedical) applications such as drug delivery, medical diagnostics and imaging, tissue engineering and biosensing.

"Smart" materials that are of special interest are the ones that can undergo conformational or chemical changes in response to variations in temperature and/or pH. In the context of this project, only thermoresponsive materials will be discussed in further detail.

1.2.1 Thermoresponsive polymers

Among the various applicable stimuli, temperature is on of the most extensively exploited in the field of "smart" polymers. This is mainly because of their high applicability in the biomedical sector, surface modification, nanotechnology and catalysis.[70,71]

When a change in temperature induces a phase separation of a polymer solution, it is possible to determine the exact temperature(s) where phase separation takes place. This is called the cloud point temperature (T_{CP}), which depends on the concentration of the solution. If the different T_{CP}'s at different concentrations are measured, a phase diagram can be produced from which the lower and/or upper critical solution temperatures can be derived. The lower and upper critical solution temperature (LCST and UCST) are respectively defined as the critical temperature below or above which a mixture is miscible. Hence, the minimum and maximum phase separation temperatures in the phase diagrams of Figure 1.5, respectively. If both the LCST and UCST are present, they will give rise to a miscibility gap which is observed at temperatures below the UCST and above the LCST and indicates the region where at least two phases are coexisting. This means that below the LCST and above the UCST, a single phase exists for all compositions. The LCST and UCST values are both dependent upon the pressure and molar-mass distributions of the constituent polymer(s).

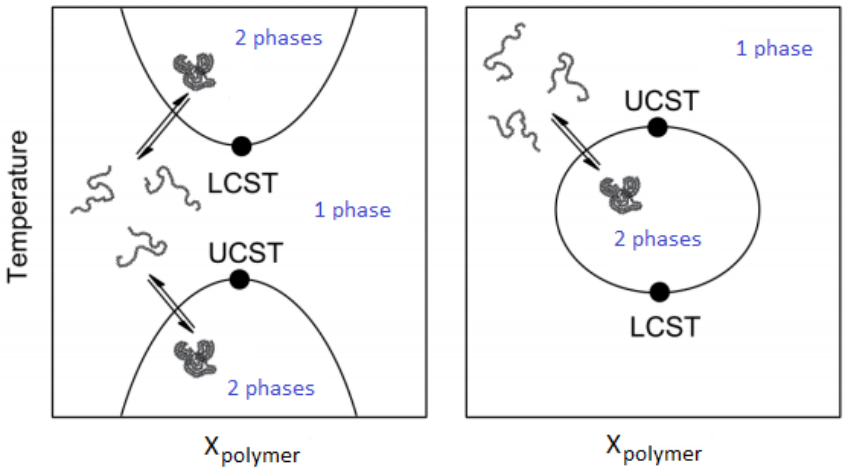

Figure 1.5: *Isobaric phase diagrams of a polymer in solution exhibiting LCST and UCST behavior. Reprinted from Seuring et al.*[72].

The first reported and most studied thermoresponsive polymer in aqueous solution is poly(*N*-isopropylacrylamide) (PNIPAM) which exhibits LCST behavior.[73–77] The polymer is water soluble, possesses a good biocompatibility and has an LCST value around 32°C, which is close to body temperature making it very interesting to be used in biomedical applications.[70] Furthermore, the LCST value is almost independent of the concentration, pH and salt concentration, leading to a robust phase transition. The LCST transition in water, which is usually the solvent in biomedical applications, is entropy driven, abrupt and is dependent on the hydrophilic-hydrophobic balance of the polymer, end-groups, polymer chain length, pH and salt concentration. For instance, a lower transition temperature is achieved with longer polymer chains because of the increased amount of polymer-polymer interactions.[78]

PNIPAM consists of hydrophilic parts, that undergo hydrogen bonding with the bulk water to keep the polymer soluble, and hydrophobic side chains that are mostly shielded from the surrounding water. When the temperature exceeds the T_{CP}, the entropy loss is no longer compensated by the enthalpy gain any more, which causes the hydrogen bonds to break up, the hydrating water to be released in the bulk water and phase separation to occur. Modifications of the polymer such as copolymerization[79] or post polymerization modifications[80,81] can be used to tune the transition temperature by adjusting the hydrophilic/hydrophobic balance of the polymer.

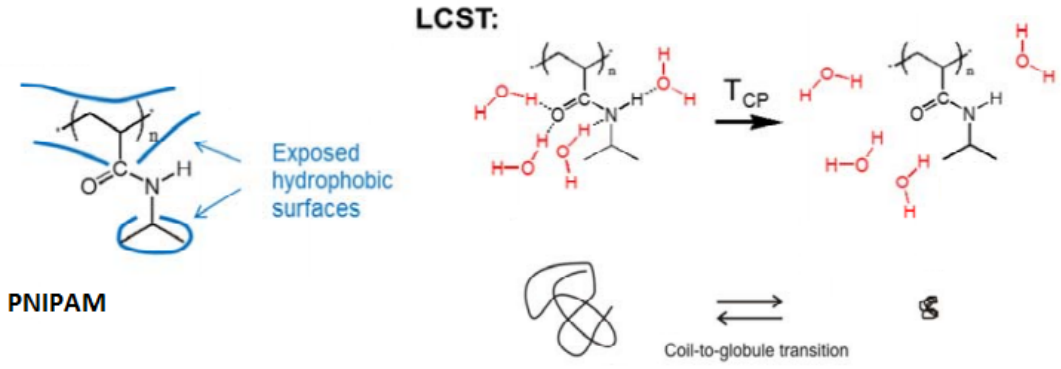

Figure 1.6: *LCST transition of PNIPAM in aqueous environment.*[82]

Apart from PNIPAM, other well-known LCST polymers including poly(*N,N*-diethylacrylamide) (PDEAAm),[83] poly(2-(*N,N*-dimethylamino)ethyl methacrylate) (PDMAEMA),[84] poly(2-oxazoline)s (POx)[85] and poly(oligo(ethyleneglycol)methylether methacrylate)s

(POEGMAs)[86] have also been widely studied and have found various applications as "smart" materials. Polymer solutions that exhibit UCST behavior undergo phase separation below a certain temperature, driven by strong enthalpic interchain interactions. Examples include polybetaines,[87] poly(methacrylamide) (PMAm),[88] poly(allylurea) (PU),[89] poly(2-dimethyl(methacryloxyethyl)ammoniumpropane sulfonate) (PDMAPS-MA)[90] and poly(*N*-acryloylglycinamide) (PNAGA).[91] A third class of thermoresponsive polymer solutions exhibit both LCST and UCST behavior. This comprises partially protonated PDMAEMA + $K_3[Co(CN)_6]$,[92] poly(ethylene oxide) (PEO),[93] poly(vinylmethylether) (PVME)[94] and poly(2-hydroxyethylmethacrylate) (PHEMA).[95]

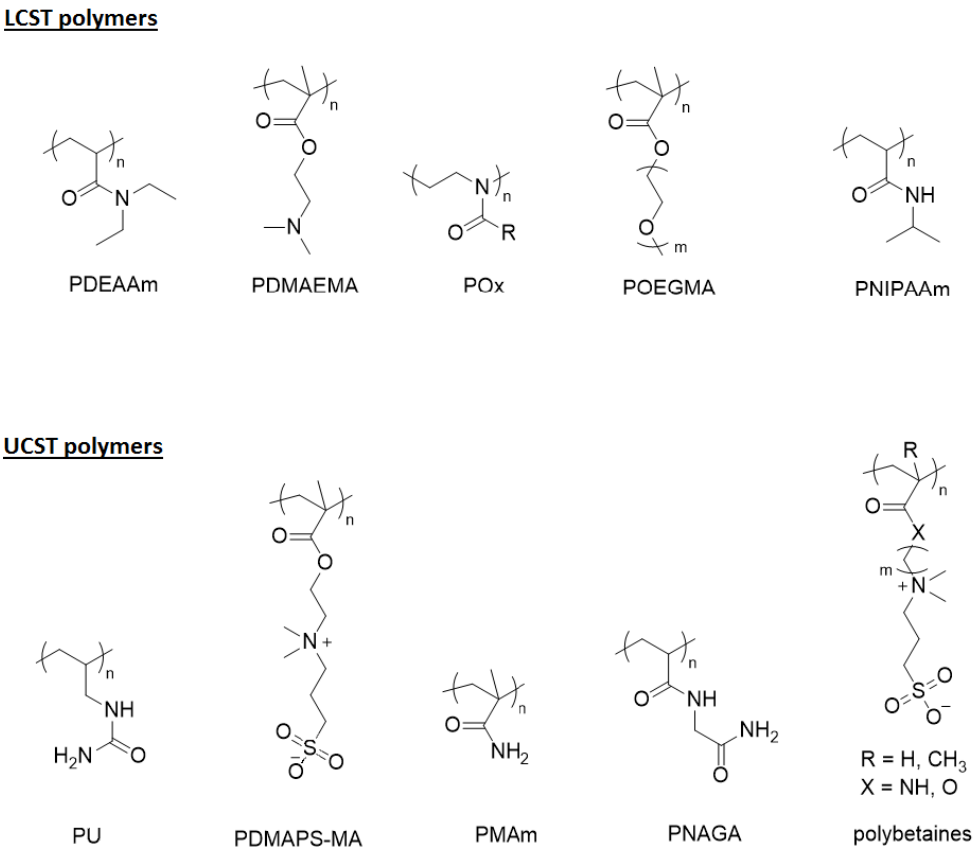

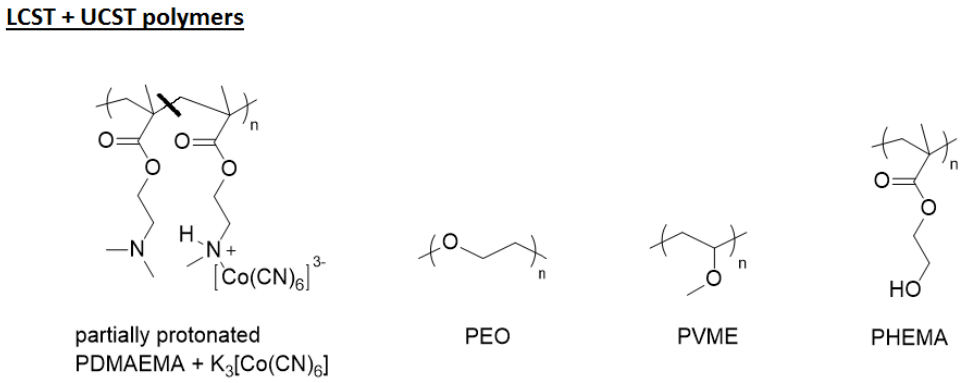

Figure 1.7: *Different examples of polymers that exhibit LCST, UCST or LCST and UCST behavior.*

1.3 Thermal memory function

Supramolecular thermometers or thermoresponsive polymers can exhibit a memory function for the thermal history of the solution, in case the phase transition shows significant hysteresis.[96–98] This means that the transition temperature will be different depending on the history of the solution. If the solution is being cooled down, the internal state of the polymer solution will be different than when the solution is heated, leading to a difference in transition temperature. The occurrence of hysteresis of the phase transition is not so common and especially a large hysteresis is exceptional.

By using a combination of static and dynamic laser scattering, Cheng *et al.*[99] revealed that the rather minor hysteresis of PNIPAM chains in water can be attributed to the additional hydrogen bonds formed between the carbonyl and amide groups in the collapsed state. These hydrogen bonds act as physical "cross-linking" points to make the chain aggregates behave like a "gel" and delay the chain dissociation. During the heating cycle of PNIPAM, the hydrogen bonds between the amide and the water dissociate and intrachain contraction occurs before interchain association. As shown in Figure 1.8,[77] the aggregates undergo an uneven swelling from the outside to the inside and a delayed chain dissociation is observed upon cooling. It is only at temperatures several degrees below the T_{CP} that complete chain dissociation occurs, at which water becomes a good solvent. During the heating cycle, the formation of aggregates occurs more uniform and only during interchain association. This leads to a sharp transition when heated and a broad hysteresis when cooled.

However, the observed hysteresis of PNIPAM is too small to result in a useful thermal memory. Therefore, supramolecular thermometers have been developed by our group by combining a thermoresponsive polymer with supramolecular host-guest chemistry. Complex formation allows for the formation of a kinetically trapped state, which results in a larger thermal memory function (hysteresis) of these thermometers. This makes them more suitable to be used in applications.[96,97]

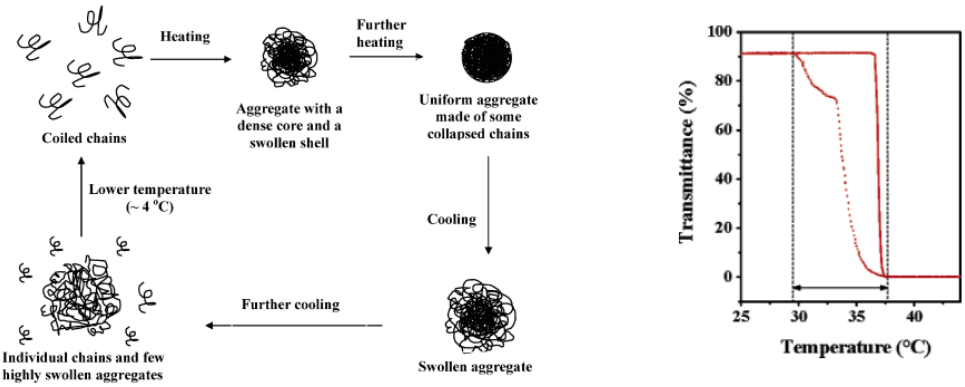

Figure 1.8: *Thermal memory function in PNIPAM. Left: schematic difference in chain dissocation and association during one heating-and-cooling cycle.*[99] *Right: plot of transmittance as function of the temperature measured for an aqueous solution of PNIPAM. The solid line is the heating cycle and the doted line is the cooling cycle.*[77]

1.4 Polymerization techniques for PNIPAM

Since PNIPAM is one of the most studied polymers in terms of thermoresponsive behavior and will be the polymer used in this project, suitable polymerization techniques to synthesize PNIPAM are searched. One of the most applied techniques is controlled radical polymerization by reversible addition-fragmentation chain transfer (RAFT).[100,101] Therefore, a brief introduction will be given on controlled radical polymerizations in general.

Controlled radical polymerization (CRP)[102] is a type of free radical polymerization (Figure 1.9) where the termination and transfer reactions are minimized, while maintaining a high enough propagation rate. It usually shows fast initiation with respect to propagation, resulting in a very narrow molecular weight distribution of the final polymer. CRP reactions are desired because of their control over the final properties of the poly-

mer such as molecular weight, molecular weight distribution (dispersity, Đ), end-group functionality and composition. Controlled radical polymerizations are often also called living radical polymerizations (LRP) and while both terms are often used interchangeable, a slight difference exists between both techniques. LRP reactions are completely living, meaning that they show a complete lack of chain transfer and termination reactions during the polymerization, whereas CRP does exhibit these type of reactions although in a suppressed way. Because the termination cannot be completely excluded, it is fundamentally impossible to get a completely living radical polymerization.[103]

During free radical polymerization, radicals are produced using heat- or light-sensitive radical initiators (e.g. benzoyl peroxide (BPO), azobisisobutyronitrile (AIBN)), which react with monomers to form a propagating chain (initiation). This active chain now possesses a radical that can react with other monomers to give a growing polymer chain (propagation) or react with another active chain to give an inactive dead chain (termination). Generally, the initiation is slow compared to the propagation and the produced radicals will propagate and terminate quickly. This means that active radicals will be formed at different times during the reaction, which results in a broader dispersity. Therefore, CRPs will slow down the rate of propagation, making this the rate determining step. This results in a more simultaneous formation of the active radicals, leading to a more monodisperse polymer. Chain transfer reactions can also occur and will induce a substantial decrease in the average molecular weight of the final polymer and will influence the structure, thus influencing the final properties of the polymer. In these reactions, the active center of a growing polymer chain gets transferred to another polymer chain (leading to branching), a monomer, the solvent (e.g. CCl_4) or a specially added chain transfer agent (CTA) to get control of the final molecular weight.

Making the propagation the rate determining step and ensuring the minimization of termination and transfer reactions can be achieved by keeping the active radicals at a low concentration, relying on the fact that the propagation has a first order relationship to the concentration of propagating radicals ($[P^*]$) and termination has a second order relationship ($[P^*]^2$). This can be done in several ways. One of the possibilities is a slow initiation of the radical initiator which keeps the radical concentration low, but gives no control over the dispersity and molecular weight of the final polymer. Another way is creating a dynamic equilibrium between the active propagating radicals (active species)

and inactive radicals (dormant species). Figure 1.10 illustrates three possible methods how to achieve a controlled radical polymerization.[103]

The first system is based on the deactivation of the growing polymer chains by using relatively stable, persistent radicals X^* (e.g. the nitroxide compound TEMPO in the NMP process). Normally this would be considered as a termination step, but due to the reversibility of this reaction, a repeated reversible coupling of the nitroxide to the growing polymer chain end occurs and termination reactions by combination of two active polymer chains get suppressed. In the second system, the deactivation proceeds *via* interaction with a species that has an even number of electrons to form a more stable, persistent radical. In the first two systems, the equilibrium is strongly shifted to the side of the dormant species allowing an adequate reduction of the concentration of the growing radicals. The third system consists of the so called *degenerative transfer process* where conventional initiators such as BPO can be used. The propagating chain radical can react with a monomer (propagation) or with a transfer reagent RX (where R resembles the dormant species and X is usually iodine) to create the inactive radical chain. Effective degenerative transfer is achieved if the exchange between the propagating radical and RX is faster than the propagation.

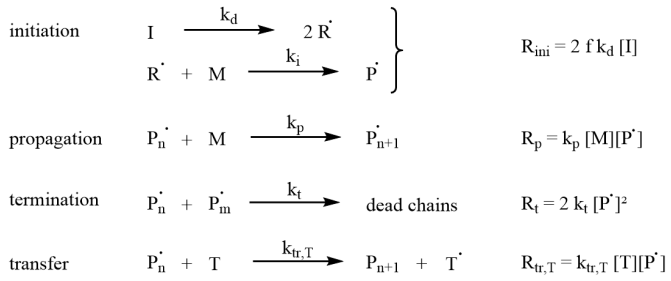

Figure 1.9: *General overview of the kinetics of a radical polymerization process.*

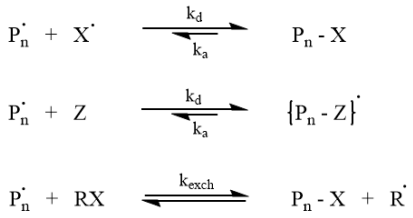

Figure 1.10: *Possibilities of dynamic equilibrium between active and dormant species. The deactivation process of the propagating radicals should be fast enough to be able to synthesize polymers in a controlled way.*

Other advantages of CRP include the broad range of molecular weights that can be obtained and the wide variety of monomers that can be used.
There are three fundamental types of controlled radical polymerizations that are commonly used in polymer synthesis: atom transfer radical polymerization (ATRP), reversible addition-fragmentation chain transfer (RAFT) polymerization and nitroxide mediated polymerization (NMP). A short introduction of each type is given.

1.4.1 ATRP

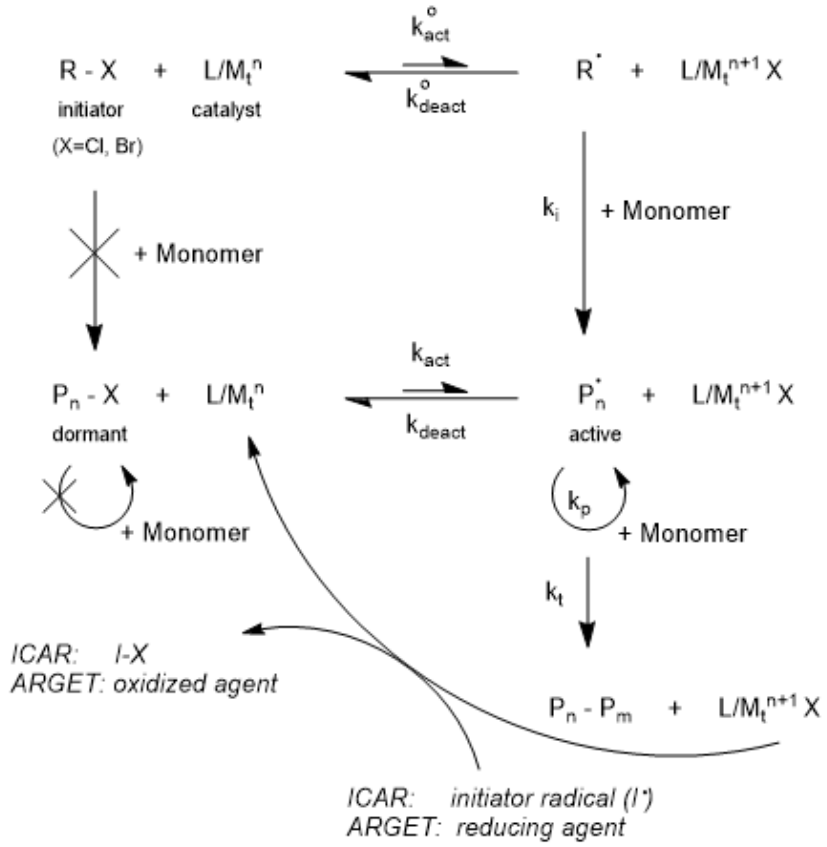

Figure 1.11: *Reaction mechanism of ATRP. The catalyst consists of a metal (mostly Cu(I)) with ligands, which can be regenerated from Cu(II), resulting from unavoidable termination reactions, using ICAR ATRP or ARGET ATRP.*

ATRP is one of the most successful methods to perform controlled polymerizations of an extensive number of monomers. Moreover, a good control is possible over the chain structure, composition and functionalities. This results in the preparation of well-defined end group-functionalized polymers and a large variety in homopolymers, block copolymers,

graft polymers and star-shaped polymers. One of the drawbacks of traditional ATRP is the use of a large amount of copper catalyst that can undergo oxidation and lead to discolorations in the final material. To obtain pure and colorless products, the catalyst needs to be removed *via* an extra purification step. To make things easier, new techniques such as ICAR ATRP (*i*nitiators for *c*ontinuous *a*ctivator *r*egeneration) and ARGET ATRP (*a*ctivators *r*e*g*enerated by *e*lectron *t*ransfer) are developed that recycle the catalyst internally and therefore only require ppm-amounts of the catalyst. This results in a shorter time to produce pure, colorless products.

1.4.2 NMP

The NMP process is a controlled radical polymerization that uses stable nitroxide compounds such as TEMPO ((2,2,6,6-tetramethylpiperidin-1-yl)oxyl) to assist in the reversible active/dormant equilibrium. The absence of metals in this process is one big advantage over the ATRP process. Drawbacks include the usage of high temperatures and the limited range of monomers that can be polymerized. NMP is mostly limited to styrene, acrylate and acrylamide derivatives.

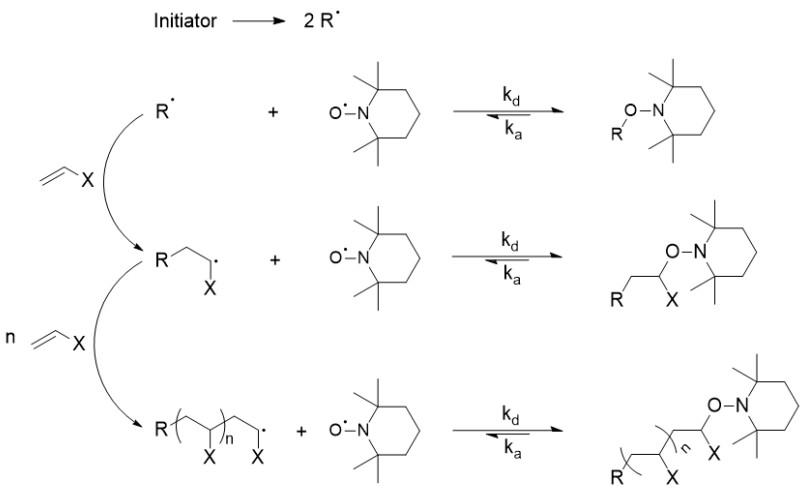

Figure 1.12: *Nitroxide Mediated Polymerization (NMP) with TEMPO as the nitroxide compound.*

1.4.3 RAFT

RAFT polymerization is a controlled radical polymerization technique that is performed in the presence of RAFT-agents where the dynamic equilibrium between the active and dormant species consists of a series of reversible addition-fragmentation steps (Figure 1.13). This allows a constant altering of the radical between different chains, leading to an alternating growth of all chains. The RAFT-agents (Figure 1.14) are chosen with care so that the exchange between the active and the dormant species occurs fast in comparison with the propagation. This gives rise to polymers with a narrow Đ. RAFT polymerizations where the employed RAFT-agents are xanthates, are also often termed MADIX polymerizations (*ma*cromolecular *d*esign *via i*nterchange of *x*anthates).[104]

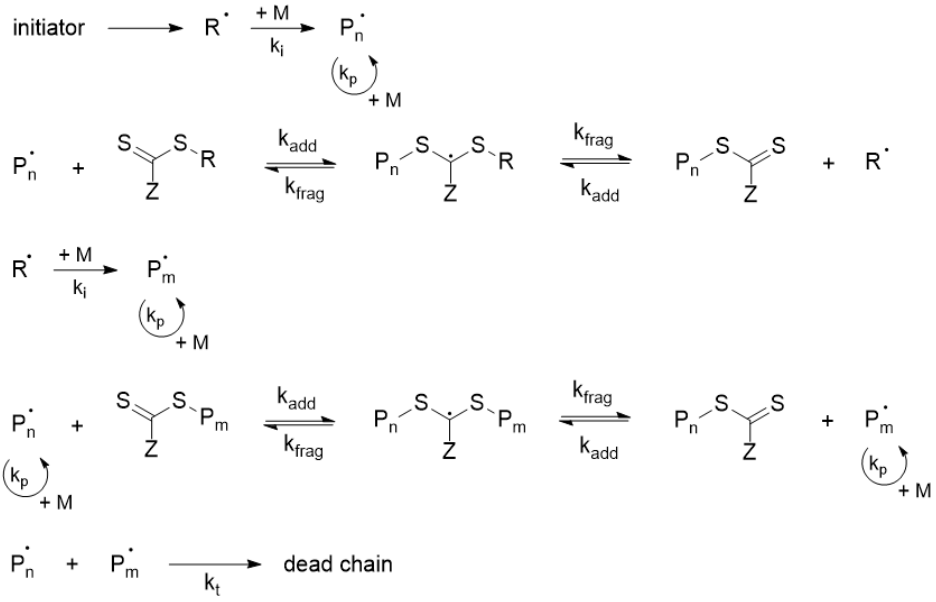

Figure 1.13: *Addition-fragmentation steps in the RAFT process.*

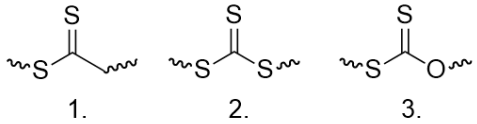

Figure 1.14: *RAFT-agents: 1. dithiocarbonates, 2. trithiocarbonates, 3. MADIX agents.*

Compared to ATRP, a larger range of polymers and more complex architectures[105] can be obtained by RAFT polymerization, but the limited large-scale commercial availability,

color and smell of the RAFT-agents limits its utilization.

Depending on the desired final properties of the polymer, a different CRP process might be advised, as is summarized in Figure 1.15.

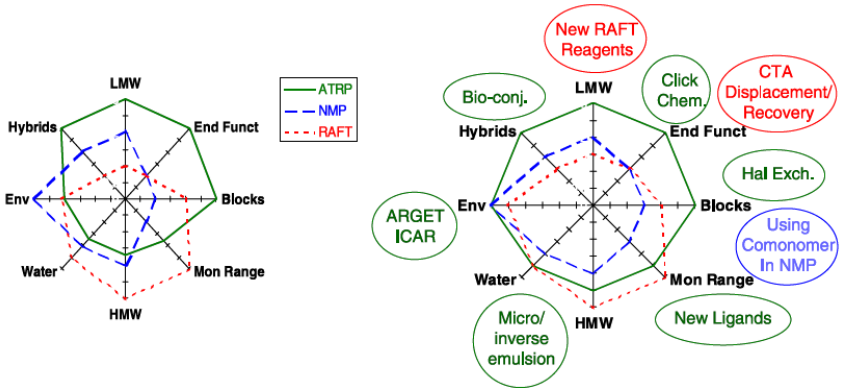

Figure 1.15: *Comparative advantages of the different CRP processes in the areas related to the synthesis of high molecular weight polymers (HMW), low molecular weight polymers (LMW), end functional polymers (End Funct), block copolymers (Blocks), range of polymerizable monomers (Mon Range), synthesis of various hybrid materials (Hybrids), environmental issues (Env) and polymerization in aqueous media (Water). The left side is a comparison from 2002,[106] while the right side is an updated situation as of 2006. Reprinted from Braunecker et al.[107].*

1.5 Hydrogels

Hydrogels are hydrophilic natural or synthetic polymer networks that can absorb large quantities of water without dissolving. This unique ability arises from the fact that the polymer backbone contains hydrophilic functional groups, which allow the hydrogel to absorb water, while the presence of crosslinks between network chains prevents the hydrogel from dissolution. The swelling capacity of the gel is determined by the nature of the polymer chains and the crosslinking density. A higher crosslinking density leads to a less stretchable polymer network and therefore a lower maximum swelling capacity.

Hydrogels can be classified in different ways such as classification based on source (natural or synthetic polymers), polymeric composition (homopolymeric, copolymeric or multipolymer hydrogels), configuration (amorphous, semicrystalline or crystalline) or the most useful one in terms of applications: classification based on type of crosslinking.[108] If the internal network structure results from molecular entanglements and/or secondary forces,

physical or reversible hydrogels are formed. These non-permanent hydrogels are driven by molecular self-assembly and hence do not need any crosslinking agents to get gel formation. Due to their dynamic nature, physical hydrogel materials exhibit shear-thinning and self-healing properties, which are desirable characteristics in a range of "smart" material applications.[109] However, the dynamic nature of the crosslinks also limits the maximal strength of such hydrogels.

Permanent or chemical hydrogels consist of covalently crosslinked networks and make use of a crosslinker (e.g. ethylene glycol dimethacrylate, EGDMA) to obtain their permanent network structure. Compared to physical hydrogels, these chemical networks are stronger because of their covalent linkage, but the absence of any dynamic character causes the hydrogels to be less flexible. The equilibrium swelling level in an aqueous solution of such covalent hydrogels is dependent on the crosslink density which can be quantified with M_c, a parameter to approximate the average molecular weight between the crosslinks of the hydrogel.[110] Chemical hydrogels are mostly used in applications that require though and stable hydrogels.[109]

Due to the difference in type of crosslinking, "smart" chemical hydrogels can only be obtained when they are based on "smart" polymers, while physical hydrogels possess a reversible nature by default. Both physical hydrogels and chemical hydrogels can exhibit defects in their network structure, influencing the elastic properties and swelling behavior of the gel.[110] In physical gels, the main defects comprise clusters of molecular entanglements or hydrophobically- or ionically-associated domains, which will create inhomogeneities, and free chain ends or chain loops, which do not contribute to the elasticity of the network. Chemical hydrogels will also exhibit reduced elasticity as a result of free chain ends or chain loops. Furthermore, due to hydrophobic aggregation of crosslinking agents, chemical hydrogels can contain regions of low water swelling and high crosslink density (clusters) that are dispersed within regions of high swelling and low crosslink density. This will lead to a difference in swelling capacity that has to be considered in the design of the hydrogel.[111]

A common use for hydrogels is as scaffolds in tissue engineering because of their structural similarity to the macromolecular-based components in the body, a similar degree of flexibility to the natural tissue (due to their significant water content) and their biocompatibility.[112,113]

1.6 Goal of the thesis

The overall goal of this project is to develop a ((re)programmable) polymeric thermometer that memorizes the thermal history of the solution and provides an associated visible readout. The thermal memory results from the employment of a thermoresponsive polymer that shows significant hysteresis in the phase transition. Hence, the internal state of the polymer solution can "remember" the previous temperature state or thermal history (Section 1.3). The visible readout is a result of the (de)complexation process that occurs during this transition. The host-guest complex formation is associated with a color change of the solution from colorless to purple.

For this project, a thermoresponsive polymer (PNIPAM) will be employed that will be functionalized with 1,5-dialkoxynaphthalene guest moieties and cyclobis(paraquat-*p*-phenylene) ($CBPQT^{4+}$) host moieties as pendants to enlarge the thermal memory window of the final polymer and provide a visible readout. Synthesis of the supramolecular host and guest monomers is followed by copolymerization with NIPAM, hydrogel formation by including a bifunctional monomer as crosslinker and characterization of the obtained structures (Figure 1.16).

Soluble polymeric thermometers have already conceptually been developed by our research group,[96] based on PNIPAM with dangling dialkoxynaphthalene guests and the supramolecular association with $CBPQT^{4+}$. However, these thermometers undergo macroscopic phase separation which strongly limits their applicability. Therefore, this project aims to develop a second generation polymeric *hydrogel* sensor with an analogous memory function as discussed in Section 1.3, which will give rise to more widely applicable sensors. Hence, the focus will be on the synthesis, characterization and copolymerization of the functional supramolecular building blocks and the thermoresponsive PNIPAM. The characterization and examination of its stimuli-responsive behavior will be studied once the hydrogel is formed.

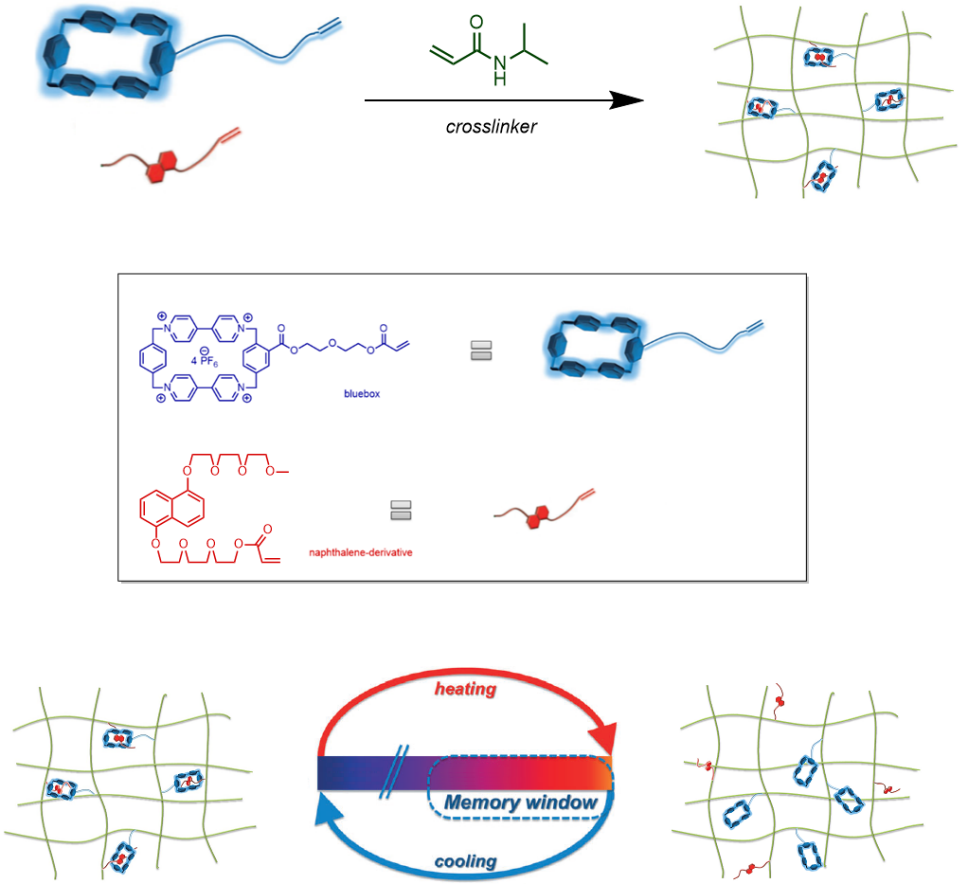

Figure 1.16: *The goal of this project is creating a NIPAM hydrogel that contains small amounts of supramolecular host and guest molecules, as thermometers with memory function.*

2 Results and discussion

The aim of this research project is the development of a hydrogel that consists of PNIPAM and some small amounts of supramolecular host and guest moieties to act as a thermometer with memory function. In a first step, these supramolecular host and guest compounds are synthesized and provided with a polymerizable double bond. Next, a copolymerization of these compounds with NIPAM should be tested and characterized. In a further stadium, hydrogels should be prepared, and their characteristics and stimuli-responsive behavior should be investigated systematically.

2.1 Synthesis of monomers

The practical work starts by synthesizing cyclobis(paraquat-*p*-phenylene) ($CBPQT^{4+}$) and 1,5-dialkoxynaphthalene derivatives, which will act as the supramolecular host and guest moieties in the polymer, respectively.

For the synthesis of the host molecule, which is a cyclobis(paraquat-*p*-phenylene) derivative **6**, three methods have been reported to combine two components into a final ring structure. The first reported method makes use of an elevated temperature to ensure ring closure.[38] The other two methods apply a template molecule (and high pressure) to combine components **A** and **B** of the host molecule at room temperature (Scheme 2.1).[114] Using a template molecule significantly increase the yield of the assembly, and since a derivative of the synthesized guest molecule is available to act as a suitable template molecule, assembly of both compounds is achieved in the presence of a template molecule at room temperature. This means that first the synthesis of the components **A** and **B** is required. Compound **A** will be produced in a two-step pathway as seen in Scheme 2.2a. First, 4,4'-dipyridyl **1** and α,α-dibromo-*p*-xylene **2** will be combined to produce the water soluble bis(pyridinium).$2Br^-$ **3**. In the second step, counterion exchange ($Br^- \longrightarrow PF_6^-$)

will be performed to change the solubility of the bis(pyridinium) from water to organic solvents.

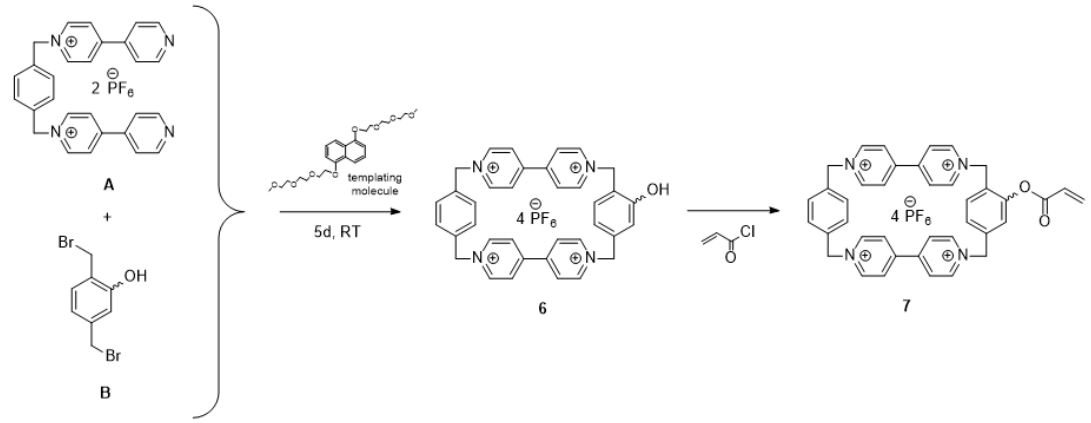

Scheme 2.1: *The synthetic route for the preparation of the supramolecular host monomer.*

To produce component **B**, a synthesis pathway is proposed as shown in Scheme 2.2b. In the first step, the commercially available 2,5-dimethylbenzoic acid **4** will be brominated using NBS to give 2,5-bis(bromomethyl)benzoic acid **5**. The carboxylic acid is then modified to provide a linker, improving the flexibility of the bluebox within the hydrogel, making complexation easier. Compound **B1** will be synthesized by reacting the carboxylic acid **5** with diethylene glycol under a variety of reaction conditions. An alternative compound **B2** will be synthesized by reducing the carboxylic acid **5** to the corresponding alcohol, in the presence of DIBAL-H.

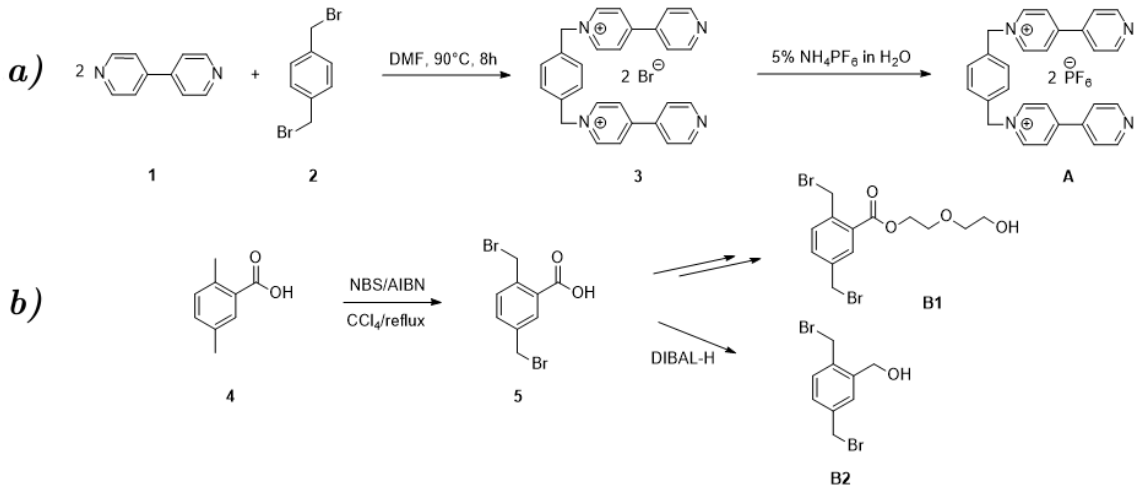

Scheme 2.2: *General synthesis routes for the preparation of compounds **A** and **B** of the supramolecular host molecule.*

If both compounds **A** and **B** are synthesized, a derivative of the supramolecular guest molecule will be used as a templating molecule to combine both compounds **A** and **B** into a functional bluebox **6**. Final reaction with acryloyl chloride will provide the functionalized monomer **7**, which is ready for polymerization (Scheme 2.1) .

For the preparation of the guest monomer (Scheme 2.3), a three-step process will be employed. A double alkylation of commercially available 1,5-dihydroxynaphthalene **8** will be performed with 2-(2-chloroethoxy)ethoxyethanol **9**, under basic conditions (K_2CO_3), to yield 1,5-bis[2-(2-(2-hydroxyethoxy)ethoxy)ethoxy]-naphthalene **10**.[115] Methylation of the diol under basic conditions (NaH) with iodomethane (MeI) will result in the mono-methylated diol **11**[51] which can be further reacted with acryloyl chloride to obtain a polymerizable guest moiety **12**.

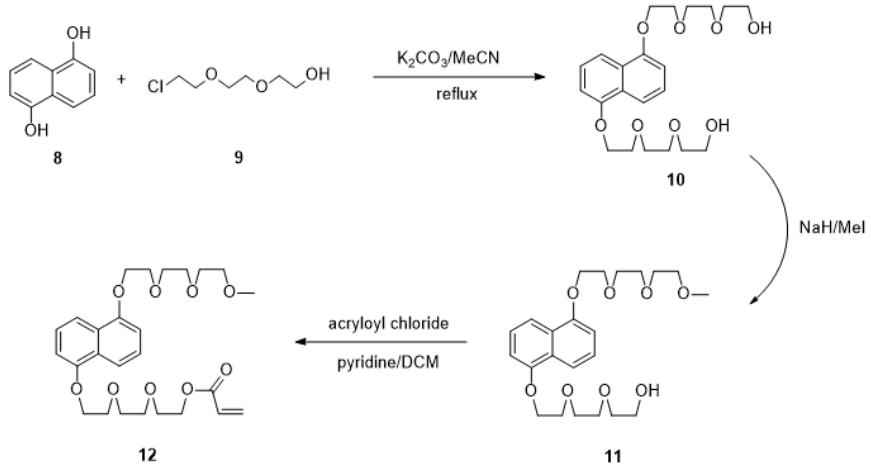

Scheme 2.3: *General synthesis route for the preparation of the supramolecular guest molecule.*

2.1.1 Synthesis of host

Synthesis of compound A: ***1,1'-(1,4-phenylenebis(methylene))bis(4,4'-pyridinium)bis(hexafluorophosphate)***

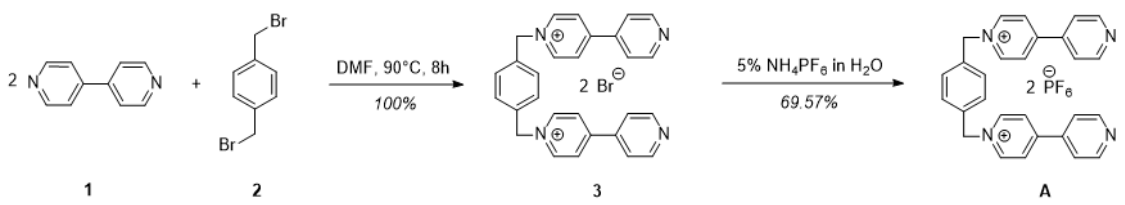

Scheme 2.4: *Synthesis of compound **A** using a two-step pathway.*

A solution of α,α-dibromo-*p*-xylene **2** in DMF was added dropwise to a solution of 4,4'-dipyridyl **1** in DMF to ensure that both sides of the dibromo-compound would react with the dipyridyl. Reacting for 8 hours in DMF at high temperature resulted in a light yellow solid that could be collected by filtration. The bis(pyridinium).2Br$^-$ **3** was dissolved in water, to which a saturated aqueous solution of NH_4PF_6 was added in excess. This allowed an interchange of all the Br^- ions for PF_6^- ions, resulting in the precipitation of bis(pyridinium).2PF_6^- **A** that could be collected by centrifugation. ^{1}H NMR spectroscopy confirmed the formation of the bis(pyridinium) **A**, which is ready for the templating reaction.

Synthesis of compound B1: *(ethylene glycol ether) 2,5-bis(bromomethyl)benzoate*

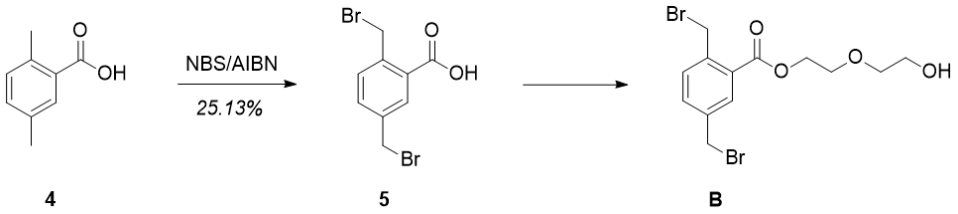

Scheme 2.5: *Synthesis of compound **B1** using a two-step pathway.*

Synthesis of compound **B1** proved to be more difficult, since most of the tested procedures did not yield the right component. Different methods were examined in the search for an operative procedure, as will be discussed below.

The initial radical bromination reaction of 2,5-dimethylbenzoic acid **4**, with AIBN as initiator, is based on the literature procedure of Ashton *et al.*[51]. To a solution of 2,5-dimethylbenzoic acid in CCl_4, NBS and a catalytic amount of AIBN were added. The suspension was refluxed under nitrogen for 4 hours, the solution cooled down to room temperature and the succinimide filtered off. Concentrating the filtrate led to a brown oil, which was dissolved in DCM and to which hexane was added. After standing in the refrigerator for 2 hours, a white solid precipitated out that was filtered off and dried under vacuum.[51] Following this exact reaction procedure did not yield the desired pure compound **5**. Therefore, extra purification steps were performed in an attempt to isolate the pure 2,5-bis(bromomethyl)benzoic acid **5**. The product was recrystallized from

toluene two times and once from hexane *via* vapor diffusion to a DCM solution (Figure 2.1). Because the volatility of DCM was too low, the precipitation process was repeated with chloroform.

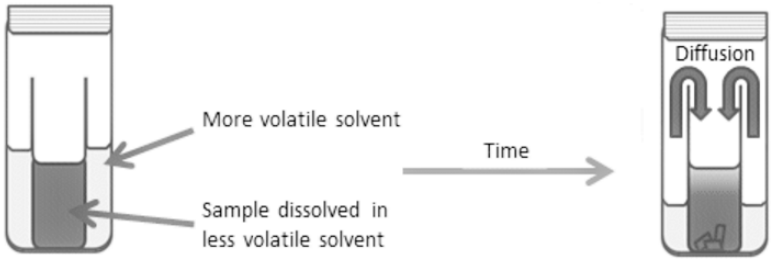

Figure 2.1: *Vapor diffusion: a recrystallization technique that allows a solvent of high volatility (e.g. hexane) to slowly diffuse into a sample of lower volatility (e.g. chloroform). Reprinted from reference[116].*

Analysis of the obtained product by ^{1}H NMR and LCMS revealed the presence of side products such as the mono-, tri- and tetrabrominated acids. Literature study suggested a possible isolation of these products *via* repetitive precipitations from chloroform in hexane.[117] Applying this technique to our mixture was successful for the separation of the mono- and tetrabrominated acids, but failed to separate the 2,5-bis(bromomethyl) benzoic acid **5** from the tribrominated acid **5.II** (Figure 2.2). The presence of these side products indicates that the reaction time was probably too long, leading to overbromination. Hence, the reaction was performed again under identical conditions, while being monitored using ^{1}H NMR spectroscopy. This allowed us to detect the approximate reaction time at which tribrominated acid was formed as a side product. ^{1}H NMR chemical shifts of possible side products formed in the synthesis of 2,5-bis(bromomethyl)benzoic acid **5** are shown in Table 2.1. Comparing the chemical shifts of compounds **5** and **5.II**, reveal distinctive differences between the two. Since the Ar(5)-C$\underline{\text{H}}$, Ar-H$_3$, Ar-H$_4$ and Ar-H$_6$ chemical shifts of compound **5.II** show a clear difference with the chemical shifts of the other compounds, these are used to monitor the formation of the tribrominated acid **5.II** during the reaction. ^{1}H NMR samples were taken after 2 and 3 hours reaction, and the resulting spectra are shown in Figure 2.3. Comparing both spectra reveals that the only clear differences appear around 8.28 ppm and 7.55 ppm. The appearance of these two signals after 3 hours reaction, can be used to verify the formation of tribrominated acid **5.II**. Therefore, the

reaction was terminated after 3 hours, forming only a small amount of side product that could still be removed by recrystallization.

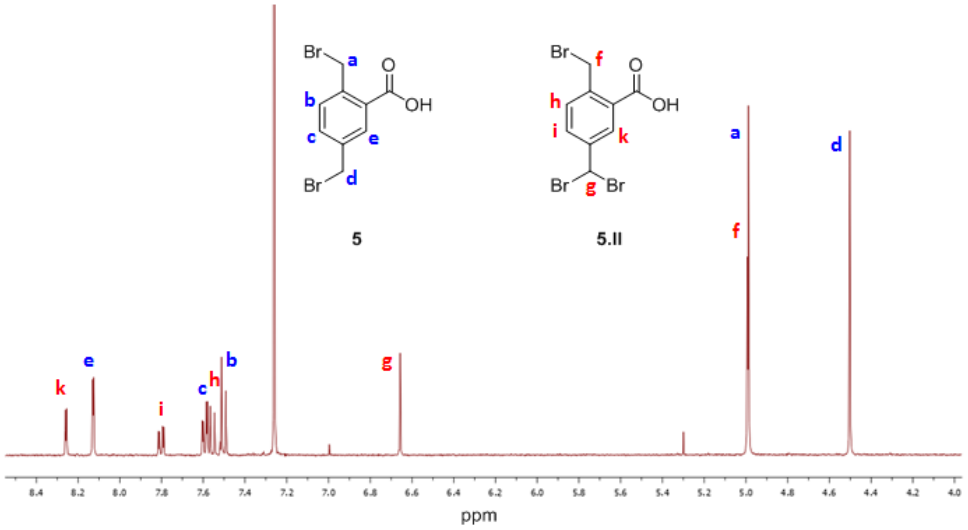

Figure 2.2: *Initial radical bromination reaction of 2,5-dimethylbenzoic acid with NBS for 4 hours refluxing. Purification steps are already performed to remove the mono- and tetrabrominated acids as side products.*

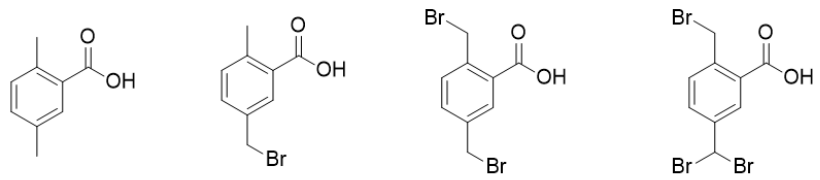

Compound	Ar(2)-C<u>H</u>	Ar(5)-C<u>H</u>	Ar-H_3	Ar-H_4	Ar-H_6
4	2.54 (CH_3)	2.29 (CH_3)	7.09 (d)	7.20 (d)	7.81 (s)
5.I	2.50 (CH_3)	4.57 (CH_2Br)	7.51 (d)	7.80 (dd)	7.92 (d)
5	4.99 (CH_2Br)	4.50 (CH_2Br)	7.50 (d)	7.61 (dd)	8.16 (d)
5.II	4.99 (CH_2Br)	6.64 ($CHBr_2$)	7.55 (d)	7.70 (dd)	8.27 (d)

Table 2.1: *^1H NMR chemical shifts (ppm) of the starting material **4** and possible byproducts (**5.I** and **5.II**) formed in the synthesis of 2,5-bis(bromomethyl)benzoic acid **5**.*[117]

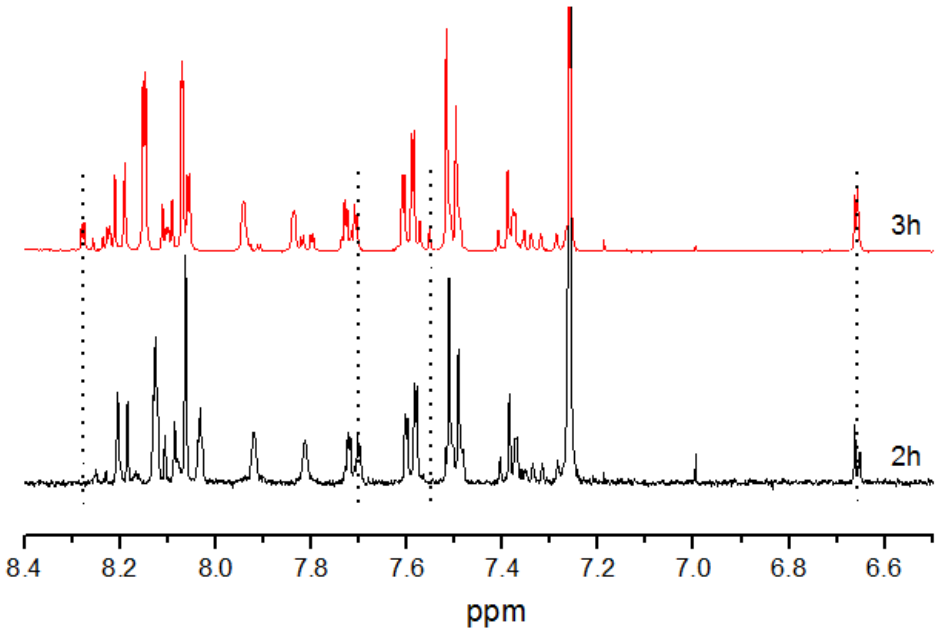

Figure 2.3: *Radical bromination reaction of 2,5-dimethylbenzoic acid with NBS: conversion after 2 hours and 3 hours refluxing.*

So, following the reaction with ^{1}H NMR spectroscopy revealed that a reaction time of 3 hours was sufficient to avoid the formation of any significant amounts of byproducts. The reaction was performed for three hours at a larger scale and was terminated by cooling to room temperature. After the reaction, the formed succinimide was filtered off under gravity and the solution was left to stand overnight upon which a white solid precipitated. The product was collected and purified by recrystallization from hexane *via* vapor diffusion to a chloroform solution. ^{1}H NMR spectroscopy and LCMS analysis confirmed the formation of the pure dibrominated acid **5**.

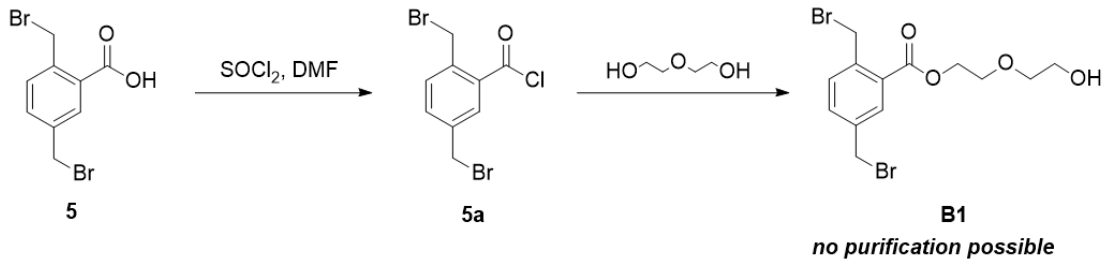

Scheme 2.6: *A first attempt to generate the desired compound* ***B1*** *via a benzoyl chloride* ***5a*** *intermediate.*

The next step consists of converting the carboxylic acid into an alcohol, with a linker

in between the bluebox and the polymerizable double bond that will be introduced onto the alcohol. In a first attempt, the 2,5-bis(bromomethyl)ben-zoic acid **5** is reacted with thionyl chloride under inert conditions to generate the benzoyl chloride **5a**.[51] This is then added dropwise to a solution of excess diethylene glycol in dry DCM. Continuing with the reaction procedure of Ashton *et al.*[51] results in the formation of an oil-like solid, in which the expected product was not detected by LCMS. Silica gel column chromatography, with DCM/hexane (10:5) as eluent, failed to separate the different fractions. Because of time limitations, no extensive attempts were made to find an effective purification technique.

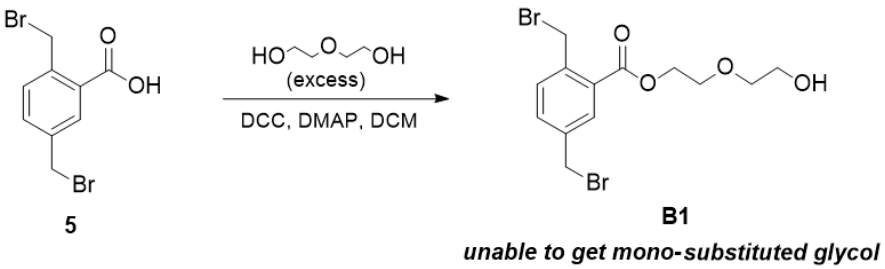

Scheme 2.7: *A second attempt to generate the desired compound **B1** via a DCC-coupling reaction.*

A second method for synthesizing the (ethylene glycol ether) 2,5-bis(bromomethyl)benzoate **B1** was performed by making use of a DCC coupling reaction.[118] The brominated acid **5**, an excess of diethylene glycol, *N,N'*-dicyclohexylcarbodiimide (DCC) and a catalytic amount of 4-dimethylaminopyridine (DMAP) in DCM was reacted overnight at room temperature under inert atmosphere. The DCC acts as an activator of the carboxylic acid so that the diethylene glycol can perform a nucleophilic attack on the carbonyl group. After an additional $3^{1/2}$ hours refluxing, the solution was allowed to cool to room temperature. The suspension was filtered, washed and concentrated, before being subjected to column chromatography. The diethylene glycol was present in large excess to the dibromide (25:1) in order to ensure the formation of the *mono*-substituted glycol. Silica gel flash column chromatography, with DCM/hexane (10:5) as eluent, revealed that only the di-substituted product was formed and a large amount of starting material was still present. To rule out coincidence, the reaction was repeated, but this did not change the outcome. A probable explanation stems from the difference in solubility of the different compounds. Since the solubility of the mono-substituted product **B1** is much better than the solubility of the

starting material **5**, a second coupling reaction could occur much faster, resulting in the di-substituted glycol.

In a third attempt, the monoesterification of the diethylene glycol was attempted in the presence of $Al_2O_3/MeSO_3H$ (AMA) and without the use of any solvents. Sharghi *et al.*[119] claims that the inexpensive reagent AMA is very effective and highly selective for the

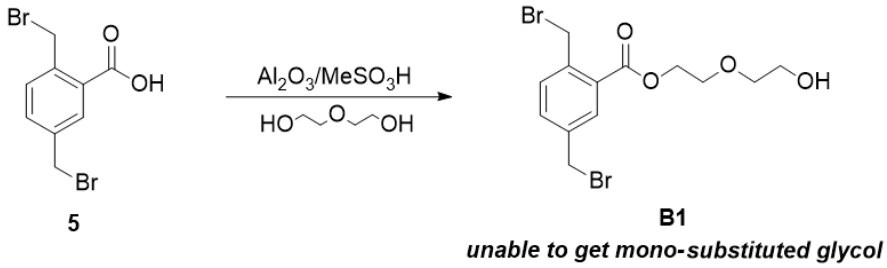

Scheme 2.8: *A third attempt to generate the desired compound **B1** via a monoesterification in the presence of AMA.*

monoesterification of diols in high yields. A mixture of $MeSO_3H$ and Al_2O_3 was prepared and the appropriate amounts of acid and diethylene glycol were added, successively. The mixture was stirred and heated at 80°C for one hour. Aqueous workup of the reaction should give the almost pure monoester product **B1**. Performing this reaction under these exact reaction conditions, with the use of a *brominated* acid as the only difference, did not yield the expected monoester product. Silica gel flash column chromatography and ^{1}H NMR spectroscopy revealed that the obtained mixture consists purely of the diester product and some unreacted starting material. Again, the reaction was repeated to rule out coincidence. The difference in solubility between the starting material **5** and the monoester product **B1** can again be adopted as a possible explanation for the failure of the reaction.

Synthesis of compound B2: *2,5-bis(bromomethyl)benzyl alcohol*

Since the radical bromination reaction did not work right away and purification was not possible, an alternative procedure was enforced based on the bromination of the ethyl-ester (Scheme 2.9). Here, the 2,5-dimethylbenzoic acid **4** was converted into the corresponding ester **4a** by esterification with ethanol, using sulfuric acid as a catalyst. Subjecting this to similar reaction conditions as before,[51] generates the ethyl 2,5-bis(bromomethyl)benzoate

4b. This can now be used to yield an alternative compound **B2** without a linker by reducing the benzoate **4b** to the corresponding alcohol **B2**.

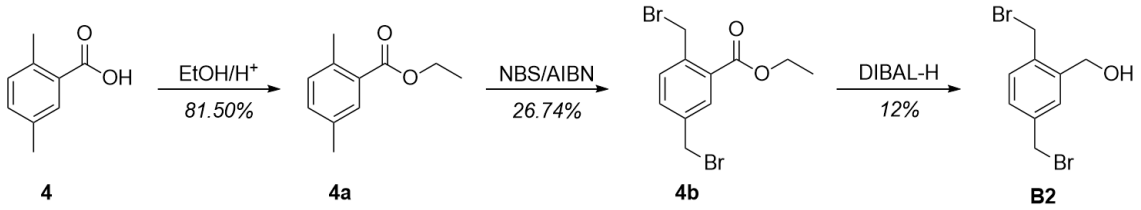

Scheme 2.9: *A final attempt to generate a suitable compound **B2** via reducing the previously synthesized 2,5-bis(bromomethyl)benzoate **4b** to the corresponding alcohol **B2**.*

Ethyl 2,5-bis(bromomethyl)benzoate **4b** is reacted with DIBAL-H at 0°C under inert atmosphere for three hours. Next, HCl is added until pH = 1 is reached, to reduce the formed aldehyde further to the corresponding alcohol **B2**. After aqueous workup, the formation of the pure alcohol **B2** was confirmed by NMR spectroscopy and LCMS analysis.

Synthesis of the polymerizable host molecule

Due to the lack of time and the unexpected difficulties that occurred during the synthesis of compound **B1**, the assembly of both components and the reaction with acryloyl chloride could not be carried out within the time frame of the master thesis.

2.1.2 Synthesis of guest

Synthesis of *1-(2-(2-(2-hydroxyethoxy)ethoxy)ethoxy)-5-(2-(2-(2-methoxyethoxy)ethoxy)ethoxy)naphthalene*

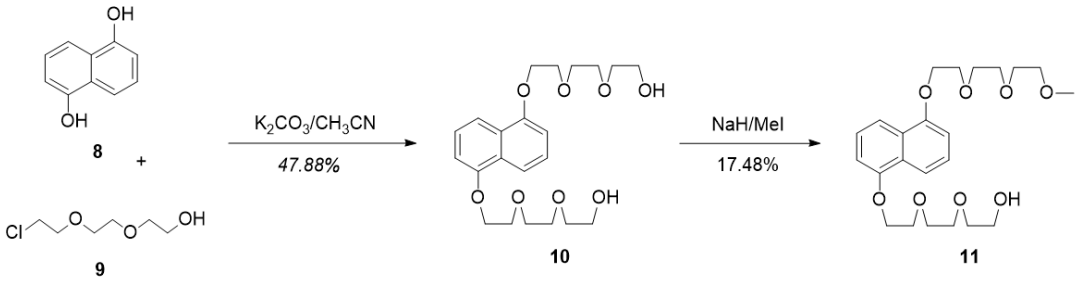

Scheme 2.10: *Synthesis of the single methylated guest molecule via a two-step pathway.*

The formation of the single methylated diol **11** was achieved in a two-step reaction. In the first step, a purple suspension of 1,5-dihydroxynaphthalene **8** and K_2CO_3 in MeCN was treated with a solution of 2-(2-chloroethoxy)ethoxyethanol **9** in MeCN and subsequently refluxed overnight to give a brown suspension. K_2CO_3 was present to neutralize the formed HCl. After filtration of the formed KCl and evaporation of the solvent, the dark brown oil was dissolved in DCM. Since the oil did not dissolve very well in the solvent, the amount of solvent was increased and the solution was left to stir for a few days. Next, the solution was washed with brine and water to remove any unreacted 2-(2-chloroethoxy)ethoxyethanol **9** and K_2CO_3, and a deep red-brown solution was obtained. Drying over $MgSO_4$ and removing most of the solvent over reduced pressure, resulted in a dark red-brown oil that was purified by column chromatography over silica. Spotting the reaction mixture on TLC revealed the presence of the starting material **8** and 1-hydroxy-5-(2-(2-(2-hydroxyethoxy)ethoxy)ethoxy)naphthalene (the compound where only one side is alkylated) in the mixture. This explains the rather low yield of the reaction, which can be resolved with a longer reaction time or a larger excess of **9**. A DCM/EtOH (30:1) mixture as eluent was used for column chromatography, resulting in a good separation of the different components. Since the first column did not give complete separation of the different compounds, a second purification was done by column chromatography (silica, DCM/EtOH, 30:1). ^{1}H NMR spectroscopy confirmed the formation of the pure 1,5-bis[2-(2-(2-hydroxyethoxy)ethoxy)ethoxy]-naphthalene **10**.
For the large scale synthesis of this compound, a slightly different purification technique was used. Since normal silica gel column chromatography failed to separate the large amount of crude product, a different stationary phase was used in an attempt to get a good separation. TLC analysis with neutral alumina (Al_2O_3) revealed a good separation for the mixture. The crude mixture was separated successfully on a neutral alumina column (DCM/EtOH, 30:1) in two batches.

In the second step, the conversion to the single methylated product **11** was achieved *via* reaction of the diol **10** with MeI under basic conditions (NaH), as described in the literature procedure[51]. After reacting for 24 hours under reflux, the solution was cooled and methanol was added to react with the excess of NaH. Aqueous workup of the reaction results in a dark, red-brown oil that can be subjected to silica gel column chromatography. Analysis of the crude mixture *via* TLC revealed that a small amount of the *double* methy-

lated product was also formed. The mixture was separated by column chromatography with EtOAc/hexane (19:1) as eluent, and the formation of the pure, single methylated compound **11** was confirmed by ^{1}H NMR spectroscopy and LCMS analysis.

Synthesis of *1-(2-(2-(2-acryloxyethoxy)ethoxy)ethoxy)-5-(2-(2-(2-methoxyethoxy)ethoxy)ethoxy)naphthalene*

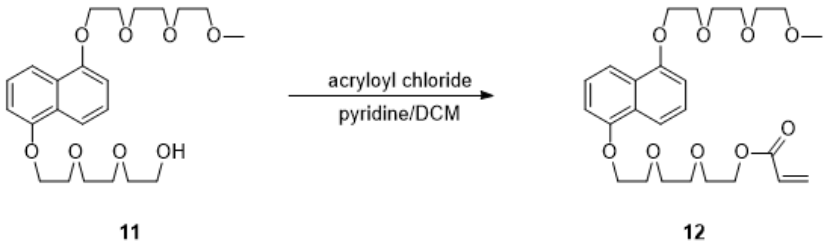

11 **12**

Scheme 2.11: *Synthesis of the polymerizable guest molecule by reaction with acryloyl chloride.*

Finally, component **11** was reacted with acryloyl chloride to synthesize the polymerizable guest molecule **12**. The acryloyl chloride was added dropwise to a solution of compound **11** and pyridine in DCM at 0°C under inert atmosphere. The reaction was executed in the presence of a base (pyridine), which is used to trap the formed HCl. After stirring the solution at 0°C for 2 hours and an additional 24 hours at room temperature, the formation of a white solid was observed. This is the pyridine hydrochloride that is insoluble in DCM and can easily be removed by filtration. After concentration, the obtained product was dissolved in EtOAc, filtered and washed with water to remove any residual pyridine. Purification was done by column chromatography with EtOAc/hexane (9:1) as eluent, and the formation of the product **12** was confirmed by LCMS. Due to the small amount of product, NMR analysis was not possible.

2.2 Polymer synthesis

The aim of this project was to synthesize a copolymer of NIPAM together with small amounts of host and guest moieties. Since the supramolecular host molecule was not ready in time, only a test RAFT polymerization of NIPAM could be executed.
The performed RAFT polymerization is a type of controlled radical polymerization, which

is discussed in Section 1.4. These "living" polymerizations are characterized by a) an almost complete absence of any chain termination or irreversible transfer reactions, and b) a fast rate of activation (effective degenerative transfer) with respect to the rate of propagation ($R_{eq} > R_p$). If there is no significant termination and $R_{eq} > R_p$, the concentration of the propagating species will be almost constant during polymerization. Looking at Equation 2.2, this means that for "living" systems, there is a linear relationship between $ln\frac{[M]_0}{[M]}$ and the time.

The polymerization rate (R_p) at which the monomer is converted into polymer:

$$R_p = \frac{-d[M]}{dt} = k_p[M][P^*] \tag{2.1}$$

Integration of this equation gives:

$$ln\frac{[M]_0}{[M]} = k_p[P^*]t \tag{2.2}$$

Here, [P*] is the concentration of the propagating species (which is constant during CRPs), [M] is the concentration of monomer at each time, k_p is the propagation rate constant and t is the time.

The relative concentration of monomer at each time during the polymerization can be determined by gas chromatography (GC) by comparing its area with the unchanging area of the solvent (internal standard). Plotting Equation 2.2 allows us to see if our polymerization follows this first order kinetic behavior. An increase in the slope of the curve may indicate slow initiation, whereas a decrease of the slope is typical for the presence of termination reactions (Figure 2.4).

Further, rapid equilibrium between the active and dormant species (R_{eq}) ensures an equal growth rate for all chains. This results in a linear increase of the average molecular weight M_n with respect to the monomer conversion, and a very narrow dispersity of the final polymer (Equation 2.3). When the molecular weight in the beginning of the polymerization is higher than predicted, this reflects slow initiation. In the case of transfer reactions, an increased amount of dead chains appears, which gives rise to lower molecular weights than theoretically expected (Figure 2.4). Since the average molecular weight and degree of polymerization (DP) exhibit a linear relationship (Equation 2.4), DP will also increase linearly with the monomer conversion. The average molecular weight (M_n) and dispersity (Đ) are determined by size exclusion chromatography (SEC), while conversion is determined by GC.

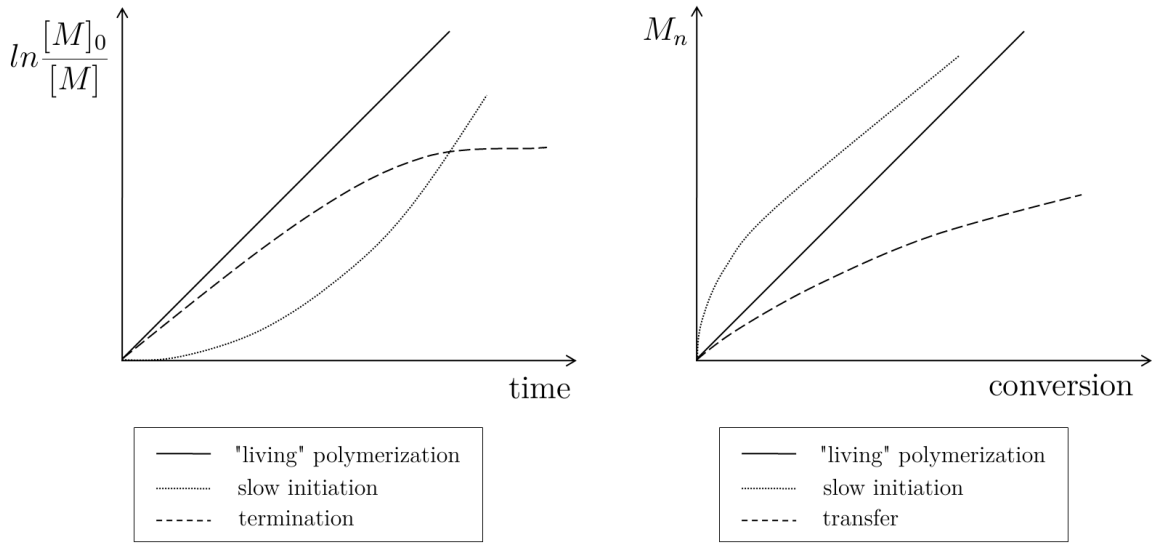

Figure 2.4: *Typical graphs for the kinetics of "living" polymerizations and the effects of slow initiation, termination and/or transfer reactions. Reprinted from reference[120].*

$$M_n = \frac{[M]_0}{[CTA]_0} * conversion * M_M + M_{CTA} \tag{2.3}$$

$$DP = \frac{M_n}{M_M} \tag{2.4}$$

$$conversion = \frac{[M]_0 - [M]}{[M]_0} = 1 - e^{-k_p[P^*]t} \tag{2.5}$$

$$Đ = \frac{M_w}{M_n} \tag{2.6}$$

Here, M_n is the number average molecular weight, M_w is the weight average molecular weight, $[M]_0$ is the initial monomer concentration, [M] is the concentration of monomer at each time, $[CTA]_0$ is the initial concentration of RAFT-agents, M_M is the molecular weight of the monomer and M_{CTA} is the molecular weight of the RAFT-agent.
Equation 2.3 assumes that each RAFT-agent is attached to a polymer chain (100% efficiency), neglects possible termination reactions and disregards the small amount of chains formed by the initiator.[121]

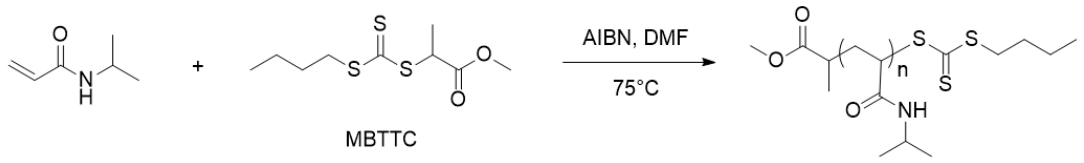

Figure 2.5: *Synthesis of PNIPAM polymers by RAFT polymerization.*

Poly(*N*-isopropylacrylamide) was synthesized by RAFT polymerization under argon atmosphere. The monomer (NIPAM), RAFT-agent (methyl 2-(butylthiocarbonothioylthio)propanoate, MBTTC), initiator (AIBN) and solvent (DMF) were brought together in a schlenk flask at a molar ratio of 250:1:0.25 and a monomer concentration of 2 M. After three freeze-pump-thaw cycles to deoxygenate the solution completely, the mixture was placed in a preheated oil bath at appropriate temperature to start the polymerization. Samples were taken every half hour for the kinetic study. The solvents used for GC and SEC samples were acetone and dimethylacetamide (DMA), respectively. After a reaction time of 3 hours, the reaction was quenched by placing it in liquid nitrogen. The resulting polymer was obtained *via* repetitive precipitation in Et_2O/hexane (4:1) and Et_2O. The resulting white, powdery polymer was obtained *via* centrifugation and a final SEC sample was made for analysis of the molar mass and Đ.

GC and SEC analysis:

GC samples are taken every half hour during the reaction to follow the concentration of monomer periodically ([M]) during the polymerization. These values can be used to plot an $ln\frac{[M]_0}{[M]}$ versus time diagram and a conversion versus time diagram. Looking at the propagation rate, $ln\frac{[M]_0}{[M]} = k_p[P^*]t$ (2.2), and assuming that the concentration of propagating species is constant, a linear relationship should be obtained. Figure 2.6 shows the GC results for the polymerization at 70°C and 75°C, and a linear fit at the data (dotted line). One can see that the data for 75°C follows an almost straight line until 120 minutes, after which a decrease in slope is observed. This indicates the loss of propagating species at longer reaction times, possibly due to termination reactions. The polymerization at 70°C exhibits a more linear relationship in the first order kinetic plot. This indicates a better "livingness" of the polymerization. In the second plot, a typical exponential relationship is observed between the conversion and the time for first order kinetics (Equation 2.5).

Again, a slight deviation is observed at longer reaction times for the polymerization at 75°C.

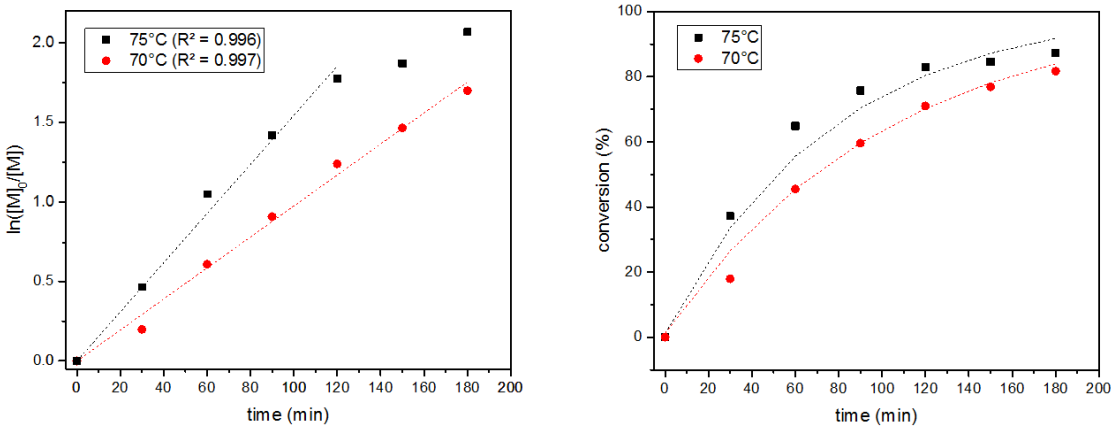

Figure 2.6: *Overview of the GC results for the RAFT polymerization of NIPAM using [NIPAM]:[MBTTC]:[I] = 250:1:0.25, 2M monomer concentration in DMF at 70° C and 75° C. Left: first order kinetic plot. Right: degree of conversion versus time.*

SEC samples are also taken every half hour during the polymerization, allowing to follow the change in molecular weight (M_n) and dispersity (Đ). The data is plotted in Figure 2.7 in function of the monomer conversion. A linear relationship is expected for "living" polymerizations. Looking at the left graph, a high degree of conversion and a high molecular weight are observed after only 30 minutes for the polymerization at 75°C. To reveal the real trend of this data, more samples should have been taken in the beginning of the polymerization. Comparing with the other data, the polymerization will probably have shown an approximately linear relationship at lower conversion and a decrease of slope at higher conversion. The observed decrease suggest the presence of transfer or termination reactions, which will still increase the conversion (consumption of monomer), but will contribute less to the increase in molecular weight. This phenomenon will also lead to an increased dispersity, causing a noticeable peak broadening in the second graph. The polymerization at 70°C again exhibits a more linear trend, which proves again the better "livingness" of the polymerization. Also, the dispersity of the 70°C polymerization is better than the polymerization at 75°C, as it shows more constant and narrow values. The second graph of Figure 2.7 exhibits the SEC traces and dispersities of the final, purified polymers. A perfect Gaussian curve is desired for the final polymer, which would

correspond to a very narrow dispersity. The polymer synthesized at 70°C exhibits a good Gaussian distribution and narrow dispersity, while the 75°C polymer shows some slight low molecular weight tailing. This means that a fraction of the polymer has a (slightly) lower molecular weight than the rest of the polymer either due to termination or irreversible chain transfer. Hence, the 75°C polymer is not as monodisperse as the 70°C polymer.

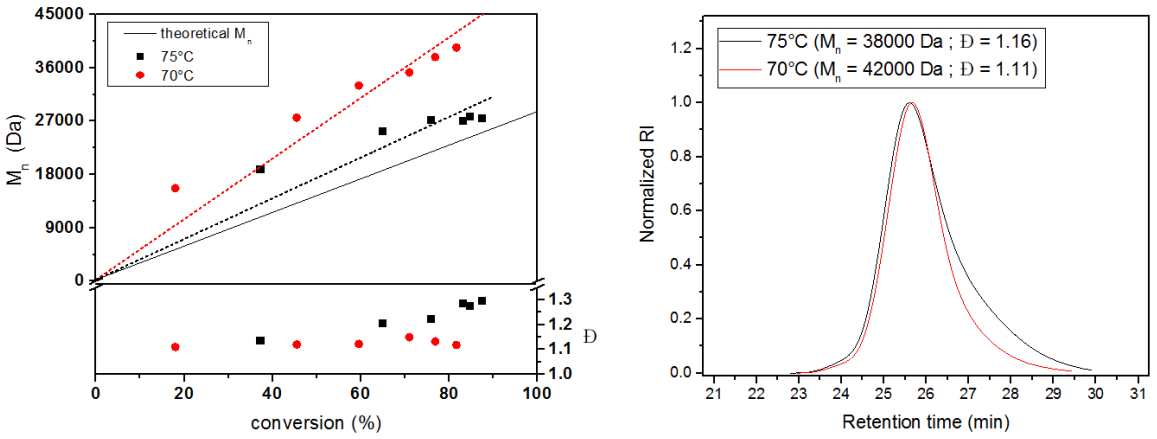

Figure 2.7: *Overview of the SEC results for the RAFT polymerization of NIPAM using [NIPAM]:[MBTTC]:[I] = 250:1:0.25, 2M monomer concentration in DMF at 70°C and 75°C. Left: molecular weight and dispersity versus degree of conversion. Right: normalized intensity signal versus retention time.*

To conclude, the livingness of this polymerization is confirmed by the experimental data shown in Figures 2.6 and 2.7. One can clearly see that the polymerization at 70°C shows a much more controlled behavior than the polymerization at 75°C. This results in a final polymer that possesses a more narrow Đ. Hence, the 70°C polymer is more monodisperse and this temperature should be used for future copolymerizations with the supramolecular comonomers.

2.3 Conclusion and outlook

During this project, we were able to partially synthesize a supramolecular host and guest compound and provide them with a polymerizable double bond.

The supramolecular host compound is a cyclobis(paraquat-*p*-phenylene) ($CBPQT^{4+}$) deriva-

tive, also known as bluebox. While the synthesis of a 'normal' bluebox is extensively described in literature, applying a linker to this molecule proves to be more difficult. Section 2.1.1 displays the different approaches that were tested in an attempt to generate the desired compound. The first part of the supramolecular host **A** was synthesized by reacting 4,4'-dipyridyl **1** with α,α-dibromo-*p*-xylene **2** at elevated temperature, under inert conditions. To change the solubility of the bis(pyridinium) from water to organic solvents, the intermediate was reacted with a saturated, aqueous NH_4PF_6 solution to change the counterion from Br^- to $PF_6{}^-$. Synthesizing the second part of the supramolecular host **B** was a bit more difficult since the introduction of the linker did not go as planned. In the first step, 2,5-dimethylbenzoic acid **4** was brominated using NBS and AIBN, based on a literature procedure. The supposedly straightforward procedure turned out to be more time consuming due to overbromination and the separation from the tribrominated product was almost impossible. Following the reaction with ^{1}H NMR spectroscopy revealed the appropriate reaction time necessary to still get a good purification of the compound **5**. In the second step, the carboxylic acid **5** was modified with a linker and different methods were attempted in the search for a successful procedure. Initially, the proposed linker consisted of a ethylene glycol ether unit that was long enough to ensure a good flexibility of the host in the hydrogel. Several methods were employed but none was successful in yielding the expected compound **B1**. This was probably due to the difference in solubility between the starting material **5** and the final compound **B1**. Since the mono-substituted glycol **B1** is much better soluble than the carboxylic acid **5**, a second reaction occurs much faster, resulting in the di-substituted glycol. Therefore, an alternative compound **B2** was produced without a linker. This was done by reducing the already synthesized ethyl 2,5-bis(bromomethyl)benzoate **4b** to the corresponding alcohol **B2**. Because of time limitations, the assembly of both components and the reaction with acryloyl chloride could not be carried out. All unsuccessful reactions were performed at least twice to exclude coincidence.

The supramolecular guest compound is a 1,5-dialkoxynaphthalene derivative and was successfully synthesized *via* a three-step process. Since someone of our research group already had experience with this type of synthesis route, the execution of this reaction sequence was rather straightforward. First, double alkylation of 1,5-dihydroxynaphthalene **8** was achieved by reaction with 2-(2-chloroethoxy)ethoxyethanol **9** under basic conditions. This

was followed by a single methylation reaction of the diol **10** with NaH/MeI, which was further reacted with acryloyl chloride to obtain a polymerizable guest moiety **12**.

For the second part of the project, a RAFT copolymerization of these supramolecular compounds with NIPAM was planned. But since the supramolecular host molecule was not ready in time, only a test homopolymerization of NIPAM could be executed. *N*-isopropylacrylamide RAFT polymerizations at 70°C and 75°C were performed, together with kinetic studies to analyze the livingness and controlled behavior of the polymerization reactions at different temperatures. The livingness of this polymerization is confirmed by the experimental data shown in Figures 2.6 and 2.7. One can clearly see that the polymerization at 70°C shows a much more controlled behavior than the polymerization at 75°C. This results in a final polymer that possesses a more narrow Đ. Hence, the 70°C polymer is more monodisperse.

For future research, a suitable synthesis route can be developed to provide the supramolecular host molecule with a suited linker. We propose to use a mono-protected alcohol to allow the formation of the mono-substituted glycol over the di-substituted product. If this succeeds, an additional two steps (assembly and reaction with acryloyl chloride) will produce the final host monomer. Copolymerization reactions can then be performed, together with the characterization of the obtained polymers. In a further stadium, hydrogels can be prepared by including a bifunctional monomer as crosslinker and characterized, and the stimuli-responsive behavior can be investigated.

3 Appendix - experimental section

3.1 Materials

The commonly used solvents were of HPLC grade and include: dichloromethane (DCM, ≥99.8%, Sigma-Aldrich), ethanol (EtOH, disinfectol, Chem-Lab), methanol (MeOH, ≥ 99.9%, Sigma-Aldrich), *n*-hexane (98.72%, Fisher Chemical), *N,N*-dimethylformamide (DMF, 99.8%, Acros Organics), toluene (99.99%, Fisher Chemical), ethyl acetate (EtOAc, ≥99.7%, Sigma-Aldrich), diethyl ether (Et_2O, ≥99.8%, Sigma-Aldrich) and chloroform ($CHCl_3$, Fisher Chemical).

Deuterated solvents for ^{1}H NMR and ^{13}C NMR spectroscopy like chloroform-*d* ($CDCl_3$, ≥99.8% D, water <0.01%) and dimethylsulfoxide-*d*6 (DMSO-*d*6, ≥99.8% D, water <0.02 %), were purchased from Euriso-top.

Dry dichloromethane (DCM), acetonitrile (MeCN), tetrahydrofuran (THF) and *N,N*-dimethylformamide (DMF) were obtained from a custom made JW Meyer solvent purification system by drying over aluminium oxide columns. Dry toluene was obtained by a reflux setup under nitrogen atmosphere.

The following chemicals were used as received: 4,4'-dipyridyl (98%, Sigma-Aldrich), α,α-dibromo-*p*-xylene (Fluka), ammonium hexafluorophosphate (NH_4PF_6, ≥ 98%, Fluka), 2,5-dimethylbenzoic acid (>98.0%, TCI), sulfuric acid (H_2SO_4, >95%, Fisher Chemical), N-bromosuccinimide (NBS, 99%, Sigma-Aldrich), carbon tetrachloride (CCl_4, 99%, Acros Organics, molecular sieves), diethylene glycol (99%, ucb), 4-(dimethylamino)pyridine (DMAP, 99%, Sigma-Aldrich), *N,N*'-dicyclohexylcarbodiimide (DCC, 99%, Sigma-Aldrich), thionyl chloride ($SOCl_2$, ≥99.5%, Acros Organics), methanesulfonic acid ($MeSO_3H$, ≥99%, Fluka), aluminium oxide (Al_2O_3, Merck KGaA), sodium bicarbonate ($NaHCO_3$, VWR In-

ternational), calcium chloride ($CaCl_2$, ≥97%, Sigma-Aldrich), 2-(2-chloroethoxy)ethoxyethanol (>96.0%, TCI), 1,5-dihydroxynapthalene (97%, Sigma-Aldrich), potassium carbonate (K_2CO_3, ≥99%, Acros Organics), sodium hydride (NaH, 60% dispersion in mineral oil, Sigma-Aldrich), iodomethane (MeI, ≥99%, Sigma-Aldrich), acryloyl chloride (≥97%, Sigma-Aldrich), pyridine (99.5%, Acros Organics), sodium carbonate (Na_2CO_3, 99.5%, Acros Organics) and magnesium sulfate ($MgSO_4$, Fisher Chemical).
Azobis(isobutyronitrile) (AIBN, 98%, Sigma-Aldrich) was recrystallized from diethyl ether and stored at -7°C.
N-isopropylacrylamide (NIPAM, 97%, Sigma-Aldrich) was recrystallized two times from hexane prior to use.
Methyl-2-(n-butyltrithiocarbonyl)propanoate (MBTTCP) was prepared according to the established procedure.[122]

3.2 Equipment

Reactions and chromatographic columns were followed by TLC on Macherey-Nagel SILG-25 UV254 glass plates (silica TLC) and TLC Aluminium oxide 60 F254 neutral (alumina TLC). Column chromatography was performed with a *Biosolve* silica gel stationary phase or a *Merck KGaA* neutral alumina phase.

Column flash chromatography was performed on a Reveleris Flash Chromatography System using a cartridge containing the stationary phase and a mobile phase that can be varied. A number of stationary phases and four solvent reservoirs are available. A UV dectector is present that can monitor two wavelengths simultaneously as well as an evaporative light scattering detector (ELSD). The ELSD provides the ability to monitor all non-volatile compounds in the eluent and allows the user to detect for compounds that do not absorb UV radiation. An additional benefit of the ELSD is the ability to employ mobile phases that absorb light at the same wavelength as the compound(s) of interest.

Centrifugation was performed on an ALC multispeed refrigerated centrifuge PK 121R from Thermo Scientific using 50 mL centrifuging tubes with screw caps from VWR or 15 mL high clarity polypropylene conical tubes from Falcon.

Liquid chromatography mass spectrometry (LCMS) analysis was performed on an Agilent 1100 HPLC with quaternary pump and UV-DAD detection, coupled to an Agilent

G1956B MSD. Ionization of the samples was achieved through electronspray ionization (ESI).

Nuclear magnetic resonance spectra were recorded on a Bruker Avance 300 MHz and 400 MHz spectrometer and at room temperature. ^{1}H NMR and ^{13}C NMR spectra were measured in chloroform-*d* ($CDCl_3$) and dimethylsulfoxide-*d*6 (DMSO-*d*6) purchased from Euriso-top .

Gas chromatography (GC) was used to determine the monomer conversion during the reaction progress. GC was performed on an Agilent Technologies 7890A system equipped with an Agilent J&W Advanced Capillary GC column (30 m, 0.320 mm, and 0.25 µm). Injections were performed with an Agilent Technologies 7693 auto sampler. Detection was done with a FID detector. Injector and detector temperatures were kept constant at 250°C and 280°C, respectively. The column was initially set at 50°C, followed by two heating stages: from 50°C to 100°C with a rate of 20°C/min, and from 100°C to 300°C with a rate of 40°C/min. This temperature was held for 30 seconds. Conversion was determined based on the integration of monomer peaks using solvent (DMF) as internal standard.

Size exclusion chromatography (SEC) was performed on a Agilent 1260-series HPLC system equipped with a 1260 online degasser, a 1260 ISO-pump, a 1260 automatic liquid sampler (ALS), a thermostatted column compartment (TCC), a 1260 diode array detector (DAD) and a 1260 refractive index detector (RID). DMAc containing 50 mM of LiCl was used as eluent at a flow rate of 0.6 mL/min. The SEC traces were analysed using the Agilent Chemstation software with the GPC add on. Molar mass and PDI values were calculated against PMMA standards.

3.3 Synthesis of monomers

1,1'-(1,4-phenylenebis(methylene))bis(4,4'pyridinium)bis(hexafluorophosphate) A

A solution of 4,4'-dipyridyl **1** (2 g, 12.8 mmol) in 30 mL dry DMF was heated to 90°C under inert atmosphere. To this, a solution of α,α-dibromo-*p*-xylene **2** (0.338 g, 1.28 mmol) in 10 mL dry DMF was added dropwise and the solution was stirred overnight at 90°C. The obtained precipitate was filtered and washed four times with Et_2O before being

dissolved in water to give a light yellow solution. A saturated NH_4PF_6 aqueous solution (589.75 mg, 3.618 mmol) was added and the solution was stirred for 1h. The precipitate was collected by centrifugation (6°C, 10000 rpm, 8 min.) and washed with water to give a light brown, solid product **A** (0.629 g, 0.891 mmol, 69.6%).

^{1}**H NMR** (400 MHz, DMSO-*d*6) δ_H = 9.33 (d, J = 7.0 Hz, 4H, $-^+NC_5H_2H_2-$), 8.87 (d, J = 6.2 Hz, 4H, $-^+NC_5H_2H_2-$), 8.64 (d, J = 7.0 Hz, 4H, $-C_5H_2H_2N$), 8.00 (d, J = 6.2 Hz, 4H, $-C_5H_2H_2N$), 7.66 (s, 4H, $C_6H_4[CH_2-^+NC_5H_4-C_5H_4N]_2$), 5.88 (s, 4H, $C_6H_4[CH_2-^+NC_5H_4-C_5H_4N]_2$).

^{13}**C NMR** (101 MHz, DMSO) δ_C = 152.92 (C_q), 150.98 (CH), 145.35 (CH), 140.75 (C_q), 135.36 (C_q), 129.58 (CH), 125.88 (CH), 121.92 (CH), 62.41 (CH_2).

ESI-MS: $[M]^{2+}$ = 208.10

ethyl 2,5-dimethylbenzoate 4a[51]

Sulfuric acid (2.857 mL, 53.603 mmol) and 2,5-dimethylbenzoic acid **4** (2 g, 13.317 mmol) were dissolved in 30 mL ethanol and heated under reflux overnight. After cooling and concentrating, the obtained residue was dissolved in 30 mL DCM and washed with saturated aqueous Na_2CO_3 and water. The organic layer was dried over $MgSO_4$, filtered and the filtrate was concentrated to yield a clear, colorless oil (1.934 g, 10.853 mmol, 81.5%).

^{1}**H NMR** (400 MHz, $CDCl_3$) δ_H = 7.72 (s, 1H, $-C_6H_3-$), 7.19 (d, J = 9.4 Hz, 1H, $-C_6H_3-$), 7.12 (d, J = 7.8 Hz, 1H, $-C_6H_3-$), 4.36 (q, J = 7.1 Hz, 2H, $-C_6H_3-CO_2CH_2CH_3$), 2.55 (s, 3H, $[CH_3]_2-C_6H_3-$), 2.35 (s, 3H, $[CH_3]_2-C_6H_3-$), 1.40 (t, J = 7.1 Hz, 3H, $-C_6H_3-CO_2CH_2CH_3$).

^{13}**C NMR** (101 MHz, $CDCl_3$) δ_C = 167.88 (C_q), 136.83 (C_q), 135.18 (C_q), 132.57 (CH), 131.57 (CH), 130.91 (CH), 129.75 (C_q), 60.62 (CH_2), 21.22 (CH_3), 20.77 (CH_3), 14.36 (CH_3).

ESI-MS: $[M+H]^+$ = 179.10

ethyl 2,5-bis(bromomethyl)benzoate 4b[51]

NBS (2.96 g, 14.03 mmol) and a catalytic amount of AIBN were added to a solution of ethyl 2,5-dimethylbenzoate **4a** (1.25 g, 7.013 mmol) in CCl_4 and the suspension was refluxed for 3h under nitrogen. After cooling and filtration of the succinimide, the filtrate was concentrated and the resulting oil dissolved in 15 mL DCM. To this, 90 mL hexane

was added and the solution produced a white precipitate after overnight cooling at -30°C. The product was collected and its purity confirmed by ^{1}H NMR spectroscopy (630 mg, 1.88 mmol, 26.7%).

^{1}H NMR (400 MHz, $CDCl_3$) δ_H = 7.98 (s, J = 1.9 Hz, 1H, $-C_6H_3[CH_2Br]_2$), 7.52 (dd, J = 7.9, 1.9 Hz, 1H, $-C_6H_3[CH_2Br]_2$), 7.44 (d, J = 7.9 Hz, 1H, $-C_6H_3[CH_2Br]_2$), 4.93 (s, 2H, $-C_6H_3[CH_2Br]_2$), 4.49 (s, 2H, $-C_6H_3[CH_2Br]_2$), 4.42 (q, J = 7.1 Hz, 2H, -$CO_2CH_2CH_3$), 1.44 (t, J = 7.1 Hz, 3H, -$CO_2CH_2CH_3$).

^{13}C NMR (101 MHz, $CDCl_3$) δ_C = 166.07 (C_q), 139.23 (C_q), 138.30 (C_q), 132.84 (CH), 132.26 (CH), 131.71 (CH), 129.97 (C_q), 61.59 (CH_2), 31.89 (CH_2), 30.95 (CH_2), 14.80 (CH_3).

ESI-MS: $[M+H]^+$ = 336.9

2,5-bis(bromomethyl)benzyl alcohol B2[123]

Ethyl 2,5-bis(bromomethyl)benzoate **4b** (294 mg, 0.875 mmol) in 5 mL toluene was added dropwise to a cooled (0°C) solution of DIBAL-H (2 mL, 17.3 mmol)(1M in THF) in 10 mL toluene, under inert conditions. The mixture was stirred for 3h at 0°C, after which HCl was added until a pH of 1 was reached. The organic phase was extracted, washed with water, dried over $MgSO_4$ and filtered. After concentrating over reduced pressure, the product was washed with ice-cold ether to give a white powder **B2** (30.82 mg, 0.11 mmol, 12%).

^{1}H NMR (300 MHz, $CDCl_3$) δ_H = 7.48 (s, 1H, $-C_6H_3^-$), 7.34 (s, 1H, $-C_6H_3^-$), 7.33 (d, J = 1.7 Hz, 1H, $-C_6H_3^-$), 4.84 (s, 2H, $-C_6H_3-CH_2-OH$), 4.60 (s, 2H, $-C_6H_3[CH_2Br]_2$), 4.48 (s, 2H, $-C_6H_3[CH_2Br]_2$).

^{13}C NMR (101 MHz, $CDCl_3$) δ_C = 139.90 (C_q), 138.8 (C_q), 135.78 (C_q), 131.15 (CH), 129.36 (CH), 128.88 (CH), 62.41 (CH_2), 32.68 (CH_2), 30.19 (CH_2).

2,5-bis(bromomethyl)benzoic acid 5[51]

NBS (39.12 g, 219.80 mmol) and a catalytic amount of AIBN (0.05 g, 0.304 mmol) were added to a solution of 2,5-dimethylbenzoic acid **4** (15.06 g, 100.26 mmol) in CCl_4 and the suspension was refluxed for 3h under nitrogen. After cooling and filtration of the succinimide, the solution was left to stand overnight. The obtained precipitate was filtered and dried under vacuum. Purification was done by recrystallization (vapor diffusion): the

product was dissolved in chloroform and put in a hexane environment to produce white, needle-like crystals **5** (7.76 g, 25.19 mmol, 25.1%).

^{1}**H NMR** (300 MHz, $CDCl_3$) δ_H = 8.13 (s, 1H, $-C_6H_3[CH_2Br]_2$), 7.59 (dd, J = 8.0, 2.0 Hz, 1H, $-C_6H_3[CH_2Br]_2$), 7.50 (d, J = 7.9 Hz, 1H, $-C_6H_3[CH_2Br]_2$), 4.99 (s, 2H, $-C_6H_3[CH_2Br]_2$), 4.50 (s, 2H, $-C_6H_3[CH_2Br]_2$).

^{13}**C NMR** (126 MHz, $CDCl_3$) δ_C = 170.49 (C_q), 140.29 (C_q), 138.54 (C_q), 133.99 (CH), 132.74 (CH), 132.64 (CH), 127.98 (C_q), 31.61 (CH_2), 30.68 (CH_2).

ESI-MS: $[M+H]^+$ = 306.90

(ethylene glycol ether) 2,5-bis(bromomethyl)benzoate B1

First attempt - via a 2,5-bis(bromomethyl)benzoyl chloride intermediate:[51]

A mixture was prepared of 2,5-bis(bromomethyl)benzoic acid **5** (0.2 g, 0.65 mmol), thionyl chloride (1.638 mL, 1.38 mmol) and 1 drop DMF in 15 mL dry toluene. The solution was allowed to reflux for 3h, before being cooled to room temperature and concentrated. The resulting yellow oil **5a** was used as such in the following step without further purification. Under inert conditions, the benzoyl chloride derivative **5a** was dissolved in 20 mL dry DCM and added dropwise to a solution of diethylene glycol (0.2 g, 1.89 mmol) in 30 mL dry DCM. The mixture was stirred for 4h at room temperature, and an additional 24h at reflux. The solution was cooled, washed with water and the organic layer dried over $MgSO_4$. After concentration, a dark orange oil is obtained that is unsuccesfully purified by subjecting it to column chromatography (DCM/hexane, 10:5).

Second attempt - DCC coupling reaction:[118]

2,5-bis(bromomethyl)benzoic acid **5** (1 g, 3.25 mmol), diethylene glycol (6 g, 56.54 mmol) and a catalytic amount of DMAP (0.02 g, 0.164 mmol) were dissolved in 30 mL pure DCM, cooled to 0°C and degassed for 30 min. A solution of DCC (1 g, 4.85 mmol) in 20 mL pure DCM was added dropwise under 0°C and the solution was allowed to stir overnight at room temperature before being refluxed for an additional 3 *à* 4h. After filtration, the filtrate was washed with brine and water and the organic layer was dried over $MgSO_4$. Filtration and concentration resulted in a light yellow oil that was purified using silica gel flash column chromatography (DCM/hexane, 10:5). This revealed the formation of only the di-substituted glycol and a large amount of unreacted starting material.

Third attempt - monoesterification with AMA without the use of any solvents:[119]
To a mixture of $MeSO_3H$ (1 mL, 15 mmol) and Al_2O_3 (0.27 g, 3 mmol), 2,5-bis(bromomethyl)benzoic acid **5** (0.308 g, 1 mmol) and diethylene ether (0.095 mL, 1 mmol) were added successively. The solution was stirred at 80°C for 1h. The mixtures was then poured into an excess of water, extracted two times with EtOAc and the organic layer washed with saturated aqueous $NaHCO_3$. Drying over $CaCl_2$, concentrating over reduced pressure and purification by silica gel flash column chromatography, resulted again in the di-substituted glycol.

1,5-bis[2-(2-(2-hydroxyethoxy)ethoxy)ethoxy]-naphthalene 10[124]
Under nitrogen, a solution of 2-(2-chloroethoxy)ethoxyethanol **9** (31.37 g, 186 mmol) in 40 mL dry MeCN was added dropwise over 1h to a purple suspension of naphthalene-1,5-diol **8** (10 g, 62.43 mmol) and K_2CO_3 (51.77 g, 374.6 mmol) in 90 mL dry MeCN. The solution was heated under reflux overnight to give a brown, turbid solution. After removing the solvent, the resulting brown oil was dissolved in DCM, stirred for a few days and washed with brine and water. The organic layer was dried over $MgSO_4$, filtered, concentrated and the resulting red-brown oil was subjected to column chromatography over silica gel (DCM/EtOH, 30:1) to give a brown, solid product **10** (12.69 g, 29.9 mmol, 47.9%)
^{1}**H NMR** (400 MHz, $CDCl_3$) δ_H 7.87 (d, J = 8.6 Hz, 2H, $[C_6H_3{-}OC_6H_{13}O_3]_2$), 7.36 (dd, J = 13.4, 5.7 Hz, 2H, $[C_6H_3{-}OC_6H_{13}O_3]_2$), 6.85 (d, J = 7.6 Hz, 2H, $[C_6H_3{-}OC_6H_{13}O_3]_2$), 4.31 (m, 4H, $[C_6H_3{-}OCH_2CH_2{-}]_2$), 4.00 (dd, J = 5.4, 4.3 Hz, 4H, $[C_6H_3{-}OCH_2CH_2{-}]_2$), 3.81 (m, 4H, $[{-}OCH_2CH_2OH]_2$), 3.72 (m, 8H, $[C_6H_3{-}OC_2H_4OC_2H_4OC_2H_4OH]_2$), 3.62 (m, 4H, $[{-}OCH_2CH_2OH]_2$).
^{13}**C NMR** (101 MHz, $CDCl_3$) δ_C = 154.31 (C_q), 126.80 (C_q), 125.13 (CH), 114.66 (CH), 105.76 (CH), 72.52 (CH_2), 71.05 (CH_2), 70.52 (CH_2), 69.85 (CH_2), 67.92 (CH_2), 61.83 (CH_2).
ESI-MS: $[M+NH_4]^+$ = 442.20

1-(2-(2-(2-hydroxyethoxy)ethoxy)ethoxy)-5-(2-(2-(2-methoxyethoxy)ethoxy) ethoxy)naphthalene 11[51]
1,5-bis[2-(2-(2-hydroxyethoxy)ethoxy)ethoxy]-naphthalene **10** (376 mg, 0.886 mmol) was dissolved in 15 mL dry THF, to which a suspension of NaH (60% dispersion in mineral

oil ; 0.6 g, 25 mmol) in 25 mL dry THF was dropwise added under inert atmosphere. The solution was stirred at room temperature for 30 min, and an additional 30 min under reflux. A solution of iodomethane (0.1285 g, 0.905 mmol) in 10 mL dry THF was added dropwise over 15 min. The solution was further refluxed for 24h, cooled and methanol (2.5 mL, 61.8 mmol) was added to react with the excess of NaH. After concentration, the resulting oil was dissolved in DCM and washed with saturated aqueous Na_2CO_3 and water. The organic layer was dried over $MgSO_4$, filtered, concentrated and the resulting red-brown oil was purified by silica gel column chromatography (EtOAc/hexane, 95:5) to give the final compound **11** (67.9 mg, 0.155 mmol, 17.5%).

^{1}**H NMR** (400 MHz, $CDCl_3$) δ_H 7.86 (dd, J = 8.5, 3.4 Hz, 2H, [C_6H_3−]$_2$), 7.34 (m, 2H, [C_6H_3−]$_2$), 6.84 (d, J = 7.6 Hz, 2H, [C_6H_3−]$_2$), 4.30 (dd, J = 9.6, 4.4 Hz, 4H, [C_6H_3−O$CH_2$$CH_2$−]$_2$), 4.00 (dt, J = 4.7, 3.5 Hz, 4H, [C_6H_3−OCH_2CH_2−]$_2$), 3.81 (m, 4H, [C_6H_3−OC_2H_4−$OC_4H_8O_2$−]$_2$), 3.71 (ddd, J = 7.6, 5.9, 3.9 Hz, 6H, [C_6H_3−OC_2H_4 − $OC_4H_8O_2$−]$_2$), 3.67 (m, 2H, [C_6H_3−OC_2H_4−$OC_4H_8O_2$−]$_2$), 3.62 (m, 2H, [C_6H_3−OC_2H_4 − $OC_4H_8O_2$−]$_2$), 3.54 (m, 2H, [C_6H_3−OC_2H_4−$OC_4H_8O_2$−]$_2$), 3.37 (s, 3H, −$OC_4H_8O_2$−CH_3).

^{13}**C NMR** (101 MHz, $CDCl_3$) δ_C = 154.33 (C_q), 126.79 (C_q), 125.09 (CH), 114.64 (CH), 105.71 (CH), 72.52 (CH_2), 71.94 (CH_2), 71.01 (CH_2), 70.73 (CH_2), 70.59 (CH_2), 70.50 (CH_2), 69.83 (CH_2), 67.91 (CH_2), 61.79 (CH_2), 60.40 (CH_2), 59.03 (CH_3).

ESI-MS: $[M+H]^+$ = 439.20

1-(2-(2-(2-acryloxyethoxy)ethoxy)ethoxy)-5-(2-(2-(2-methoxyethoxy)ethoxy) ethoxy)naphthalene 12

Acryloyl chloride (21.02 mg, 0.232 mmol) in 3 mL dry DCM was added dropwise to a solution of 1-(2-(2-(2-hydroxyethoxy)ethoxy)ethoxy)-5-(2-(2-(2-methoxyethoxy)ethoxy)-ethoxy)naphthalene **11** (67.9 mg, 0.155 mmol) and pyridine (24.5 mg, 0.310 mmol) in 7 mL dry DCM at 0°C, under inert atmosphere. The solution was stirred for 2h at 0°C and then at room temperature overnight. After filtration of the pyridine hydrochloride, the mixture is concentrated, dissolved in EtOAc, filtered again and washed with water to remove any residual pyridine. Purification is performed by column chromatography (EtOAc/hexane, 9:1). Due to the small amount of the product, only confirmation by LCMS was possible.

ESI-MS: $[M + NH_4]^+$ = 510.20

3.4 Polymerizations

poly(*N*-isopropylacrylamide) [125]

PNIPAM was synthesized by RAFT polymerization under argon atmosphere. *N*-isopropylacrylamide (1.132 g, 10 mmol), methyl 2-(butylthiocarbonothioyl-thio)propanoate (10.1 mg, 0.04 mmol) and AIBN (1.64 mg, 0.01 mmol) were dissolved in 5 mL DMF in a schlenk flask to obtain a molar ratio of 250:1:0.25 and a monomer concentration of 2 M. The mixture was subjected to three freeze-pump-thaw cycles to completely deoxygenate the solution. One cycle consists of freezing the solution in liquid nitrogen for at least 10 minutes, after which vaccuum is applied (10 min) to remove the air present in the flask. Next, the flask is put in a beaker of water to defrost, upon which air bubbles appear from the solution. Due to the low pressure above the solution (vaccuum), the air gets released from the solution (bubbles). This cycle is repeated at least 3 to 4 times till no more gas is present in the solution. An argon atmosphere is applied to the flask and after taking the first kinetic samples, the polymerization is started by placing the mixture in a preheated oil bath (70°C/75°C). Samples are taken every half hour for kinetic studies. The solvents used for GC and SEC samples were respectively acetone and dimethylacetamide (DMA). After a reaction time of 3 hours, the flask was removed from the oil bath and placed in liquid nitrogen to stop the polymerization. The resulting polymer was obtained *via* precipitation in Et_2O/hexane (4:1) and twice in pure Et_2O. Centrifugation resulted in the final white, powdery polymer.

Polymerization at 70°C: M_n = 42 kDa ; Đ= 1.11

Polymerization at 75°C: M_n = 38 kDa ; Đ= 1.16

Bibliography

1. N. Avakyan, A. A. Greschner, F. Aldaye, C. J. Serpell, V. Toader, A. Petitjean, and H. F. Sleiman. Reprogramming the assembly of unmodified DNA with a small molecule. *Nature Chem.*, 8(4):368–376, 2016.
2. S. M. Douglas, H. Dietz, T. Liedl, B. Hogberg, F. Graf, and W. M. Shih. Self-assembly of DNA into nanoscale three-dimensional shapes. *Nature*, 459:414–418, 2009.
3. J. Sharma, R. Chhabra, C. Anchi, J. Brownell, Y. Liu, and H. Yan. Control of self-assembly of DNA tubules through integration of gold nanoparticles. *Science*, pages 112–116, 2009.
4. M. N. Namchuk and S. G. Withers. Mechanism of Agrobacterium β-glucosidase: Kinetic analysis of the role of noncovalent enzyme/substrate interactions. *Biochemistry*, 34(49):16194–16202, 1995.
5. B. Nidetzky, C. Eis, and M. Albert. Role of non-covalent enzyme-substrate interactions in the reaction catalysed by cellobiose phosphorylase from Cellulomonas uda. *Biocatal. Biotransform.*, 659:649–659, 2000.
6. D. Sellmann and J. Sutter. Elementary reactions, structure-function relationships, and the potential relevance of low molecular weight metal-sulfur ligand complexes to biological N2 fixation. *J. Biol. Inorg. Chem.*, 1(6):587–593, 1996.
7. W. Antholine, J. Knight, H. Whelan, and D. H. Petering. Studies of the reaction of 2-formylpyridine thiosemicarbazone and its iron and copper complexes with biological systems. *Molecular pharmacology*, 13(1):89–98, 1977.
8. S. G. Zhang, D. M. Marini, W. Hwang, and S. Santoso. Design of nanostructured biological materials through self- assembly of peptides and proteins. *Curr. Opin. Chem. Biol.*, 6(6):865–871, 2002.
9. P. L. Privalov and G. I. Makhatadze. Contribution of hydration and non-covalent

interactions to the heat capacity effect on protein unfolding. *J. Mol. Biol.*, 224(3): 715–723, 1992.

10. D. Schmaljohann. Thermo- and pH-responsive polymers in drug delivery. *Adv. Drug Deliv. Rev.*, pages 1655–1670, 2006.

11. V. Kumar, S. Palazzolo, S. Bayda, G. Corona, G. Toffoli, and F. Rizzolio. DNA Nanotechnology for Cancer Therapeutics. *Theranostics*, 6(5):710–725, 2016.

12. S. Mura, J. Nicolas, and P. Couvreur. Stimuli-responsive nanocarriers for drug delivery. *Nature Mater.*, 12(11):991–1003, 2013.

13. Z. Ge and S. Liu. Functional block copolymer assemblies responsive to tumor and intracellular microenvironments for site-specific drug delivery and enhanced imaging performance. *Chem. Soc. Rev.*, 42(17):7289–325, 2013.

14. C. Heinzmann, C. Weder, and L. M. de Espinosa. Supramolecular polymer adhesives: advanced materials inspired by nature. *Chem. Soc. Rev.*, 45:342–358, 2015.

15. N. Holten-Andersen, M. J. Harrington, H. Birkedal, B. P. Lee, P. B. Messersmith, K. Y. C. Lee, and J. H. Waite. pH-induced metal-ligand cross-links inspired by mussel yield self-healing polymer networks with near-covalent elastic moduli. *Proc. Nat. Acad. Sci. USA*, 108(7):2651–2655, 2011.

16. T. Okano. Molecular Design of Temperature-Responsive Polymers As Intelligent Materials. *Adv. Polym. Sci.*, 110:179–197, 1993.

17. M. Ortega Lorenzo, C. J. Baddeley, C. Muryn, and R. Raval. Extended surface chirality from supramolecular assemblies of adsorbed chiral molecules. *Nature*, 404 (6776):376–379, 2000.

18. J. Lothe, G. Rao, T. A. Dobbins, D. P. Pope, A. H. Heuer, J. Castaing, T. E. Mitchell, S. Kumar, P. Hazzledine, D. E. Jesson, B. J. Pletka, D. S. Phillips, T. Yamamoto, Y. Ikuhara, and J. P. Remeika. Acid Catalysis in Basic Solution : A Supramolecular Host Promotes Orthoformate Hydrolysis. *Science*, pages 85–88, 2007.

19. S. R. Roy and A. K. Chakraborti. Supramolecular assemblies in ionic liquid catalysis for aza-michael reaction. *Org. Lett.*, 12(17):3866–3869, 2010.

20. B. L. Feringa, W. F. Jager, and B. de Lange. Organic materials for reversible optical data storage. *Tetrahedron*, 49(37):8267–8310, 1993.

21. H. Tian and S. Yang. Recent progresses on diarylethene based photochromic switches. *Chem. Soc. Rev.*, 33(2):85–97, 2004.

22. F. M. Raymo. Digital Processing and Communication with Molecular Switches. *Adv. Mater.*, 14(6):401–414, 2002.

23. Y. Zakrevskyy, J. Stumpe, and C. F. J. Faul. A supramolecular approach to optically anisotropic materials: Photosensitive ionic self-assembly complexes. *Adv. Mater.*, 18 (16):2133–2136, 2006.

24. A. I. Taylor, F. Beuron, S. Peak-Chew, E. P. Morris, P. Herdewijn, and P. Holliger. Nanostructures from Synthetic Genetic Polymers. *Chem. Biochem.*, 2016.

25. K. Rajagopal and J. P. Schneider. Self-assembling peptides and proteins for nanotechnological applications. *Curr. Opin. Struct. Biol.*, 14(4):480–486, 2004.

26. E. Frieden. Non-Covalent Interactions: Key to biological flexibility and specificity. *J. Chem. Educ.*, pages 754–761, 1975.

27. Http://ch301.cm.utexas.edu/section2.php?target=imfs/forces/forces-attraction-all.php.

28. J. Dowden, J. D. Kilburn, and P. Wright. Synthetic developments in host–guest chemistry. *Contemp. Org. Synth.*, 2(5):289–314, 1995.

29. G. M. Whitesides and B. Grzybowski. Self-assembly at all scales. *Science*, 295(5564): 2418–21, 2002.

30. A. Tiwari and L. Uzun. *Advanced Functional Materials*. Wiley Online Library, 2015.

31. T. Kato. Self-assembly of phase-segregated liquid crystal structures. *Science*, 295: 2414–2418, 2002.

32. G. M. Whitesides, J. P. Mathias, and T. Christoph. Molecular self-assembly and nanochemistry: a chemical strategy for the synthesis of nanostructures. *DTIC document*, (611), 1991.

33. K. Ariga, J. P. Hill, M. V. Lee, A. Vinu, R. Charvet, and S. Acharya. Challenges and breakthroughs in recent research on self-assembly. *Sci. Technol. Adv. Mater.*, 9 (1):014109, 2008.

34. S. Vauthey. Molecular self-assembly of surfactant-like peptides to form nanotubes and nanovesicles. *Proc. Nat. Acad. Sci. USA*, 99(8):5355–5360, 2002.

35. H. Park, A. Afzali, S. Han, G. S. Tulevski, A. D. Franklin, J. Tersoff, J. B. Hannon,

and W. Haensch. High-density integration of carbon nanotubes via chemical self-assembly. *Nature Nanotechn.*, 7(12):787–791, 2012.

36. A. Khaled, S. Guo, F. Li, and P. Guo. Controllable self-assembly of nanoparticles for specific delivery of multiple therapeutic molecules to cancer cells using RNA nanotechnology. *Nano Lett.*, 5(9):1797–1808, 2005.
37. V. Balzani, M. Gomez-Lopez, and J. F. Stoddart. Molecular machines. *Acc. Chem. Res.*, 31(7):405–414, 1998.
38. B. Odell, M. V. Reddington, A. M. Z. Slawin, N. Spencer, J. F. Stoddart, and D. J. Williams. Cyclobis(paraquat-p-phenylene): a tetracationic multipurpose receptor. *Angew. Chem. Int. Ed.*, 100(I):1547–1550, 1988.
39. A. R. Bernardo, J. F. Stoddart, and A. E. Kaifer. Cyclobis(paraquat-p-phenylene) as a synthetic receptor for electron-rich aromatic compounds: electrochemical and spectroscopic studies of neurotransmitter binding. *J. Amer. Chem. Soc.*, pages 10624–10631, 1992.
40. S. Andersen, M. Jensen, A. Sørensen, E. Miyazaki, K. Takimiya, Bo W. Laursen, A. H. Flood, and J. O. Jeppesen. Anion effects on the cyclobis(paraquat-p-phenylene) host. *Chem. Commun.*, 48:5157, 2012.
41. M. A. C. Stuart, W. T. S. Huck, J. Genzer, M. Müller, C. Ober, M. Stamm, G. B. Sukhorukov, I. Szleifer, V. V. Tsukruk, M. Urban, F. Winnik, S. Zauscher, I. Luzinov, and S. Minko. Emerging applications of stimuli-responsive polymer materials. *Nature Mater.*, 9(2):101–113, 2010.
42. A. Malfait, F. Coumes, D. Fournier, G. Cooke, and P. Woisel. A water-soluble supramolecular polymeric dual sensor for temperature and pH with an associated direct visible readout. *Eur. Polym. J.*, pages 552–558, 2015.
43. C. Pietsch, R. Hoogenboom, and U. S. Schubert. PMMA based soluble polymeric temperature sensors based on UCST transition and solvatochromic dyes. *Polym. Chem.*, page 1005, 2010.
44. C. Gota, S. Uchiyama, and T. Ohwada. Accurate fluorescent polymeric thermometers containing an ionic component. *Analyst*, pages 121–6, 2007.
45. S. W. Hong, C. H. Ahn, J. Huh, and W. H. Jo. Synthesis of a PEGylated polymeric pH sensor and its pH sensitivity by fluorescence resonance energy transfer. *Macromolecules*, 39(22):7694–7700, 2006.

46. L. Zhu, S. Powell, and S. G. Boyes. Synthesis of tertiary amine-based pH-responsive polymers by RAFT Polymerization. *J. Polym. Sci., Part A: Polym. Chem.*, 53(8): 1010–1022, 2015.

47. G. Filipcsei, I. Csetneki, A. Szilagyi, and M. Zrinyi. Magnetic field-responsive smart polymer composites. *Adv. Polym. Sci.*, 206(1):137–189, 2007.

48. S. Bhattacharya, F. Eckert, V. Boyko, and A. Pich. Temperature-, pH-, and magnetic-field-sensitive hybrid microgels. *Small*, 3(4):650–657, 2007.

49. M. Karg, I. Pastoriza-Santos, B. Rodriguez-González, R. Von Klitzing, S. Wellert, and T. Hellweg. Temperature, pH, and ionic strength induced changes of the swelling behavior of PNIPAM-poly(allylacetic acid) copolymer microgels. *Langmuir*, 24(12): 6300–6306, 2008.

50. M. Shibayama, F. Ikkai, S. Inamoto, S. Nomura, and C. C. Han. pH and salt concentration dependence of the microstructure of poly(N-isopropylacrylamide-co-acrylic acid) gels. *J. Chem. Phys.*, 105(10):4358, 1996.

51. P. R. Ashton, R. Ballardini, V. Balzani, S. E. Boyd, A. Credi, M. T. Gandolfi, M. Gómez-López, S. Iqbal, D. Philp, J. A. Preece, L. Prodi, H. G. Ricketts, J. F. Stoddart, M. S. Tolley, M. Venturi, A. J. P. White, and D. J. Williams. Simple Mechanical Molecular and Supramolecular Machines: Photochemical and Electrochemical Control of Switching Processes. *Chem. Eur. J.*, pages 152–170, 1997.

52. A. Suzuki and T. Tanaka. Phase transition in polymer gels induced by visible light. *Nature*, 346(6282):345–347, 1990.

53. F. Li, C. Xie, Z. Cheng, and H. Xia. Ultrasound responsive block copolymer micelle of poly(ethylene glycol)-poly(propylene glycol) obtained through click reaction. *Ultrason. Sonochem.*, 30:9–17, 2016.

54. W. Chen and J. Du. Ultrasound and pH Dually Responsive Polymer Vesicles for Anticancer Drug Delivery. *Sci. Rep.*, 3:1–9, 2013.

55. C. de Las Heras Alarcon, S. Pennadam, and C. Alexander. Stimuli responsive polymers for biomedical applications. *Chem. Soc. Rev.*, 34(3):276–285, 2005.

56. E. G. Kelley, J. N. L. Albert, M. O. Sullivan, and T. H. Epps. Stimuli-responsive copolymer solution and surface assemblies for biomedical applications. *Chem. Soc. Rev.*, 141(4):520–529, 2008.

57. W. Wang, Y. Li, and Z. Lu. Coil to globule transition of homo- and block-copolymer

with different topological constraint and chain stiffness. *Sci. China Chem.*, 58(9): 1471–1477, 2015.

58. K. A. Dill. The protein folding problem. *Physics Today*, 1993.
59. E. Sherman and G. Haran. Coil-globule transition in the denatured state of a small protein. *Proc. Nat. Acad. Sci. USA*, 103(31):11539–43, 2006.
60. V. A. Bloomfield. DNA condensation. *Curr. Opin. Struct. Biol.*, 6(3):334–341, 1996.
61. C. E. Immoos, S. J. Lee, and M. W. Grinstaff. DNA-PEG-DNA triblock macromolecules for reagentless DNA detection. *J. Amer. Chem. Soc.*, 126(35):10814–10815, 2004.
62. U. Rant, K. Arinaga, S. Scherer, E. Pringsheim, S. Fujita, N. Yokoyama, M. Tornow, and G. Abstreiter. Switchable DNA interfaces for the highly sensitive detection of label-free DNA targets. *Proc. Nat. Acad. Sci. USA*, 104(44):17364–9, 2007.
63. R. J. Mart, R. D. Osborne, M. M. Stevens, and R. V. Ulijn. Peptide-based stimuli-responsive biomaterials. *Soft Matter*, 2(10):822, 2006.
64. M. Yamada, M. Kondo, R. Miyasato, Y. Naka, J. Mamiya, M. Kinoshita, A. Shishido, Y. Yu, C. J. Barrett, and T. Ikeda. Photomobile polymer Materials—Various Three-dimensional movements. *J. Mater. Chem.*, 19(1):60, 2009.
65. M. Zrinyi. Intelligent polymer gels controlled by magnetic fields. *Colloid Polym. Sci.*, 278(2):98–103, 2000.
66. D. Roy, J. N. Cambre, and B. S. Sumerlin. Future perspectives and recent advances in stimuli-responsive materials. *Prog. Polym. Sci.*, 35(1-2):278–301, 2010.
67. W. Weng, J. B. Beck, A. M. Jamieson, and S. J. Rowan. Understanding the mechanism of gelation and stimuli-responsive nature of a class of metallo-supramolecular gels. *J. Amer. Chem. Soc.*, 128(35):11663–11672, 2006.
68. S. Qin, Y. Geng, D. E. Discher, and S. Yang. Temperature-controlled assembly and release from polymer vesicles of poly(ethylene oxide)-block-poly(N-isopropylacrylamide). *Adv. Mater.*, 18(21):2905–2909, 2006.
69. Y. Sagara and T. Kato. Stimuli-responsive luminescent liquid crystals: Change of photoluminescent colors triggered by a shear-induced phase transition. *Angew. Chem. Int. Ed.*, 47(28):5175–5178, 2008.
70. E. S. Gil and S. M. Hudson. Stimuli-reponsive polymers and their bioconjugates. *Prog. Polym. Sci.*, pages 1173–1222, 2004.

71. M. A. Ward and T. K. Georgiou. Thermoresponsive polymers for biomedical applications. *Polymers*, pages 1215–1242, 2011.

72. J. Seuring and S. Agarwal. Polymers with upper critical solution temperature in aqueous solution. *Macromol. Rapid Commun.*, pages 1898–1920, 2012.

73. H. G. Schild. Poly(N-isopropylacrylamide): experiment, theory and application. *Prog. Polym. Sci.*, 17(2):163–249, 1992.

74. Y. Xia, N. A. D. Burke, and H. D. H. Stöver. End group effect on the thermal response of narrow-disperse poly(N-isopropylacrylamide) prepared by atom transfer radical polymerization. *Macromolecules*, pages 2275–2283, 2006.

75. S. Carter, S. Rimmer, R. Rutkaite, L. Swanson, J. P. Fairclough, A. Sturdy, and M. Webb. Highly branched poly(N-isopropylacrylamide) for use in protein purification. *Biomacromolecules*, pages 1124–1130, 2006.

76. P. Kujawa, F. Segui, S. Shaban, C. Diab, Y. Okada, F. Tanaka, and F. M. Winnik. Impact of end-group association and main-chain hydration on the thermosensitive properties of hydrophobically modified telechelic poly(N-isopropylacrylamides) in water. *Macromolecules*, pages 341–348, 2006.

77. J. F. Lutz, Ö. Akdemir, and A. Hoth. Point by point comparison of two thermosensitive polymers exhibiting a similar LCST: Is the age of poly(NIPAM) over? *J. Amer. Chem. Soc.*, pages 13046–13047, 2006.

78. A. K. Tucker and M. J. Stevens. Study of the Polymer Length Dependence of the Single Chain Transition Temperature in Syndiotactic Poly(N-isopropylacrylamide) Oligomers in Water. *Macromolecules*, 45(16):6697–6703, 2012.

79. J. S. Park and K. Kataoka. Precise control of lower critical solution temperature of thermosensitive poly(2-isopropyl-2-oxazoline) via gradient copolymerization with 2-ethyl-2-oxazoline as a hydrophilic comonomer. *Macromolecules*, 39(19):6622–6630, 2006.

80. M. Jamroz-Piegza, A. Utrata-Wesolek, B. Trzebicka, and A. Dworak. Hydrophobic modification of high molar mass polyglycidol to thermosensitive polymers. *Eur. Polym. J.*, 42(10):2497–2506, 2006.

81. A. Dworak, B. Trzebick, and A. Utrata. Hydrophobically modified polyglycidol - the control of lower critical solution temperature. *Polym. Bull.*, 54:47–54, 2003.

82. Y. Zhang, S. Furyk, D. E. Bergbreiter, and P. S. Cremer. Specific ion effects on the

water solubility of macromolecules: PNIPAM and the Hofmeister series. *J. Amer. Chem. Soc.*, 127(41):14505–14510, 2005.

83. B. V. K. J. Schmidt, M. Hetzer, H. Ritter, and C. Barner-Kowollik. Modulation of the thermoresponsive behavior of poly(N,N-diethylacrylamide) via cyclodextrin host/guest interactions. *Macromol. Rapid Commun.*, pages 1306–1311, 2013.
84. F. A. Plamper, M. Ruppel, A. Schmalz, O. Borisov, M. Ballauff, and A. H. E. Müller. Tuning the Thermoresponsive Properties of Weak Polyelectrolytes: Aqueous Solutions of Star-Shaped and Linear Poly(N,N -dimethylaminoethyl Methacrylate). *Macromolecules*, 40(23):8361–8366, 2007.
85. R. Hoogenboom, H. M. L. Thijs, M. J. H. C. Jochems, B. M. van Lankvelt, M. W. M. Fijten, and U. S. Schubert. Tuning the LCST of poly(2-oxazoline)s by varying composition and molecular weight: alternatives to poly(N-isopropylacrylamide)? *Chem. Commun.*, pages 5758–5760, 2008.
86. G. Vancoillie, D. Frank, and R. Hoogenboom. Thermoresponsive poly(oligo ethylene glycol acrylates). *Prog. Polym. Sci.*, pages 1074–1095, 2014.
87. F. Dai, P. Wang, Y. Wang, L. Tang, J. Yang, W. Liu, H. Li, and G. Wang. Double thermoresponsive polybetaine-based ABA triblock copolymers with capability to condense DNA. *Polymer*, pages 5322–5328, 2008.
88. X. Huang, F. Du, R. Ju, and Z. Li. Novel acid-labile, thermoresponsive poly(methacrylamide)s with pendent ortho ester moieties. *Macromol. Rapid Commun.*, 28(5):597–603, 2007.
89. N. Shimada, M. Nakayama, A. Kano, and A. Maruyama. Design of UCST polymers for chilling capture of proteins. *Biomacromolecules*, pages 1452–1457, 2013.
90. L. Chen, Y. Honma, T. Mizutani, D. J. Liaw, J. P. Gong, and Y. Osada. Effects of polyelectrolyte complexation on the UCST of zwitterionic polymer. *Polymer*, pages 141–147, 2000.
91. F. Liu and S. Agarwal. Thermoresponsive gold nanoparticles with positive UCST-type thermoresponsivity. *Macromol. Chem. Phys.*, 216(4):460–465, 2015.
92. F. A. Plamper, A. Schmalz, M. Ballauff, and A. H. E. Müller. Tuning the thermoresponsiveness of weak polyelectrolytes by pH and light: Lower and upper critical-solution temperature of poly(N,N-dimethylaminoethyl methacrylate). *J. Amer. Chem. Soc.*, pages 14538–14539, 2007.

93. B. Hammouda, D. L. Ho, and S. Kline. Insight into Clustering in Poly(ethylene oxide) Solutions. *Macromolecules*, pages 6932–6937, 2004.

94. K. Van Durme, G. Van Assche, E. Nies, and B. Van Mele. Phase transformations in aqueous low molar mass poly(vinyl methyl ether) solutions: Theoretical prediction and experimental validation of the peculiar solvent melting line, bimodal LCST, and (adjacent) UCST miscibility gaps. *J. Phys. Chem. B*, pages 1288–1295, 2007.

95. J. V. M. Weaver, I. Bannister, K. L. Robinson, X. Bories-Azeau, S. P. Armes, M. Smallridge, and P. McKenna. Stimulus-Responsive Water-Soluble Polymers Based on 2-Hydroxyethyl Methacrylate. *Macromolecules*, 37(7):2395–2403, 2004.

96. L. Sambe, V. R. Delarosa, K. Belal, F. Stoffelbach, J. Lyskawa, F. Delattre, M. Bria, G. Cooke, R. Hoogenboom, and P. Woisel. Programmable polymer-based supramolecular temperature sensor with a memory function. *Angew. Chem. Int. Ed.*, pages 5044–5048, 2014.

97. V. R. de la Rosa and R. Hoogenboom. Solution polymeric optical temperature sensors with long-term memory function powered by supramolecular chemistry. *Chem. Eur. J.*, 21(3):1302–1311, 2015.

98. O. Kahn and C. J. Martinez. MOF76-Spin-Transition Polymers: From Molecular Materials Toward Memory Devices. *Science*, 279(5347):44–48, 1998.

99. H. Cheng, L. Shen, and C. Wu. LLS and FTIR studies on the hysteresis in association and dissociation of poly(N-isopropylacrylamide) chains in water. *Macromolecules*, pages 2325–2329, 2006.

100. A. P. Vogt and B. S. Sumerlin. Tuning the Temperature Response of Branched Poly(N-isopropylacrylamide) Prepared by RAFT Polymerization. *Macromolecules*, 41(20):7368–7373, 2008.

101. Y. Yang, X. Song, L. Yuan, M. Li, J. Liu, R. Ji, and H. Zhao. Synthesis of PNIPAM polymer brushes on reduced graphene oxide based on click chemistry and RAFT polymerization. *J. Polym. Sci., Part A: Polym. Chem.*, 50(2):329–337, 2012.

102. Sigma. Controlled radical polymerization guide. pages 12–14, 2012.

103. D. Greszta, D. Mardare, and K. Matyjaszewski. "Living" Radical Polymerization. 1. Possibilities and Limitations. *Macromolecules*, (27):638–644, 1994.

104. M. H. Stenzel, L. Cummins, G. E. Roberts, T. P. Davis, P. Vana, and C. Barner-Kowollik. Xanthate mediated living polymerization of vinyl acetate: A systematic

variation in MADIX/RAFT agent structure. *Macromol. Chem. Phys.*, 204(9):1160–1168, 2003.

105. R. Plummer, D. J. T. Hill, and A. K. Whittaker. Solution properties of star and linear poly(N-isopropylacrylamide). *Macromolecules*, 39(24):8379–8388, 2006.
106. K. Matyjaszewski. Controlled/living radical polymerization: State of the art in 2002. *ACS Symp. Ser.*, 2003.
107. W. A. Braunecker and K. Matyjaszewski. Controlled/living radical polymerization: Features, developments, and perspectives. *Prog. Polym. Sci.*, 32(1):93–146, 2007.
108. E. M. Ahmed. Hydrogel: Preparation, characterization, and applications: A review. *J. Adv. Res.*, 6(2):105–121, 2015.
109. E. A. Appel, J. del Barrio, X. J. Loh, and O. A. Scherman. Supramolecular polymeric hydrogels. *Chem. Soc. Rev.*, 41(18):6195, 2012.
110. A. S. Hoffman. Hydrogels for biomedical applications. *Adv. Drug Deliv. Rev.*, 64: 18–23, 2012.
111. B. Lindemann, U. P. Schro, and W. Oppermann. Influence of the Cross-Linker Reactivity on the Formation of Inhomogeneities in Hydrogels. *Macromolecules*, 30 (4):4073–4077, 1997.
112. K. Y. Lee and D. J. Mooney. Hydrogels for tissue engineering. *Chem. Rev.*, 101(7): 1869–1879, 2001.
113. N. Boucard, C. Viton, D. Agay, E. Mari, T. Roger, Y. Chancerelle, and A. Domard. The use of physical hydrogels of chitosan for skin regeneration following third-degree burns. *Biomaterials*, 28(24):3478–3488, 2007.
114. M. Asakawa, W. Dehaen, L. Gerrit, S. Menzer, J. Nouwen, M. Raymo, J. F. Stoddart, and D. J. Williams. Improved Template-Directed Synthesis of Cyclobis (paraquat-p-phenylene) atoms that are able to enter into edge-to-face T-type the plots illustrated in Figure 2b , determined by measur- and guest having molar concentration C , where C is. *J. Org. Chem.*, 3263(15):9591–9595, 1996.
115. S. Fujii and J.M. Lehn. Structural and Functional Evolution of a Library of Constitutional Dynamic Polymers driven by Recognition of Alkali Metal Ions. *Angew. Chem. Int. Ed.*, pages 3128–3132, 2009.
116. Http://www.chemistryviews.org/details/education/2538941/Tips_and_Tricks_for._the_Lab_Growing_Crystals_Part_3.html.

117. M. P. L. Werts, M. Van Den Boogaard, G. M. Tsivgoulis, and G. Hadziioannou. Mechanically linked polyrotaxanes: A stepwise approach. *Macromolecules*, 36(19): 7004–7013, 2003.

118. D. Meza, E. Arias, I. Moggio, J. Romero, J. M. Mata, R. M. Jiménez-Barrera, R. F. Ziolo, O. Rodríguez, and M. Ottonelli. Synthesis and photophysical and supramolecular study of π-conjugated (diethylene glycol methyl ether) benzoateethynylene oligomers and polymers. *Polym. Chem.*, pages 1639–1648, 2015.

119. H. Sharghi and M. H. Sarvari. Al2O3/MeSO3H (AMA) as a new reagent with high selective ability for monoesterification of diols. *Tetrahedron*, pages 3627–3633, 2003.

120. https://www.cmu.edu/maty/crp/features.html.

121. A. Favier, M. Charreyre, and C. Pichot. A detailed kinetic study of the RAFT polymerization of a bi-substituted acrylamide derivative: influence of experimental parameters. *Polymer*, 45(26):8661–8674, 2004.

122. C. N. Urbani and M. J. Monteiro. Nanoreactors for aqueous RAFT-mediated polymeriz ations. *Macromolecules*, pages 3884–3886, 2009.

123. G. Cooke, P. Woisel, M. Bria, F. Delattre, J. F. Garety, S. G. Hewage, G. Rabani, and G. M. Rosair. A tuneable self-complexing molecular switch. *Org. Lett.*, pages 1423–1426, 2006.

124. A. L. Kieran, S. I. Pascu, T. Jarrosson, M. J. Gunter, and J. K. M. Sanders. Dynamic synthesis of a macrocycle containing a porphyrin and an electron donor. *Chem. Commun.*, pages 1842–1844, 2005.

125. Z. Zhang, S. Maji, A. B. Antunes, R. De Rycke, Q. Zhang, R. Hoogenboom, and B. G. De Geest. Salt Plays a Pivotal Role in the Temperature-Responsive Aggregation and Layer-by-Layer Assembly of Polymer-Decorated Gold Nanoparticles. *Chem. Mater.*, pages 4297–4303, 2013.

4 Scientific article

Towards Responsive Polymer Hydrogel Sensors and Actuators

Annelore Podevyn[a], Zhanyao Hou[a], and Richard Hoogenboom[a*]

[a] Supramolecular Chemistry Group, Ghent University, Department of Organic and Macromolecular Chemistry, Ghent 9000, Belgium

*Richard.Hoogenboom@ugent.be

The design of a second generation polymeric hydrogel thermometers with a memory function is reported, based on thermoresponsive PNIPAM functionalized with 1,5-dialkoxynaphthalene guest moieties and cyclobis-(paraquat-*p*-phenylene)($CBPQT^{4+}$) host moieties as pendants. This supramolecular thermometer should possess an enlarged thermal memory function for the thermal history of the hydrogel and provides a visible readout. The synthesis of the polymerizable supramolecular host and guest molecules is described, together with the study of the RAFT polymerization of PNIPAM, providing the first steps towards this hydrogel sensor.

Keywords: host-guest chemistry, thermoresponsive polymers, poly(*N*-isopropylacrylamide)

Introduction

Biological processes have always been a source of inspiration for scientists to develop new materials. The specificity, high adaptability and dynamic nature of these processes encouraged scientist to investigate the intermolecular interactions between molecules that

are of a reversible nature. These non-covalent interactions are generally weaker than the covalent interactions, but can be used in a multiple and cooperative manner to give the strength needed to form stable complexes and provide the required adaptability and specificity. Hence, the research field that focusses on these intermolecular interactions between molecules, and analyzes how different molecules can recognize each other, assemble and function on a molecular scale is called supramolecular chemistry. One interesting type of mechanism that occurs in nature and relies on non-covalent interactions is the recognition between an enzyme and its substrate. This mechanism is based on host-guest interactions, which arise from the fact that the significantly larger "host" enzyme is capable of enclosing the smaller "guest" substrate via non-covalent interactions. Compatible geometry (lock-key principle) and complementary distribution of the active groups are required to get a maximum specificity and stability between both molecules.[1] The strength of the host-guest complexation generally depends on the size of both molecules (compatible geometry) and the type and number of interactions.

Within this study, the focus will be on host-guest chemistry where the host is a macrocyclic cyclobis(paraquat-*p*-phenylene) ($CBPQT^{4+}$, bluebox) structure and the guest is a 1,5-dialkoxynaphthalene derivative. The size and electron-accepting properties of the bluebox' cavity, make it ideal for the inclusion of electron-rich aromatic subunits such as the 1,5-dialkoxynaphthalene derivative.[2]

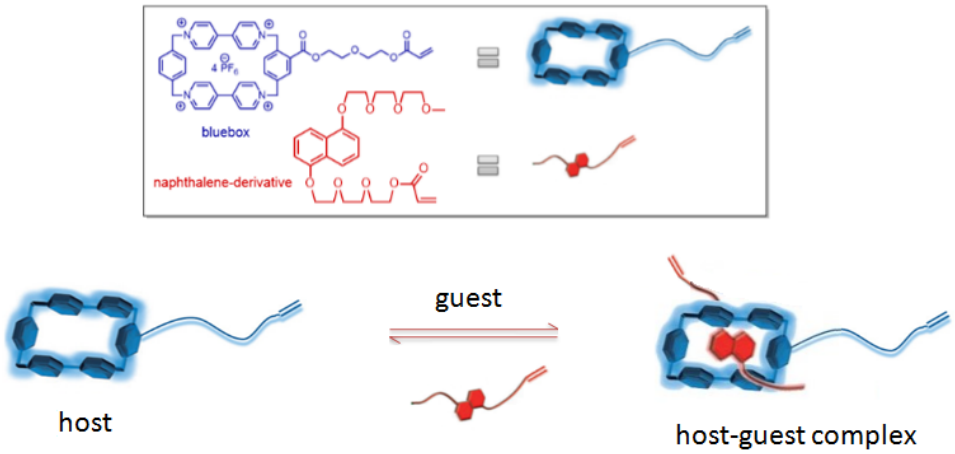

Figure 4.1: *Overview of the supramolecular host and guest molecules used in this project and the association equilibrium.*

Another important feature of biological processes is their ability to respond to small

changes in their local environment through a property change. This is responsible for the high adaptivity of living species and stems form the possibility to alter the non-covalent intermolecular bonds *via* a change in amount or nature of the interactions or a variation in conditions, such as concentration or temperature. Thermoresponsive polymers are of special interest for a wide range of applications,[3–7] and undergo a phase transition upon a change in temperature. These polymers can exhibit LCST and/or UCST behavior[8–13] (lower or upper critical solution temperature) depending on if the polymer solution is miscible below or above this critical temperature, respectively. The polymer used in this study is PNIPAM, which exhibits LCST behavior.[14–16] The solubility in water, good biocompatibility and LCST value around body temperature (32°C) make this polymer very interesting to be used in biomedical applications.[17] Furthermore, PNIPAM exhibits a hysteresis in temperature.[16,18] This means that this thermoresponsive polymer exhibits a memory function for the thermal history of the solution. Since the observed hysteresis is too small to result in a useful thermal memory, PNIPAM can be combined with supramolecular host-guest chemistry to develop supramolecular thermometers. These thermometers possess a larger thermal memory function since complexation allows the formation of a kinetically trapped state, making them more suitable to be used in applications.

Such soluble polymeric thermometers have already conceptually been developed by our research group based on PNIPAM with dangling dialkoxynaphthalene guests and the supra-molecular association with $CBPQT^{4+}$.[19] However, these thermometers undergo macroscopic phase separation which strongly limits their applicability. Therefore, this study aims to develop a second generation polymeric hydrogel sensor with an analogous memory function, which will give rise to more widely applicable sensors. These hydrogels are composed of thermoresponsive PNIPAM, functionalized with 1,5-dialkoxynapthalene guest moieties and cyclobis(paraquat-*p*-phenylene)($CBPQT^{4+}$) host moieties as pendants to enlarge the thermal memory window and provide a visible readout. The synthesis of monomers bearing supramolecular host and guest moieties and the RAFT polymerization of NIPAM were studied. The copolymerization of NIPAM with the functionalized monomers and the memory function of the copolymer will be investigated in future research.

Experimental

The used materials, equipment and synthesis routes for the target compounds is described in the supporting information.

Results and Discussion

Synthesis of the supramolecular host

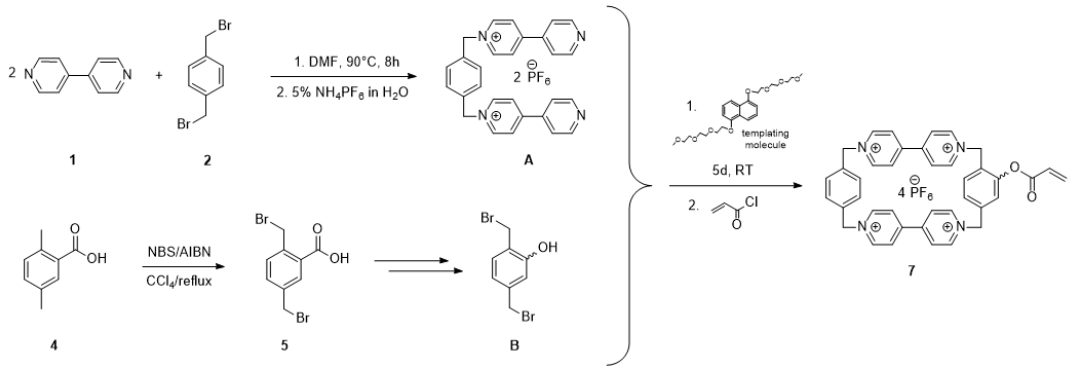

Scheme 4.1: *Synthetic pathway for the supramolecular host molecule, a CBPQT^{4+} derivative.*

The supramolecular host molecule, which is a CBPQT^{4+} derivative, was synthesized from two parts **A** and **B** as seen in Scheme 4.1. Compound **A** was prepared by first combining 4,4'-dipyridyl **1** and α,α-dibromo-*p*-xylene **2** at elevated temperature to produce the water soluble bis(pyridinium).2Br. This was then treated with an excess of saturated aqueous NH_4PF_6 solution, ensuring counterion exchange (Br^- to PF_6^-) and inevitably changing the solubility of the bis(pyridinium) from water to organic solvents. Ultimately, bis(pyridinium).2PF_6 was obtained with a yield of 69.6%.

The synthesis of compound **B** started with a radical bromination reaction, based on the literature procedure of Ashton *et al.*[20]. In the second step, it was attempted to provide the 2,5-bis(bromomethyl)benzoic acid **5** with a linker, to improve the flexibility of the bluebox within the hydrogel. This proved to be more difficult, since most of the tested procedures did not yield the right compound. As shown in Scheme 4.2, different methods were examined in the search for an operative procedure.

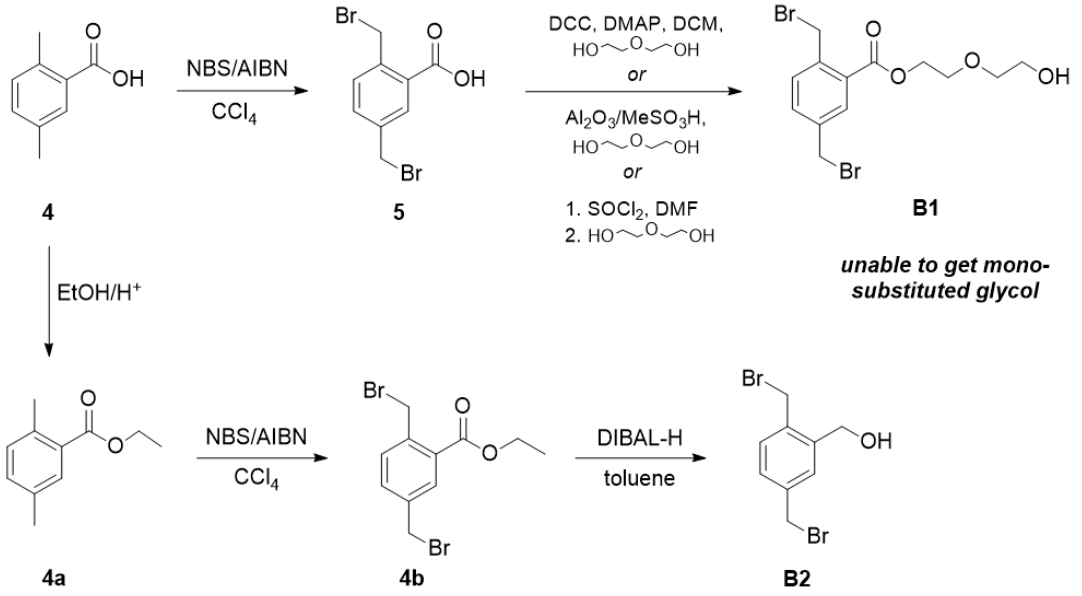

Scheme 4.2: *Different reaction procedures tested in an attempt to generate the desired compound* ***B****.*

Following the literature procedure[20] for the initial radical bromination reaction of 2,5-dimethylbenzoic acid **4**, with AIBN as initiator, did not yield the expected pure compound. Additional purification steps did not allow to isolate the pure 2,5-bis(bromomethyl) benzoic acid **5**. Analysis of the obtained product by ^{1}H NMR spectroscopy and LCMS revealed the presence of side products such as the mono-, tri- and tetrabrominated acids. Removal of the mono- and tetrabrominated acid was achieved by recrystallization from hexane vapor diffusion in a chloroform solution, but it failed to separate the 2,5-bis(bromomethyl)benzoic acid **5** from the tribrominated acid **5.II**. The presence of these side products indicates that the reaction time was too long. Hence, the reaction was performed again under identical conditions, while being monitored using ^{1}H NMR spectroscopy (Figure 4.2). This revealed that a maximum reaction time of 3 hours was sufficient to not generate the tribrominated acid as a side product that could not be removed by recrystallization. Therefore, the reaction was terminated after 3 hours, forming only a small amount of side product that could still be removed by recrystallization. The pure dibrominated acid **5** was isolated with a yield of 25.1%.

In the next step, the carboxylic acid was converted to create a linker between the bluebox and the polymerizable double bond and different methods were attempted in the search for an successful procedure (Scheme 4.2). Initially, the proposed linker consisted of a

ethylene glycol ether unit that was long enough to ensure a good flexibility of the host in the hydrogel. In a first attempt, the 2,5-bis(bromomethyl)benzoic acid **5** was reacted with thionyl chloride under inert conditions to generate the benzoyl chloride **5a**.[20] This was then added dropwise to a solution of diethylene glycol in dry DCM to attach the linker.

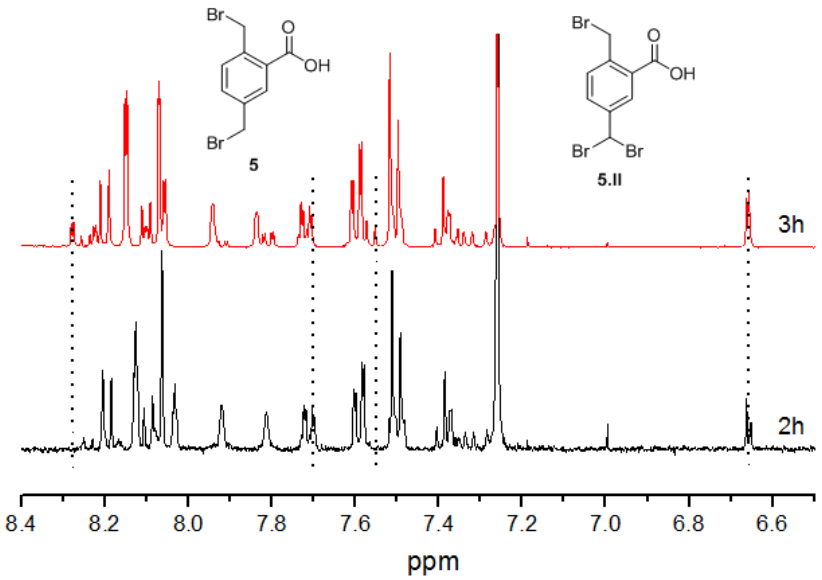

Figure 4.2: *Radical bromination reaction of 2,5-dimethylbenzoic acid with NBS: conversion after 2 hours and 3 hours. The dotted lines represent the* ^1H *chemical shifts of tribrominated acid* ***5.II*** *as side product, which are used to determine the maximum reaction time.*

Continuing with the reaction procedure of Ashton *et al.*[20] resulted in the formation of an oil-like solid, in which the desired product was not detected by LCMS. A second method for synthesizing the (ethylene glycol ether) 2,5-bis(bromomethyl) benzoate **B1** was attempted, based on the use of a DCC-coupling reaction[21] to attach the linker to the 2,5-bis(bromomethyl)benzoic acid **5**. Unfortunately, only the disubstituted glycol was formed in small amount, together with a large amount of unreacted starting material. A third method was attempted, where the monoesterification was performed in the presence of $Al_2O_3/MeSO_3H$ (AMA), without the use of any solvents. Sharghi *et al.*[22] claimed this reagent very effective and highly selective for the monoesterification of diols in high yields. Performing this reaction under exact the same reaction conditions did not yield the expected monoester product and ^{1}H NMR spectroscopy revealed that the obtained mixture consisted purely of the diester product and some unreacted starting material. Since these three literature procedures, that clearly stated that this type of reaction should work, did

not yield the desired compound, an alternative compound **B2** was produced without a linker. This was done by reducing the already synthesized 2,5-bis(bromomethyl)benzoate **4b** to the corresponding alcohol **B2**[23]. Reacting the 2,5-bis(bromomethyl)benzoate **4b** with DIBAL-H for three hours at 0°C and acidic workup, generated the pure alcohol **B2** with a 12% yield.

Because of time limitations, the assembly of compounds **A** and **B** and the reaction with acryloyl chloride could not be carried out. All unsuccessful reactions were performed at least twice to exclude coincidence.

Synthesis of the supramolecular guest

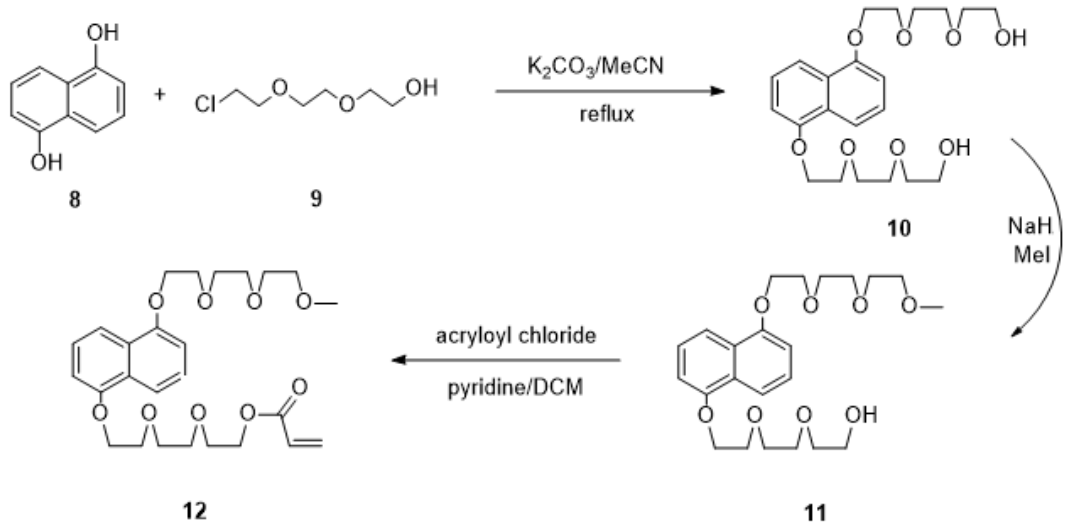

Scheme 4.3: *Synthetic pathway for the supramolecular guest molecule, a 1,5-dialkoxynaphthalene derivative.*

The supramolecular guest molecule is a 1,5-dialkoxynaphthalene derivative and was synthesized according to optimized literature procedures. First, double alkylation of 1,5-dihydroxynaphthalene **8** was achieved by reaction with 2-(2-chloroethoxy)ethoxyethanol **9** under basic conditions (K_2CO_3), which resulted in the formation of the diol **10** with a yield of 47.9%.[24] The yielded 1,5-bis[2-(2-(2-hydroxyethoxy)ethoxy)ethoxy]-naphthalene **10** was subsequently methylated under basic conditions (NaH) with iodomethane (MeI) to generate the mono-methylated diol **11**, as described in literature.[20] The desired product was isolated with a yield of 17.5%. Further reaction of component **11** with acryloyl

chloride in the presence of a base (pyridine) resulted in the formation of the polymerizable guest molecule **12**.

Polymer synthesis

For the second part of this study, a RAFT copolymerization of these supramolecular compounds with NIPAM was planned. But since the supramolecular host molecule was not ready in time, only a test homopolymerization of NIPAM could be executed. *N*-isopropylacrylamide RAFT polymerizations at 70°C and 75°C were performed, together with kinetic studies to analyze the livingness and controlled behavior of the polymerization reactions at different temperatures. Figure 4.3 (left) shows the first order kinetic plot that was constructed by measuring the concentration of monomer periodically ([M]) during the polymerization *via* GC analysis. An expected linear relationship is obtained for the polymerization at 70°C, confirming the living character of the polymerization. The polymerization at 75°C follows an almost linear relationship until 120 minutes, after which a decrease in slope is observed. This indicates the presence of termination reactions at longer reaction times.

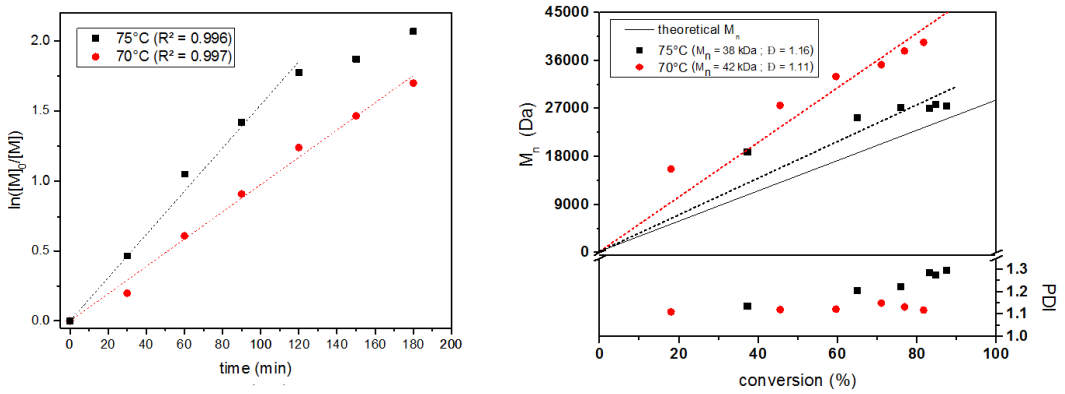

Figure 4.3: *Kinetic study of the RAFT polymerization of NIPAM using [NIPAM]:[MBTTC]:[I] = 250:1:0.25, 2M monomer concentration in DMF at 70°C and 75°C. Left: first order kinetic plot. Right: number average molecular weight (M_n) and dispersity (Đ) as function of degree of conversion.*

The number average molecular weight (M_n) and polydispersity (Đ) were determined during the polymerization *via* SEC analysis. This data is plotted in function of the monomer conversion in Figure 4.3 (right) . Again, a linear correlation is expected for "living" polymerizations. The polymerization at 75°C shows a high degree of conversion and a high

molecular weight after only 30 minutes. To reveal the real trend of this data, more samples should have been taken in the beginning of the polymerization. Comparing with the other data, the polymerization will probably have shown an approximately linear relationship at lower conversion and a decrease of slope at higher conversion. The observed decrease suggest the presence of transfer or termination reactions, which will still increase the conversion (consumption of monomer), but will contribute less to the increase in molecular weight. This phenomenon will also lead to an increased polydispersity, causing a noticeable increase in polydispersity at higher conversions. The polymerization at 70°C exhibits a more linear trend, which proves the better "livingness" of the polymerization. Also, the polydispersity of the 70°C polymerization is better than the polymerization at 75°C, as it shows more constant and narrow values. By combining both graphs, we can conclude that the RAFT polymerization proceeds in a living manner, but that the polymerization temperature should no be too high to avoid termination and transfer reactions.

Conclusion

Synthesis routes for the supramolecular host and guest molecules were designed and developed. While the supramolecular guest was successfully synthesized without any major problems, the synthesis of the supramolecular host showed some issues. The supposedly straightforward procedure for the radical bromination of the second part of the host, turned out to be more time consuming in finding the ideal reaction conditions. Furthermore, applying the initially proposed ethylene glycol ether linker turned out to be more difficult than expected, probably due to the low solubility of the acid, and was due to time limitations replaced by a shorter ethyl alcohol linker. Hence, the assembly of compounds **A** and **B** of the host and the reaction with acryloyl chloride could not be carried out and remain an item for further research. In addition, successful homopolymerizations were carried out with NIPAM at 70°C and 75°C. The polymerization reaction at 70°C reflected a better livingness and much more controlled behavior.
Future research will focus on developing a suitable synthesis route for the preparation of a host molecule with an appropriate linker, and copolymerization reactions of the obtained supramolecular host and guest molecules with NIPAM.

Acknowlegdements

I would like to thank my promotor, Prof. dr. Richard Hoogenboom for giving me the opportunity to be part of his research group. And a special thanks to my supervisor Zhanyao Hou for his guidance and advice during this project.

References

1. E. Frieden. Non-Covalent Interactions: Key to biological flexibility and specificity. *J. Chem. Educ.*, pages 754–761, 1975.
2. A. R. Bernardo, J. F. Stoddart, and A. E. Kaifer. Cyclobis(paraquat-p-phenylene) as a synthetic receptor for electron-rich aromatic compounds: electrochemical and spectroscopic studies of neurotransmitter binding. *J. Amer. Chem. Soc.*, pages 10624–10631, 1992.
3. D. Schmaljohann. Thermo- and pH-responsive polymers in drug delivery. *Adv. Drug Deliv. Rev.*, pages 1655–1670, 2006.
4. C. Gota, S. Uchiyama, and T. Ohwada. Accurate fluorescent polymeric thermometers containing an ionic component. *Analyst*, pages 121–6, 2007.
5. C. Pietsch, R. Hoogenboom, and U. S. Schubert. PMMA based soluble polymeric temperature sensors based on UCST transition and solvatochromic dyes. *Polym. Chem.*, page 1005, 2010.
6. A. Malfait, F. Coumes, D. Fournier, G. Cooke, and P. Woisel. A water-soluble supramolecular polymeric dual sensor for temperature and pH with an associated direct visible readout. *Eur. Polym. J.*, pages 552–558, 2015.
7. M. A. Ward and T. K. Georgiou. Thermoresponsive polymers for biomedical applications. *Polymers*, pages 1215–1242, 2011.
8. L. Chen, Y. Honma, T. Mizutani, D. J. Liaw, J. P. Gong, and Y. Osada. Effects of polyelectrolyte complexation on the UCST of zwitterionic polymer. *Polymer*, pages 141–147, 2000.
9. F. Dai, P. Wang, Y. Wang, L. Tang, J. Yang, W. Liu, H. Li, and G. Wang. Double thermoresponsive polybetaine-based ABA triblock copolymers with capability to condense DNA. *Polymer*, pages 5322–5328, 2008.
10. R. Hoogenboom, H. M. L. Thijs, M. J. H. C. Jochems, B. M. van Lankvelt, M. W. M. Fijten, and U. S. Schubert. Tuning the LCST of poly(2-oxazoline)s by varying composition and molecular weight: alternatives to poly(N-isopropylacrylamide)? *Chem. Commun.*, pages 5758–5760, 2008.
11. B. V. K. J. Schmidt, M. Hetzer, H. Ritter, and C. Barner-Kowollik. Modulation of the thermoresponsive behavior of poly(N,N-diethylacrylamide) via cyclodextrin host/guest interactions. *Macromol. Rapid Commun.*, pages 1306–1311, 2013.
12. N. Shimada, M. Nakayama, A. Kano, and A. Maruyama. Design of UCST polymers for chilling capture of proteins. *Biomacromolecules*, pages 1452–1457, 2013.

13. J. Seuring and S. Agarwal. Polymers with upper critical solution temperature in aqueous solution. *Macromol. Rapid Commun.*, pages 1898–1920, 2012.
14. H. G. Schild. Poly(N-isopropylacrylamide): experiment, theory and application. *Prog. Polym. Sci.*, pages 163–249, 1992.
15. P. Kujawa, F. Segui, S. Shaban, C. Diab, Y. Okada, F. Tanaka, and F. M. Winnik. Impact of end-group association and main-chain hydration on the thermosensitive properties of hydrophobically modified telechelic poly(N-isopropylacrylamides) in water. *Macromolecules*, pages 341–348, 2006.
16. J. F. Lutz, Ö. Akdemir, and A. Hoth. Point by point comparison of two thermosensitive polymers exhibiting a similar LCST: Is the age of poly(NIPAM) over? *J. Amer. Chem. Soc.*, pages 13046–13047, 2006.
17. E. S. Gil and S. M. Hudson. Stimuli-reponsive polymers and their bioconjugates. *Prog. Polym. Sci.*, pages 1173–1222, 2004.
18. H. Cheng, L. Shen, and C. Wu. LLS and FTIR studies on the hysteresis in association and dissociation of poly(N-isopropylacrylamide) chains in water. *Macromolecules*, pages 2325–2329, 2006.
19. L. Sambe, V. R. Delarosa, K. Belal, F. Stoffelbach, J. Lyskawa, F. Delattre, M. Bria, G. Cooke, R. Hoogenboom, and P. Woisel. Programmable polymer-based supramolecular temperature sensor with a memory function. *Angew. Chem. Int. Ed.*, pages 5044–5048, 2014.
20. P. R. Ashton, R. Ballardini, V. Balzani, S. E. Boyd, A. Credi, M. T. Gandolfi, M. Gómez-López, S. Iqbal, D. Philp, J. A. Preece, L. Prodi, H. G. Ricketts, J. F. Stoddart, M. S. Tolley, M. Venturi, A. J. P. White, and D. J. Williams. Simple Mechanical Molecular and Supramolecular Machines: Photochemical and Electrochemical Control of Switching Processes. *Chem. Eur. J.*, pages 152–170, 1997.
21. D. Meza, E. Arias, I. Moggio, J. Romero, J. M. Mata, R. M. Jiménez-Barrera, R. F. Ziolo, O. Rodríguez, and M. Ottonelli. Synthesis and photophysical and supramolecular study of π-conjugated (diethylene glycol methyl ether) benzoateethynylene oligomers and polymers. *Polym. Chem.*, pages 1639–1648, 2015.
22. H. Sharghi and M. H. Sarvari. Al2O3/MeSO3H (AMA) as a new reagent with high selective ability for monoesterification of diols. *Tetrahedron*, pages 3627–3633, 2003.
23. G. Cooke, P. Woisel, M. Bria, F. Delattre, J. F. Garety, S. G. Hewage, G. Rabani, and G. M. Rosair. A tuneable self-complexing molecular switch. *Org. Lett.*, pages 1423–1426, 2006.
24. A. L. Kieran, S. I. Pascu, T. Jarrosson, M. J. Gunter, and J. K. M. Sanders. Dynamic synthesis of a macrocycle containing a porphyrin and an electron donor. *Chem. Commun.*, pages 1842–1844, 2005.
25. C. N. Urbani and M. J. Monteiro. Nanoreactors for aqueous RAFT-mediated polymeriz ations. *Macromolecules*, pages 3884–3886, 2009.
26. Z. Zhang, S. Maji, A. B. Antunes, R. De Rycke, Q. Zhang, R. Hoogenboom, and B. G. De Geest. Salt Plays a Pivotal Role in the Temperature-Responsive Aggregation and Layer-by-Layer Assembly of Polymer-Decorated Gold Nanoparticles. *Chem. Mater.*, pages 4297–4303, 2013.

Supporting Information

Materials

Unless otherwise specified, all reagents were used as received. Commonly used solvents were of HPLC grade and were purchased from Sigma-Aldrich (DCM, MeOH, EtOAc, Et_2O), Fisher Chemical (*n*-hexane, toluene, $CHCl_3$), Acros Organics (DMF) and Chem-lab (EtOH). Deuterated solvents for ^{1}H NMR and ^{13}C NMR spectroscopy like chloroform-*d* ($CDCl_3$, ≥99.8% D) and dimethylsulfoxide-*d*6 (DMSO-*d*6, ≥99.8% D), were purchased from Euriso-top. Dry solvents were obtained from a custom made JW Meyer solvent purification system by drying over aluminium oxide columns (DCM, MeCN, THF, DMF) or by a reflux setup under nitrogen atmosphere (toluene). All chemicals were purchased from Sigma-Aldrich, with the exception of diethylene glycol (ucb), Al_2O_3 (Merck KGaA), $NaHCO_3$ (VWR International), H_2SO_4 and $MgSO_4$ (Fisher Chemical), 2,5-dimethylbenzoic acid and 2-(2-chloro-ethoxy)ethoxy-ethanol (TCI), α,α-dibromo-*p*-xylene, ammonium hexafluorophosphate and methanesulfonic acid (Fluka), CCl_4, thionyl chloride, K_2CO_3, pyridine and Na_2CO_3 (Acros Organics). Azobis(isobutyronitrile) (Sigma-Aldrich) was recrystallized from diethyl ether and stored at -7°C. N-isopropylacrylamide (Sigma-Aldrich) was recrystallized two times from hexane prior to use. Methyl-2-(n-butyltrithiocarbonyl)propanoate (MBTTCP) was prepared according to the established procedure.[25]

Equipment

Column chromatography was performed with a *Biosolve* silica gel stationary phase or a *Merck KGaA* neutral alumina phase. Column flash chromatography was performed on a Reveleris Flash Chromatography System using a cartridge containing the stationary phase and a mobile phase that can be varied. A number of stationary phases and four solvent reservoirs are available. A UV dectector is present that can monitor two wavelengths simultaneously as well as an evaporative light scattering detector (ELSD). The ELSD provides the ability to monitor all non-volatile compounds in the eluent and allows the user to detect for compounds that do not absorb UV radiation. An additional benefit of the ELSD is the ability to employ mobile phases that absorb light at the same wavelength as the compound(s) of interest. Centrifugation was performed on

an ALC multispeed refrigerated centrifuge PK 121R from Thermo Scientific using 50 mL centrifuging tubes with screw caps from VWR or 15 mL high clarity polypropylene conical tubes from Falcon. Liquid chromatography mass spectrometry (LCMS) analysis was performed on an Agilent 1100 HPLC with quaternary pump and UV-DAD detection, coupled to an Agilent G1956B MSD. Ionization of the samples was achieved through electronspray ionization (ESI). Nuclear magnetic resonance spectra were recorded on a Bruker Avance 300 MHz and 400 MHz spectrometer and at room temperature. ^{1}H NMR and ^{13}C NMR spectra were measured in chloroform-*d* ($CDCl_3$) and dimethylsulfoxide-*d*6 (DMSO-*d*6) purchased from Euriso-top. Gas chromatography (GC) was performed on an Agilent Technologies 7890A system equipped with an Agilent J&W Advanced Capillary GC column (30 m, 0.320 mm, and 0.25 µm). Injections were performed with an Agilent Technologies 7693 auto sampler. Detection was done with a FID detector. Injector and detector temperatures were kept constant at 250°C and 280°C, respectively. The column was initially set at 50°C, followed by two heating stages: from 50°C to 100°C with a rate of 20°C/min, and from 100°C to 300°C with a rate of 40°C/min. This temperature was held for 30 seconds. Conversion was determined based on the integration of monomer peaks using solvent (DMF) as internal standard. Size exclusion chromatography (SEC) was performed on a Agilent 1260-series HPLC system equipped with a 1260 online degasser, a 1260 ISO-pump, a 1260 automatic liquid sampler (ALS), a thermostatted column compartment (TCC), a 1260 diode array detector (DAD) and a 1260 refractive index detector (RID). DMAc containing 50 mM of LiCl was used as eluent at a flow rate of 0.6 mL/min. The SEC traces were analysed using the Agilent Chemstation software with the GPC add on. Molar mass and PDI values were calculated against PMMA standards.

Monomer synthesis

1,1'-(1,4-phenylenebis(methylene))bis(4,4'pyridinium)bis(hexafluorophosphate) **A**

A solution of 4,4'-dipyridyl **1** (2 g, 12.8 mmol) in 30 mL dry DMF was heated to 90°C under inert atmosphere. To this, a solution of α,α-dibromo-*p*-xylene **2** (0.338 g, 1.28 mmol) in 10 mL dry DMF was added dropwise and the solution was stirred overnight at 90°C. The obtained precipitate was filtered and washed four times with Et_2O before being dissolved in water to give a light yellow solution. A saturated NH_4PF_6 aqueous solution (589.75 mg, 3.618 mmol) was added and the solution was stirred for 1h. The

precipitate was collected by centrifugation (6°C, 10000 rpm, 8 min.) and washed with water to give a light brown, solid product **A** (0.629 g, 0.891 mmol, 69.6%).

^{1}**H NMR** (400 MHz, DMSO-*d*6) δ_H = 9.33 (d, J = 7.0 Hz, 4H, $-^{+}NC_5H_2H_2-$), 8.87 (d, J = 6.2 Hz, 4H, $-^{+}NC_5H_2H_2-$), 8.64 (d, J = 7.0 Hz, 4H, $-C_5H_2H_2N$), 8.00 (d, J = 6.2 Hz, 4H, $-C_5H_2H_2N$), 7.66 (s, 4H, $C_6H_4[CH_2-^{+}NC_5H_4-C_5H_4N]_2$), 5.88 (s, 4H, $C_6H_4[CH_2-^{+}NC_5H_4-C_5H_4N]_2$).

^{13}**C NMR** (101 MHz, DMSO) δ_C = 152.92 (C_q), 150.98 (CH), 145.35 (CH), 140.75 (C_q), 135.36 (C_q), 129.58 (CH), 125.88 (CH), 121.92 (CH), 62.41 (CH_2).

ESI-MS: $[M]^{2+}$ = 208.10

ethyl 2,5-dimethylbenzoate **4a**[20] Sulfuric acid (2.857 mL, 53.603 mmol) and 2,5-dimethylbenzoic acid **4** (2 g, 13.317 mmol) were dissolved in 30 mL ethanol and heated under reflux overnight. After cooling and concentrating, the obtained residue was dissolved in 30 mL DCM and washed with saturated aqueous Na_2CO_3 and water. The organic layer was dried over $MgSO_4$, filtered and the filtrate was concentrated to yield a clear, colorless oil (1.934 g, 10.853 mmol, 81.5%).

^{1}**H NMR** (400 MHz, $CDCl_3$) δ_H = 7.72 (s, 1H, $-C_6H_3^-$), 7.19 (d, J = 9.4 Hz, 1H, $-C_6H_3-$), 7.12 (d, J = 7.8 Hz, 1H, $-C_6H_3-$), 4.36 (q, J = 7.1 Hz, 2H, $-C_6H_3-CO_2CH_2CH_3$), 2.55 (s, 3H, $[CH_3]_2-C_6H_3-$), 2.35 (s, 3H, $[CH_3]_2-C_6H_3-$), 1.40 (t, J = 7.1 Hz, 3H, $-C_6H_3-C$
$O_2CH_2CH_3$).

^{13}**C NMR** (101 MHz, $CDCl_3$) δ_C = 167.88 (C_q), 136.83 (C_q), 135.18 (C_q), 132.57 (CH), 131.57 (CH), 130.91 (CH), 129.75 (C_q), 60.62 (CH_2), 21.22 (CH_3), 20.77 (CH_3), 14.36 (CH_3).

ESI-MS: $[M+H]^+$ = 179.10

ethyl 2,5-bis(bromomethyl)benzoate **4b**[20] NBS (2.96 g, 14.03 mmol) and a catalytic amount of AIBN were added to a solution of ethyl 2,5-dimethylbenzoate **4a** (1.25 g, 7.013 mmol) in CCl_4 and the suspension was refluxed for 3h under nitrogen. After cooling and filtration of the succinimide, the filtrate was concentrated and the resulting oil dissolved in 15 mL DCM. To this, 90 mL hexane was added and the solution produced a white precipitate after overnight cooling at -30°C. The product was collected and its purity confirmed by ^{1}H NMR spectroscopy (630 mg, 1.88 mmol, 26.7%).

^{1}H NMR (400 MHz, $CDCl_3$) δ_H = 7.98 (s, J = 1.9 Hz, 1H, $-C_6H_3[CH_2Br]_2$), 7.52 (dd, J = 7.9, 1.9 Hz, 1H, $-C_6H_3[CH_2Br]_2$), 7.44 (d, J = 7.9 Hz, 1H, $-C_6H_3[CH_2Br]_2$), 4.93 (s, 2H, $-C_6H_3[CH_2Br]_2$), 4.49 (s, 2H, $-C_6H_3[CH_2Br]_2$), 4.42 (q, J = 7.1 Hz, 2H, $-CO_2CH_2CH_3$), 1.44 (t, J = 7.1 Hz, 3H, $-CO_2CH_2CH_3$).
^{13}C NMR (101 MHz, $CDCl_3$) δ_C = 166.07 (C_q), 139.23 (C_q), 138.30 (C_q), 132.84 (CH), 132.26 (CH), 131.71 (CH), 129.97 (C_q), 61.59 (CH_2), 31.89 (CH_2), 30.95 (CH_2), 14.80 (CH_3).
ESI-MS: $[M+H]^+$ = 336.9

2,5-bis(bromomethyl)benzyl alcohol **B2**[23] Ethyl 2,5-bis(bromomethyl)benzoate **4b** (294 mg, 0.875 mmol) in 5 mL toluene was added dropwise to a cooled (0°C) solution of DIBAL-H (2 mL, 17.3 mmol)(1M in THF) in 10 mL toluene, under inert conditions. The mixture was stirred for 3h at 0°C, after which HCl was added until a pH of 1 was reached. The organic phase was extracted, washed with water, dried over $MgSO_4$ and filtered. After concentrating over reduced pressure, the product was washed with ice-cold ether to give a white powder **B2** (30.82 mg, 0.11 mmol, 12%).
^{1}H NMR (300 MHz, $CDCl_3$) δ_H = 7.48 (s, 1H, $-C_6H_3^-$), 7.34 (s, 1H, $-C_6H_3^-$), 7.33 (d, J = 1.7 Hz, 1H, $-C_6H_3^-$), 4.84 (s, 2H, $-C_6H_3-CH_2-OH$), 4.60 (s, 2H, $-C_6H_3[CH_2Br]_2$), 4.48 (s, 2H, $-C_6H_3[CH_2Br]_2$)
^{13}C NMR (101 MHz, $CDCl_3$) δ_C = 139.90 (C_q), 138.8 (C_q), 135.78 (C_q), 131.15 (CH), 129.36 (CH), 128.88 (CH), 62.41 (CH_2), 32.68 (CH_2), 30.19 (CH_2).

2,5-bis(bromomethyl)benzoic acid **5**[20] NBS (39.12 g, 219.80 mmol) and a catalytic amount of AIBN (0.05 g, 0.304 mmol) were added to a solution of 2,5-dimethylbenzoic acid **4** (15.06 g, 100.26 mmol) in CCl_4 and the suspension was refluxed for 3h under nitrogen. After cooling and filtration of the succinimide, the solution was left to stand overnight. The obtained precipitate was filtered and dried under vacuum. Purification was done by recrystallization (vapor diffusion): the product was dissolved in chloroform and put in a hexane environment to produce white, needle-like crystals **5** (7.76 g, 25.19 mmol, 25.1%).
^{1}H NMR (300 MHz, $CDCl_3$) δ_H = 8.13 (s, 1H, $-C_6H_3[CH_2Br]_2$), 7.59 (dd, J = 8.0, 2.0 Hz, 1H, $-C_6H_3[CH_2Br]_2$), 7.50 (d, J = 7.9 Hz, 1H, $-C_6H_3[CH_2Br]_2$), 4.99 (s, 2H,

$-C_6H_3[CH_2Br]_2$), 4.50 (s, 2H, $-C_6H_3[CH_2Br]_2$).

^{13}C NMR (126 MHz, $CDCl_3$) δ_C = 170.49 (C_q), 140.29 (C_q), 138.54 (C_q), 133.99 (CH), 132.74 (CH), 132.64 (CH), 127.98 (C_q), 31.61 (CH_2), 30.68 (CH_2).

ESI-MS: $[M+H]^+$ = 306.90

(ethylene glycol ether) 2,5-bis(bromomethyl)benzoate **B1**

First attempt - via a 2,5-bis(bromomethyl)benzoyl chloride intermediate[20]: A mixture was prepared of 2,5-bis(bromomethyl)benzoic acid **5** (0.2 g, 0.65 mmol), thionyl chloride (1.638 mL, 1.38 mmol) and 1 drop DMF in 15 mL dry toluene. The solution was allowed to reflux for 3h, before being cooled to room temperature and concentrated. The resulting yellow oil **5a** was used as such in the following step without further purification. Under inert conditions, the benzoyl chloride derivative **5a** was dissolved in 20 mL dry DCM and added dropwise to a solution of diethylene glycol (0.2 g, 1.89 mmol) in 30 mL dry DCM. The mixture was stirred for 4h at room temperature, and an additional 24h at reflux. The solution was cooled, washed with water and the organic layer dried over $MgSO_4$. After concentration, a dark orange oil is obtained that is unsuccesfully purified by subjecting it to column chromatography (DCM/hexane, 10:5).

Second attempt - DCC coupling reaction[21]: 2,5-bis(bromomethyl)benzoic acid **5** (1 g, 3.25 mmol), diethylene glycol (6 g, 56.54 mmol) and a catalytic amount of DMAP (0.02 g, 0.164 mmol) were dissolved in 30 mL pure DCM, cooled to 0°C and degassed for 30 min. A solution of DCC (1 g, 4.85 mmol) in 20 mL pure DCM was added dropwise under 0°C and the solution was allowed to stir overnight at room temperature before being refluxed for an additional 3 *à* 4h. After filtration, the filtrate was washed with brine and water and the organic layer was dried over $MgSO_4$. Filtration and concentration resulted in a light yellow oil that was purified using silica gel flash column chromatography (DCM/hexane, 10:5). This revealed the formation of only the di-substituted glycol and a large amount of unreacted starting material.

Third attempt - monoesterification with AMA without the use of any solvents[22]: To a mixture of $MeSO_3H$ (1 mL, 15 mmol) and Al_2O_3 (0.27 g, 3 mmol), 2,5-bis(bromomethyl)benzoic acid **5** (0.308 g, 1 mmol) and diethylene ether (0.095 mL, 1 mmol) were added successively. The solution was stirred at 80°C for 1h. The mixtures was then poured into an excess of water, extracted two times with EtOAc and the organic layer washed with saturated aqueous $NaHCO_3$. Drying over $CaCl_2$, concentrating over reduced

pressure and purification by silica gel flash column chromatography, resulted again in the di-substituted glycol.

1,5-bis[2-(2-(2-hydroxyethoxy)ethoxy)ethoxy]-naphthalene **10**[24] Under nitrogen, a solution of 2-(2-chloroethoxy)ethoxyethanol **9** (31.37 g, 186 mmol) in 40 mL dry MeCN was added dropwise over 1h to a purple suspension of naphthalene-1,5-diol **8** (10 g, 62.43 mmol) and K_2CO_3 (51.77 g, 374.6 mmol) in 90 mL dry MeCN. The solution was heated under reflux overnight to give a brown, turbid solution. After removing the solvent, the resulting brown oil was dissolved in DCM, stirred for a few days and washed with brine and water. The organic layer was dried over $MgSO_4$, filtered, concentrated and the resulting red-brown oil was subjected to column chromatography over silica gel (DCM/EtOH, 30:1) to give a brown, solid product **10** (12.69 g, 29.9 mmol, 47.9%)

^{1}**H NMR** (400 MHz, $CDCl_3$) δ_H 7.87 (d, J = 8.6 Hz, 2H, $[C_6H_3{-}OC_6H_{13}O_3]_2$), 7.36 (dd, J = 13.4, 5.7 Hz, 2H, $[C_6H_3{-}OC_6H_{13}O_3]_2$), 6.85 (d, J = 7.6 Hz, 2H, $[C_6H_3{-}OC_6H_{13}O_3]_2$), 4.31 (m, 4H, $[C_6H_3{-}OCH_2CH_2{-}]_2$), 4.00 (dd, J = 5.4, 4.3 Hz, 4H, $[C_6H_3{-}OCH_2CH_2{-}]_2$), 3.81 (m, 4H, $[{-}OCH_2CH_2OH]_2$), 3.72 (m, 8H, $[C_6H_3{-}OC_2H_4OC_2H_4OC_2H_4OH]_2$), 3.62 (m, 4H, $[{-}OCH_2CH_2OH]_2$).

^{13}**C NMR** (101 MHz, $CDCl_3$) δ_C = 154.31 (C_q), 126.80 (C_q), 125.13 (CH), 114.66 (CH), 105.76 (CH), 72.52 (CH_2), 71.05 (CH_2), 70.52 (CH_2), 69.85 (CH_2), 67.92 (CH_2), 61.83 (CH_2).

ESI-MS: $[M+NH_4]^+$ = 442.20

1-(2-(2-(2-hydroxyethoxy)ethoxy)ethoxy)-5-(2-(2-(2-methoxyethoxy)ethoxy)ethoxy)-naphthalene **11**[20] 1,5-bis[2-(2-(2-hydroxyethoxy)ethoxy)ethoxy]-naphthalene **10** (376 mg, 0.886 mmol) was dissolved in 15 mL dry THF, to which a suspension of NaH (60% dispersion in mineral oil)(0.6 g, 25 mmol) in 25 mL dry THF was dropwise added under inert atmosphere. The solution was stirred at room temperature for 30 min, and an additional 30 min under reflux. A solution of iodomethane (0.1285 g, 0.905 mmol) in 10 mL dry THF was added dropwise over 15 min. The solution was further refluxed for 24h, cooled and methanol (2.5 mL, 61.8 mmol) was added to react with the excess of NaH. After concentration, the resulting oil was dissolved in DCM and washed with saturated aqueous Na_2CO_3 and water. The organic layer was dried over $MgSO_4$, filtered, concentrated and the resulting red-brown oil was purified by silica gel column chromatography

(EtOAc/hexane, 95:5) to give the final compound **11** (67.9 mg, 0.155 mmol, 17.5%).
^{1}H NMR (400 MHz, $CDCl_3$) δ_H 7.86 (dd, J = 8.5, 3.4 Hz, 2H, [C_6H_3−]$_2$), 7.34 (m, 2H, [C_6H_3−]$_2$), 6.84 (d, J = 7.6 Hz, 2H, [C_6H_3−]$_2$), 4.30 (dd, J = 9.6, 4.4 Hz, 4H, [C_6H_3−O$CH_2$$CH_2$−]$_2$), 4.00 (dt, J = 4.7, 3.5 Hz, 4H, [C_6H_3−OCH_2CH_2−]$_2$), 3.81 (m, 4H, [C_6H_3−OC_2H_4−O$C_4H_8O_2$−]$_2$), 3.71 (ddd, J = 7.6, 5.9, 3.9 Hz, 6H, [C_6H_3−OC_2H_4 − O$C_4H_8O_2$−]$_2$), 3.67 (m, 2H, [C_6H_3−OC_2H_4−O$C_4H_8O_2$−]$_2$), 3.62 (m, 2H, [C_6H_3−OC_2H_4 − O$C_4H_8O_2$−]$_2$), 3.54 (m, 2H, [C_6H_3−OC_2H_4−O$C_4H_8O_2$−]$_2$), 3.37 (s, 3H, −O$C_4H_8O_2$−CH_3).
^{13}C NMR (101 MHz, $CDCl_3$) δ_C = 154.33 (C_q), 126.79 (C_q), 125.09 (CH), 114.64 (CH), 105.71 (CH), 72.52 (CH_2), 71.94 (CH_2), 71.01 (CH_2), 70.73 (CH_2), 70.59 (CH_2), 70.50 (CH_2), 69.83 (CH_2), 67.91 (CH_2), 61.79 (CH_2), 60.40 (CH_2), 59.03 (CH_3).
ESI-MS: $[M+H]^+$ = 439.20

1-(2-(2-(2-acryloxyethoxy)ethoxy)ethoxy)-5-(2-(2-(2-methoxyethoxy)ethoxy)ethoxy)-naphthalene **12** Acryloyl chloride (21.02 mg, 0.232 mmol) in 3 mL dry DCM was added dropwise to a solution of 1-(2-(2-(2-hydroxyethoxy)ethoxy)ethoxy)-5-(2-(2-(2-methoxyethoxy)ethoxy)ethoxy)naphthalene **11** (67.9 mg, 0.155 mmol) and pyridine (24.5 mg, 0.310 mmol) in 7 mL dry DCM at 0°C, under inert atmosphere. The solution was stirred for 2h at 0°C and then at room temperature overnight. After filtration of the pyridine hydrochloride, the mixture is concentrated, dissolved in EtOAc, filtered again and washed with water to remove any residual pyridine. Purification is performed by column chromatography (EtOAc/hexane, 9:1). Due to the small amount of the product, only confirmation by LCMS was possible.
ESI-MS: $[M + NH_4]^+$ = 510.20

Polymer synthesis[26]

PNIPAM was synthesized by RAFT polymerization under argon atmosphere. *N*-isopropyl-acrylamide (1.132 g, 10 mmol), methyl 2-(butylthiocarbonothioyl-thio)propanoate (10.1 mg, 0.04 mmol) and AIBN (1.64 mg, 0.01 mmol) were dissolved in 5 mL DMF in a schlenk flask to obtain a molar ratio of 250:1:0.25 and a monomer concentration of 2 M. The mixture was subjected to three freeze-pump-thaw cycles to completely deoxygenate the solution. One cycle consists of freezing the solution in liquid nitrogen for at least 10 minutes, after which vaccuum is applied (10 min) to remove the air present

in the flask. Next, the flask is put in a beaker of water to defrost, upon which air bubbles appear from the solution. Due to the low pressure above the solution (vaccuum), the air gets released from the solution (bubbles). This cycle is repeated at least 3 to 4 times till no more gas is present in the solution. An argon atmosphere is applied to the flask and after taking the first kinetic samples, the polymerization is started by placing the mixture in a preheated oil bath (70°C/75°C). Samples are taken every half hour for kinetic studies. The solvents used for GC and SEC samples were respectively acetone and dimethylacetamide (DMA). After a reaction time of 3 hours, the flask was removed from the oil bath and placed in liquid nitrogen to stop the polymerization. The resulting polymer was obtained *via* precipitation in Et_2O/hexane (4:1) and twice in pure Et_2O. Centrifugation resulted in the final white, powdery polymer.

Polymerization at 70°C: M_n = 42 kDa ; Đ= 1.11

Polymerization at 75°C: M_n = 38 kDa ; Đ= 1.16

5 Supporting Information

^{1}H NMR spectra of the most important purified compounds.

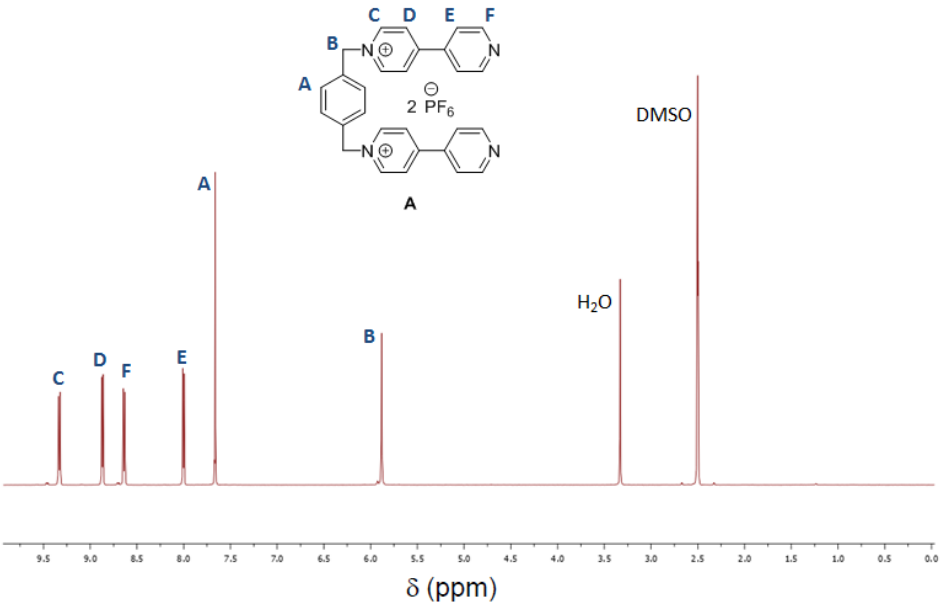

Figure 5.1: *^{1}H NMR spectrum of the purified compound* ***A****.*

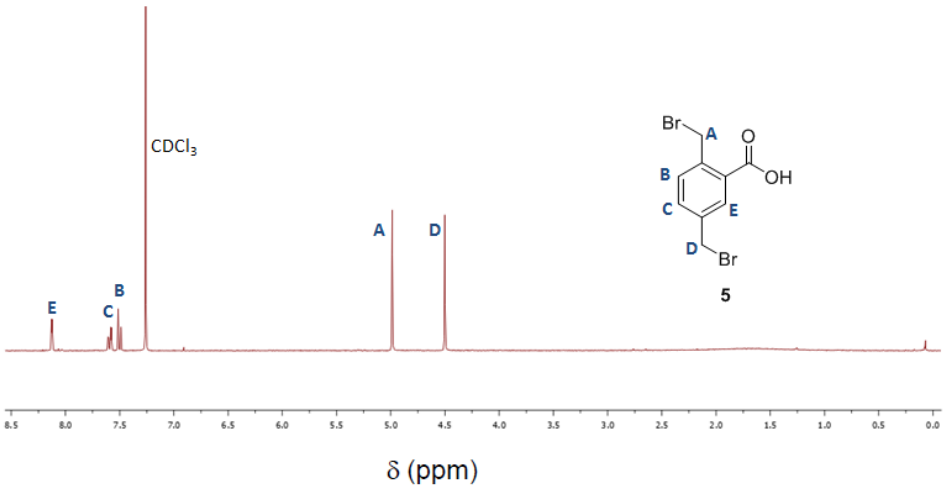

Figure 5.2: *^1H NMR spectrum of the purified compound* ***5****.*

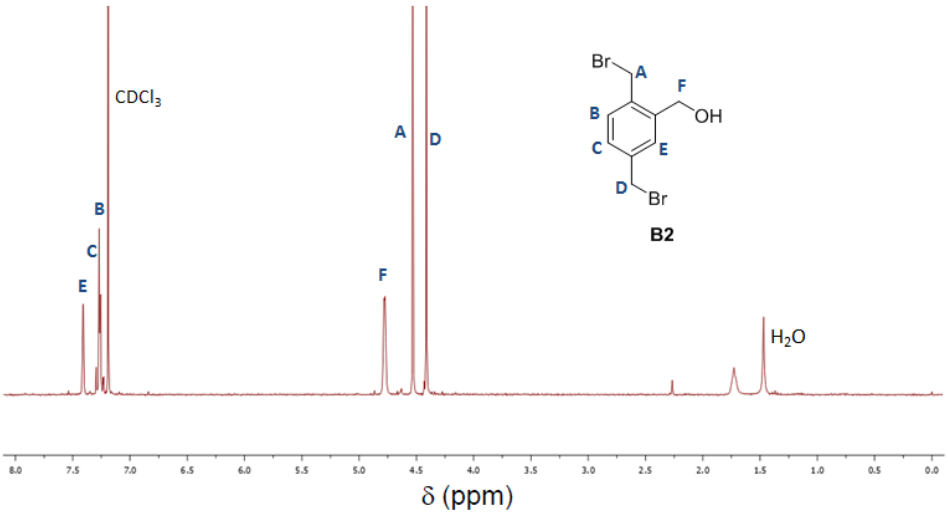

Figure 5.3: *^1H NMR spectrum of the purified compound* ***B2****.*

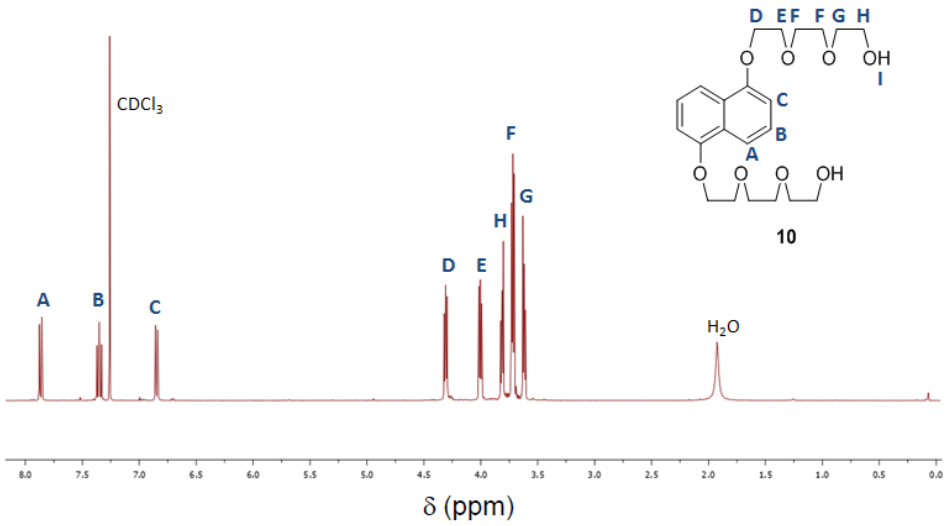

Figure 5.4: *^{1}H NMR spectrum of the purified compound* ***10****.*

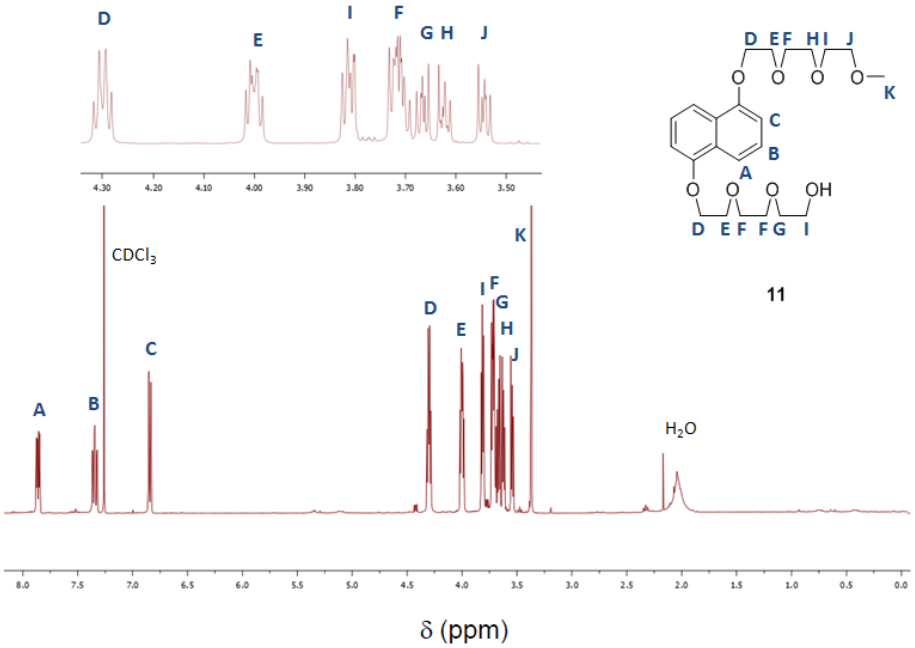

Figure 5.5: *^{1}H NMR spectrum of the purified compound* ***11****.*